MAGNETORESISTANCE AT MEDIUM AND HIGH FIELDS IN INDIUM ANTIMONIDE AND INDIUM ARSENIDE

by

Clifford Harry Champness

A thesis submitted to the Faculty of Graduate Studies and Research in partial fulfilment of the requirements for the Degree of Doctor of Philosophy

Department of Physics
(Eaton Electronic Research Laboratory)
McGill University, Montreal.

March 1962.

TABLE OF CONTENTS

TABLE OF CONTENTS (contd.)

TABLE OF CONTENTS (contd.)

ABSTRACT

Measurements have been made of the angular dependence of magnetoresistance and Hall effect of indium antimonide at room and liquid air temperatures in fields less than 7,000 oersted, and of the transverse magnetoresistance at room temperature of indium antimonide and indium arsenide in transient fields up to 3×10^5 oersted. The lower field results confirm the existence of a small positive longitudinal magnetoresistance not due to sample and field misalignment but due to either a cubical anisotropy of conduction properties or to sample inhomogeneity. Some structure in the angular variation is apparent at $77^{\circ}K$. The high field results can be explained principally by the classical two band model but show a deviation at the higher fields which could be due to Landau quantization of the conduction electrons. The measurements generally suggest that the scattering processes are only weakly dependent on the energy of the carriers.

ACKNOWLEDGEMENTS

The author wishes to express his gratitude to Dr. R. Stevenson for his support of the work and particularly for his assistance in the use of the high field techniques. He wishes to thank Professor G.A. Woonton, Director of the Eaton Laboratory, for his support and encouragement. Thanks are due to Messrs. Andrew Solandt and Peter Smith for assistance with calculations and to the staff and graduate students of the Eaton Laboratory for their help in many ways. The author is grateful for support from the Office of Naval Research (U.S. Navy), and the Defence Research Board of Canada.

INTRODUCTION

In general the resistance of an electrical conductor changes in the presence of a magnetic field and the phenomenon is referred to as the magnetoresistance effect. Usually the change is an increase and in normal laboratory magnetic fields it is often very small. It arises principally from the Lorentz force acting on the charge carriers causing them to have a sideways component of motion between collisions. Changes of resistance can also result from the effect of the magnetic field on the concentration of available electrons and on the scattering processes but these effects are smaller in most situations. Frequently only longitudinal and transverse field-current orientations are employed in magneto-resistance investigations. The transverse magnetoresistance is usually larger than the longitudinal effect.

Magnetoresistance can be used to help in understanding the conduction processes in metals and semiconductors. The effect in metals is complex but in semiconductors it is simpler and often larger. This is to some extent due to their larger mobilities and to their having a Boltzmann energy distribution of charge carriers.

This thesis presents the results of measurements of magnetoresistance made on the compound semiconductor indium antimonide. Some results on the similar semiconductor, indium arsenide, are also given. The measurements were carried out at high magnetic fields of around 200,000 oersted using pulsed techniques and at medium fields of less than 7,000 oersted with a conventional electromagnet. The choice of the terms "medium" and "high" is made by

comparison with the reciprocal of the electron mobility (which has the dimensions of magnetic induction) in the semiconductors.

The medium field work consisted of measurements of conductivity, Hall coefficient and magnetoresistance at room and liquid nitrogen temperatures. The main object of the work was to provide values of the conduction parameters needed for analysing the high field magnetoresistance. A second object was to find out if a longitudinal magnetoresistance really exists in indium antimonide, since this effect can shed light on the band structure in the material. Accordingly, the samples used were oriented in specific directions so that possible anisotropy could be detected in the longitudinal magnetoresistance and measurements were made with angular variation between current and magnetic field. Until recently all previously reported work was carried out with unoriented samples. Due to inhomogeneity in the samples this part of the study was not very conclusive. Nevertheless, the examination in its limited way, was probably the most detailed yet made and enables two explanations of the longitudinal magnetoresistance to be rejected. At liquid nitrogen temperature, the angular dependence showed some new effects.

Up to the present time practically no high field measurements have been made on semiconductors at room temperature. The high field work presented in Part II of the thesis describes room temperature measurements of transverse magnetoresistance made on some of the indium antimonide and indium arsenide samples studied in Part I. Longitudinal measurements were not made because of

orientation uncertainties in the pulsed field method.

Indium antimonide in many ways is suitable for high field magnetoresistance studies. The conduction electrons have a very small effective mass so that relatively low fields are needed to make them execute complete circular orbits in the magnetic field before being scattered. Because of the small mass, the electron mobility is very high and hence the magnetoresistance effect is very large. Even more important, fields can be reached to make the energy spacing between adjacent Landau levels much greater than kT at room temperature. Thus the quantization at high fields should be big enough to affect the conduction processes. Another advantage of indium antimonide is that its effective mass can be taken approximately to be isotropic. In Part I it is shown that any deviations of the conduction band from spherical symmetry are small. This makes a considerable simplification of the theoretical treatments.

An examination at room temperature for the appearance of transport effects, resulting from the quantization into Landau levels, was the primary purpose for doing the measurements. A second objective was to examine how far the classical conduction theory would fit the magnetoresistance results and accordingly to see what information could be obtained on the scattering processes of the carriers. Such information could then be compared with results from the medium field measurements. This aspect of the work was given added interest by the recent analysis of Weiss (1961). After allowing for spurious effects, he concluded that

magnetoresistance arising from a single band is as yet undetected in indium antimonide.

The high field studies presented here are in a range largely unexplored and the resistance increases are the greatest yet reported at room temperature. A special point of the investigation is the comparison with two band classical theory using conduction parameters measured on the individual samples.

PART I

MEDIUM FIELD

MEASUREMENTS

1. PRELIMINARY SURVEY FOR PART I

Measurements of magnetoresistance and Hall effect are readily carried out in indium antimonide at medium fields because of the high mobility of the charge carriers. They can be employed to determine the concentration of carriers and their mobilities, to estimate the total number of donors and acceptors and suggest or rule out possible scattering mechanisms. To obtain such data was the primary purpose of the measurements of Part I so that it could be used to understand the magnetoresistance at high fields.

The second objective of the work regarding the existence of longitudinal magnetoresistance was motivated by band structure considerations. Any evidence of anisotropy in the longitudinal effect could suggest deviations from spherical symmetry of the constant energy surfaces in wave vector ($\underline{k}$) space.

The band structure of indium antimonide according to some theoretical speculations of Herman (1955) is shown in figure 1. There are subsidiary minima along [100] and [111] directions in the conduction band but these lie at a higher energy than the minimum at the centre of the zone where the electrons are situated. The possibility of populating the subsidiary minima would give rise to a component of longitudinal magnetoresistance. Hence the special interest in this effect.

Before reviewing the magnetoresistance work, it is helpful first to review briefly the evidence favouring spherical energy surfaces for the conduction band of indium antimonide. Dresselhaus, Kip, Kittel and Wagoner (1955) studied microwave

cyclotron resonance at liquid helium temperature and found the effective mass of the electrons to be isotropic under rotation in a (100) plane. This indicates that the energy surfaces are either spherical or are spheroids directed along $\langle 100 \rangle$ axes at liquid helium temperature. In the room temperature cyclotron resonance experiments of Burstein, Picus and Gebbie (1956), of Keyes, Zwerdling, Foner, Kolm and Lax (1956) and of Sosniak (1961), rotation of the crystals was not carried out. Thus at room temperature the possibility of a small amount of anisotropy existing in the effective mass remains unchecked by cyclotron resonance. Evidence in favour of spherical energy surfaces at the centre of the Brillouin zone was provided by piezoresistance measurements on single crystals by Potter (1957).

Regarding magnetoresistance, measurements of the dependence on the angle between current (I) and magnetic field (H) were first reported by Pearson and Tanenbaum (1953) on a polycrystalline p-type sample. Later the measurements were repeated (Tanenbaum, Pearson and Feldman, 1954) on n- and p-type single crystal samples cut with current axes parallel to [100] and [110] directions. They reported that the magnetoresistance practically vanished when I and H were parallel, as would be expected for spherical energy surfaces. Subsequent work by other investigators, however, showed that the longitudinal magnetoresistance was not zero. Mansfield (1955) found that in polycrystalline degenerate material it was an appreciable fraction of the transverse effect. Frederikse and Hosler (1957) found that at 78° K in purer single crystal material it was an order of magnitude smaller than the

transverse effect. Complex behaviour was observed by these workers when I and H were nearly parallel on two unoriented samples; one of them showed a longitudinal magnetoresistance positive at small fields which changed to negative at higher fields, while the other sample showed a positive effect at all fields with I parallel to H but underwent changes of sign to negative and then back to positive again as the angle between I and H was increased. Using pulsed fields up to 180 kilo-oersted, Haslett and Love (1959) found longitudinal magnetoresistance values up to 25 at 78°K. At this temperature they found that no "freeze out" (Keyes and Sladek, 1956) effects occurred. Both Frederikse and Hosler, and Haslett and Love state that the nonzero longitudinal magnetoresistance can be explained on the basis of a quantum transport treatment such as that of Argyres and Adams (1956). This explanation has, however, not yet been substantiated by explicit theoretical calculations. More recent work on tellurium doped indium antimonide by Rupprecht, Weber and Weiss (1960) has given a longitudinal magnetoresistance smaller than 1% from liquid helium to room temperature.

Magnetoresistance measurements are sensitive to inhomogeneity in the samples. Influences of inhomogeneity on the transverse magnetoresistance have been considered by a number of workers. Anomalous results have been shown to occur in samples containing conductivity gradients (Bate and Beer, 1961), discontinuities (Bate, Bell and Beer, 1961) and periodic layers (Weiss, 1961). Some of the inhomogeneities are related to the direction of crystal growth (Rupprecht, 1961; Allred and Bate, 1961). The present work and the work of Frederikse and Hosler (1957) shows the

longitudinal magnetoresistance to be even more sensitive to inhomogeneity.

While there have been many previous investigations of magnetoresistance in indium antimonide few, until recently, have been carried out on oriented single crystal samples. Accordingly, in the work presented here, all the measurements were made on samples cut in specific crystallographic directions.

2. THEORETICAL CONSIDERATIONS

The general theory of the magnetoresistance effect is very complex and therefore it is usual in practice to deal with special cases, such as weak or strong magnetic fields. The semiclassical treatment of the effect using the Lorentz-Sommerfeld conduction theory is, from a formal point of view, largely complete. On the other hand the quantum mechanical treatment has been worked out only in very restricted cases and generally is not in a suitable form for direct application to experimental results.

A nondegenerate semiconductor in weak fields with a one carrier system and acoustic lattice scattering is an example of an ideal special case which cannot be realized experimentally. The real situations are intermediate cases and hence comparison with theory involves interpolation between extremes. The object in the present section, nevertheless, is to state some of the theoretical results for the special cases. The derivations of the formulae are not given and can be seen in the literature. From the outset consideration is limited only to the case where a nondegenerate distribution of carriers of one type is present. Two carrier magnetoresistance is discussed in part II of the thesis.

2.1 Semiclassical Theory

2.11 Isotropic Semiconductor

If the conduction relaxation time τ is independent of the energy (ϵ) of the electrons, the magnetoresistance, both transverse and longitudinal is zero. In the simplest treatment of conduction, the relaxation time is assumed to have an energy

dependence of the form $\tau = a\varepsilon^q$ where a and q are constants depending on the mode of scattering of the electrons. With acoustic lattice scattering $q = -1/2$, whereas with ionized impurity scattering $q = +3/2$ (approximately). For electrons with an isotropic effective mass and an isotropic relaxation time, application of the Lorentz theory of conduction (e.g. Wilson, 1953) gives the following results:

- for the longitudinal case,

$$\frac{\Delta\rho}{\rho_o} = 0 \quad \text{at all magnetic fields}$$

- and for the transverse case,

$$\frac{\Delta\rho}{\rho_o} = s(\mu_n H)^2 \qquad \ldots\ldots\ldots (1)$$

provided that $\mu_n H \ll 1$, i.e. for weak magnetic fields only. H is the magnetic field, μ_n is the electron mobility expressed in inverse magnetic units, ρ_o is the resistivity of the semiconductor in zero magnetic field and $\Delta\rho$ is the resistivity increase in the presence of the magnetic field. The dimensionless coefficient s depends on the mechanism of scattering of the electrons and may be shown to be given by the following function of the relaxation time energy exponent q.

$$s = \frac{9\pi}{16} \frac{\left[(2q+\frac{3}{2})!\right]^2}{\left[(q+\frac{3}{2})!\right]^4} \left\{ \frac{(3q+\frac{3}{2})!(q+\frac{3}{2})!}{\left[(2q+\frac{3}{2})!\right]^2} - 1 \right\} \qquad \ldots\ldots\ldots (2)$$

A plot of the variation of s as a function of q according to this formula is given in figure 2. It will be noted in particular that $s = 0$ when $q = 0$ and that for acoustic lattice

scattering $s = 0.38$. Under the same conditions the Hall coefficient R_H is related to the electron concentration n and charge e by the relation

$$R_H = \frac{r}{ne} , \qquad \ldots\ldots (3)$$

where r is a numerical factor of the order of unity. It is given specifically by the formula,

$$r = \frac{3\pi^{1/2}}{4} \frac{(2q + \frac{3}{2})!}{[(q + \frac{3}{2})!]^2} \qquad \ldots\ldots (4)$$

which goes to unity when $q = 0$. This expression squared is exactly equal to the term in front of the main bracket in the formula for s (equation (2)). Since the zero field conductivity σ_o is given by $\sigma_o = ne\mu_n$, equation (1) may be rewritten using equations (2), (3) and (4) in the following form:

$$\frac{\Delta\rho}{\rho_o} = \frac{s}{r^2} (R_H \sigma_o H)^2 . \qquad \ldots\ldots (5)$$

In indium antimonide the room temperature Hall mobility $R_H\sigma_o$ for the electrons is about 7×10^4 cm^2 $volt^{-1}$ sec^{-1} (or 7×10^{-4} $gauss^{-1}$). Hence equation (5) would apply only for fields much less than

$\frac{1}{\mu_n} = 1.4 \times 10^3$ gauss.

For strong magnetic fields, $\mu_n H >> 1$, the theory shows that the magnetoresistance saturates at a value given by

$$\frac{\Delta\rho_\infty}{\rho_o} = \frac{16}{9\pi} (q + \tfrac{3}{2})!(\tfrac{3}{2} - q)! - 1 \qquad \ldots\ldots (6)$$

For $q = -1/2$, the saturation magnetoresistance is 0.132 and for $q = 0$, it is zero. Defining a quantity $\alpha = \frac{9\pi}{16}\left[(q+\frac{3}{2})!(\frac{3}{2}-q)!\right]^{-1}$

(which will be useful later in section II of the thesis), equation (6) may be re-expressed as

$$\frac{\Delta\rho_\infty}{\rho_o} = \frac{1-\alpha}{\alpha} \qquad \ldots\ldots (7)$$

The variation of α with q is shown in figure 2.

2.12 Semiconductor with Cubic Symmetry

(a) Weak Fields. A theory of magnetoresistance in crystals having cubic symmetry in weak magnetic fields has been suggested by Seitz (1950). In the work of Pearson and Suhl (1951) on the magnetoresistance in germanium, it was shown that this theory leads to the following expression for the magnetoresistance

$$\frac{\Delta\rho}{\rho_o H^2} = b + c\left(\sum \iota\eta\right)^2 + d\sum \iota^2\eta^2 \qquad \ldots\ldots (8)$$

where ι and η are respectively the direction cosines of the current I and the magnetic field H with respect to the cubic axes of the crystal. The coefficients b, c and d are related to the conduction properties of the electrons concerned.

In general the effective electron mass in a crystal is anisotropic. Thus the constant energy surfaces in $\underline{k}$ space are ellipsoids rather than spheres. However, in a cubic crystal, symmetry requires the overall conductivity to be isotropic. Hence the energy surfaces constituting the conduction band must be several in number and arranged in the reduced zone so as to maintain cubic symmetry. Similar considerations apply to the relaxation time. Considering only ellipsoids of revolution, m_ℓ^* and τ_ℓ may be defined as the effective mass and relaxation

time respectively in the direction of axial symmetry of each spheroid and m_t^* and τ_t as the corresponding quantities transverse to this axis. A quantity K is then defined as $\frac{m_\ell^* \tau_t}{m_t^* \tau_\ell}$. Consideration of the conduction in a multi-spheroid band leads to expressions for the coefficients b, c and d in terms of $R_H \sigma_o$, K and integrals over energy involving the relaxation time (see Glicksman, 1958). Since all the coefficients turn out to be proportional to $(R_H \sigma_o)^2$, new coefficients may be redefined as follows

$$b' = b/(R_H \sigma_o)^2 \quad \ldots\ldots (9)$$

$$c' = c/(R_H \sigma_o)^2 \quad \ldots\ldots (10)$$

and $$d' = d/(R_H \sigma_o)^2 \quad , \quad \ldots\ldots (11)$$

so that equation (8) may be rewritten

$$\frac{\Delta\rho}{\rho_o (R_H \sigma_o H)^2} = b' + c' \left(\sum \iota\eta\right)^2 + d' \sum \iota^2 \eta^2 \quad \ldots\ldots (8A)$$

Further simplification using the previously mentioned results for the isotropic weak field theory, gives the following expressions for the coefficients

$$b' = \left(1 + \frac{s}{r^2}\right) \mathcal{M}_1(K) - 1 \quad \ldots\ldots (12)$$

$$c' = 1 - \left(1 + \frac{s}{r^2}\right) \mathcal{M}_2(K) \quad \ldots\ldots (13)$$

$$d' = \left(1 + \frac{s}{r^2}\right) \mathcal{M}_3(K) \quad \ldots\ldots (14)$$

and the Hall coefficient is given by

$$R_H = \frac{r'}{ne} \quad \text{where} \quad r' = \frac{3K(K+2)}{(2K+1)^2} \quad . \quad \ldots\ldots (15)$$

The functions $\mathcal{M}_1(K)$, $\mathcal{M}_2(K)$ and $\mathcal{M}_3(K)$ take different forms according to the spheroid model under consideration. Particular forms are given by Allgaier (1958).

If current flows in a fixed direction in the crystal and the direction of the magnetic field is made variable, the variation of $\Delta\rho/[\rho_o(R_H\sigma_o H)^2]$ can be mapped out in three dimensions in terms of the coefficients b', c' and d' using equation (8A). For example, if the current I flows in a [100] direction, $\Delta\rho/[\rho_o(R_H\sigma_o H)^2]$ is equal to $b' + \frac{d'}{2}$ for H in a $[1\bar{1}0]$ direction and $b' + \frac{d'}{3}$ for H in an [001] direction. It may be especially noted that with I parallel to H, longitudinal values in the [100], [110] and [111] directions are $b' + c' + d'$, $b' + c' + \frac{d'}{2}$ and $b' + c' + \frac{d'}{3}$ respectively.

Abeles and Meiboom (1954) and Shibuya (1954) considered three multi-spheroid systems for interpreting the magnetoresistance effect in germanium. Their models were (a) 6 spheroids along the $\langle 100 \rangle$ directions in k-space (b) 12 spheroids along $\langle 110 \rangle$ directions and (c) 8 spheroids along $\langle 111 \rangle$ directions. For these models certain symmetry relations were shown to hold between the coefficients b', c' and d', These relations are tabulated as follows:

Table I

Model	Conditions	
Spherical	$b' + c' = 0$	$d' = 0$
(a)	$b' + c' = -d'$	$d' < 0$
(b)	$b' + c' = d'$	$d' > 0$
(c)	$b' + c' = 0$	$d' > 0$

Note that the coefficient d' is zero for spherical energy surfaces and nonzero in the other cases for $K \neq 0$; it may thus be thought of as the magnetoresistance anisotropy parameter. Using these symmetry relations, longitudinal values of $\Delta\rho/[\rho_o(R_H\sigma_o H)^2]$

are given in table II for [100], [110] and [111] directions with the three multi-spheroid models. The longitudinal effect depends only on d', whose magnitude is in turn dependent on K and q. If K = 1, the spheroidal energy surfaces become spheres and the longitudinal magnetoresistance is zero in all directions. When this happens $M_1 = M_2 = 1$, $M_3 = d' = 0$ and

$$b' = -c' = \frac{s}{r^2} \qquad \ldots\ (16)$$

(b) Strong Fields. Abeles and Meiboom (1954) and Shibuya (1954) have worked out expressions for the saturation magnetoresistance in certain cases with the three multi-spheroid systems. The expressions for the longitudinal magnetoresistance are functions of K only and are given in table II. For a given spheroid system it is apparent that the saturation longitudinal magnetoresistance, like the weak field effect, is directionally dependent. Again if K = 1, the longitudinal magnetoresistance disappears.

It is clear from table II that the longitudinal magnetoresistance can, in principle, be used to find out the symmetry model and the spheroid shape (K value) for a particular conduction band. According to Herring (1955) the longitudinal magnetoresistance contribution from a particular ellipsoid is zero if the applied magnetic field is parallel to any principal axis of the ellipsoid. In the case of model (a) it is possible to do this for all the six ellipsoids at the same time if H is directed along any <100> axis. Table II shows the longitudinal magnetoresistance is zero for this case. With eight ellipsoids along <111> axes however, there is no direction for which the longitudinal magnetoresistance is zero; when the magnetic field is directed along a particular

$\langle 111 \rangle$ axis it is parallel to the principal axes of two of the ellipsoids, but not parallel to those of the other six ellipsoids. The same is true for ellipsoids along $\langle 110 \rangle$ axes. While most models will not have a direction where the longitudinal effect is zero, they will show a characteristic variation with angle. In general the effect might be expected to be a minimum when the magnetic field is parallel to a principal axis and a maximum when it is in a direction which is most oblique to the set of ellipsoids. Calculations show that in many cases this rule holds. The various conduction band models also lead to a modification of the transverse saturation magnetoresistance from its value for an isotropic band. Special cases of this have been worked out by Shibuya (1954).

2.2 Quantum Mechanical Theory

The quantum treatment of magnetoresistance takes into account the quantization of the electron orbits in a magnetic field. Landau wave functions which also contain the electric field, are used to determine the density matrix of the electrons and hence the electric current. This has been done by Adams and Holstein (1959) for various scattering mechanisms in the extreme quantum limit of high magnetic fields when all the electrons occupy just the lowest Landau level. The longitudinal magnetoresistance is somewhat easier to treat theoretically than the transverse effect. In the longitudinal case the magnetic field only affects the transition probability and hence the relaxation time; the magnetic field cannot alter the speed of the electrons parallel to the field.

In general it might be expected that the quantum mechanical treatment would begin to become important when $\xi = \frac{\hbar \omega_c}{kT} > 1$

i.e. when the energy separation $\hbar\omega_c$ between adjacent Landau levels is greater than kT, where $\hbar$ is Planck's constant divided by 2π, k is Boltzmann's constant, T is the absolute temperature and ω_c is the cyclotron resonance angular frequency.

The point which is specially interesting in the quantum treatment is that it leads to a nonzero longitudinal magnetoresistance for spherical energy surfaces. Hence even at small fields it may be the only contribution experimentally observable.

2.21 Longitudinal Magnetoresistance for an Isotropic Semiconductor

At weak fields, i.e. $\xi << 1$ the only expressions which appear to have been worked out are for the longitudinal magnetoresistance with acoustic lattice scattering. Even in this special case there is little agreement in the literature as to the correct expression for the effect, as can be seen from the following formulae

Appel (1956) : $$\frac{\Delta\rho}{\rho_o} = \frac{\xi^2}{12} \qquad \ldots. (17)$$

Schoenfeld (Argyres, 1958):

$$\frac{\Delta\rho}{\rho_o} = \left[1 + 17.4\,\xi^{1/2} + \frac{3}{4}\xi \ln \xi + O(\xi)\right]^{-1} - 1 \qquad \ldots. (18)$$

Miller and Omar (1961):

$$\frac{\Delta\rho}{\rho_o} = \left[1 + \xi + 0.025\,\xi^2\right]^{-1} - 1 \qquad \ldots. (19)$$

The last two formulae predict negative magnetoresistance while the first one predicts it to be positive. The equation of Schoenfeld predicts surprizingly large changes at small fields.

Barrie (1959) has made some numerical calculations for

acoustic lattice scattering but his computations do not go to very small values of ξ . However, extrapolating his data to smaller fields for the case of a conductor with a degeneracy factor $\zeta/kT=0.92$ (ζ being the Fermi energy with respect to the bottom of the conduction band), the longitudinal magnetoresistance is found to be negative and to agree very roughly in magnitude to that predicted by the formula of Miller and Omar. In the absence of better information the results of Miller and Omar are accepted. A somewhat more accurate formula than equation (19) is

$$\frac{\Delta\rho}{\rho_o} = \frac{1}{6F}\,\xi\,\mathrm{cosech}\left(\frac{\xi}{2}\right)\exp\left(\frac{\xi}{2}\right) \qquad \ldots\ (20)$$

where $$F \simeq 1 - \left(\frac{2}{3} + 0.33\,\xi + 0.074\,\xi^2\right)\exp(-\xi) \qquad \ldots\ (20A)$$

Miller and Omar have given a quantum mechanical treatment of longitudinal magnetoresistance for the multi-spheroid model (c) which applies to the conduction band of germanium.

3. SAMPLES

The indium antimonide samples were cut from three single crystals which are labelled A, B and C. These crystals were kindly supplied by Dr. T.J. Davies of Minneapolis Honeywell, Dr. M. Gransden of Canadian Marconi and Dr. A.J. Strauss of the Lincoln Laboratory. Details of the crystals are given in table III. Crystals A and C were n-type while crystal B was p-type. At room temperature the crystals were intrinsic. An approximate determination of the density of scattering centres was made from the observed mobilities using the impurity scattering formula of Conwell and Weisskopf (1946). The concentrations are shown in table III and indicate by comparison with the liquid air carrier concentrations the degree of donor-acceptor compensation in the crystals. This reveals that the apparent small hole concentration in crystal B was mainly the result of compensation. Crystal A has about four times as many extrinsic electrons per cm^3 as crystal C. The total number of impurity centres was probably in about the same ratio.

Details of a single crystal of n-type indium arsenide, obtained from the Lincoln Laboratory through the courtesy of Dr. Strauss, are also given in table III. Infrared cyclotron resonance was observed in this crystal and in the two n-type indium antimonide crystals A and C by J. Sosniak (1961).

The samples used to make the galvanomagnetic measurements were cut in the form of rectangular filaments from the crystals. The long axes of the samples were in [100], [110] and [111] directions with the lateral faces having the orientations shown in figure 3.

The cutting of the samples was done using a tungsten wire saw and the crystallographic orientations were determined from Laue X-ray photographs. The deviations from the specified crystal directions were usually within 2° for the long axes but rather more than this for the lateral faces of the samples. This error is a consequence of the rather crude method of cutting with a wire saw. However, the wire saw did not cause fractures in the brittle indium antimonide samples as tends to happen with other methods of cutting.

Indium antimonide and indium arsenide tend to cleave along [110] planes. This caused a number of breakages to occur particularly with [100] samples. The cleavage property was also put to good use in the preparation of indium antimonide samples C1a and C1b and in indium arsenide sample X1 where the lateral faces were made by cleavage.

The samples C1a, C2 and C3 all had the common orientation property of possessing a {110} lateral face. This plane was used as the plane of rotation in the angular dependence measurements on the C samples.

4. METHOD OF MEASUREMENT

The measurements of magnetoresistance and Hall effect were made as a function of the angle θ between current and magnetic field and as a function of magnetic field strength with the magnetic field parallel and transverse to the current axis.

4.1 Magnets and Sample Holders

The measurements were carried out in a 6 inch rotatable electromagnet on samples A1a, A2, A3 and B3. When this magnet became unavailable, measurements were continued on a 4 inch rotatable electromagnet with samples A1b, C1a, C1b, C2 and C3. The magnets were used with untapered pole pieces giving a sufficiently uniform field over the sample. The sample was supported horizontally between the pole pieces and the different angles between I and H obtained by rotating the electromagnet about a vertical axis (figure 4). With the angular scale set to zero, alignment of the sample axis parallel to the magnetic field was done by eye. The field of the six inch electromagnet was calibrated by Dr. J.A. Carruthers against current using proton resonance and the four inch electromagnet was indirectly calibrated in the same way.

The type of sample holder is shown in figure 5. It consisted of a micarta rod one end of which was filed to a double flat. Across this flat a small slot was filed, into which the sample was inserted. The ends of the sample were soldered with indium to two small brass screws tapped into the base of the slot. These screws were specially made from thin brass wire using a watchmaker's die; one end of each screw was turned down to

a very small diameter for ease of making contact to the sample. The end contacts served both as current electrodes and to hold the sample in place. The potential probes consisted of four short lengths of 0.003 inch diameter platinum wire coated with indium. These were passed through small transverse holes drilled in 0-80 (N.F.) screws using a watchmaker's drill. The heads of the 0-80 screws were sawn off and screwdriver slots cut in the stems. By twisting the screws in the holder, the platinum wires could be made to be in spring contact with the sides of the sample. Good electrical contact was then ensured by discharging a 2.5 μF condenser charged to 50 volts between each probe and one end of the sample. Wire leads from both the probes and sample end contacts were taken out from the opposite face of the holder and passed along the length of the rod out to the measuring circuit. Partial short circuiting of the Hall voltage by the finite size of metallic probe areas can cause spurious magnetoresistance effects (Broom, 1958). This should not have occurred with the small size of probe wire contacts used here.

4.2 Measurement Technique

The four probes on the sample (figure 6) enabled measurements to be made of two Hall voltages (from probe pairs 1 and 2) and two conductivity voltages (from the upper and lower probe pairs). A constant current of about 10 mA at room temperature and 2 mA at liquid air temperature was passed through the sample and the potential differences between the probes were measured with a Leeds and Northrup type K2 potentiometer. The current was measured with a Weston, model 280 milliammeter. The particular choice of probe pair connected to the potentiometer was made

using the five position selector switch (figure 7), one position of which was a short circuit for checking purposes. There is always a stray component of magnetoresistance between the Hall probes and also a stray component of Hall effect between the conductivity probes. The two effects can be distinguished by reversing the magnetic field direction which was done throughout the course of the measurements. The reversed polarity of the Hall voltage on reversing the field was rendered positive to the potentiometer by the reversing switch S4. The direction of the current through the sample was also reversed during the measurements to eliminate any possible thermoelectric effects. The sample current reversing switch S2 was ganged to another reversing switch S3 which was connected between switches S1 and S4. When the sample current was reversed, the potential differences between the probes were also reversed; the switch S4 then reinverted the polarity to give positive voltages again so that they could be measured by the potentiometer.

With the magnet and sample in fixed positions, the routine for taking the measurements was as follows. Four potentiometer readings were taken between the probe pairs with no magnetic field. Then four more were taken with the field on, four more with the field reversed and finally four readings with the field off again. The sample current was then reversed and a further set of sixteen readings obtained. Differences between the readings with the field on and off were taken to represent Hall voltages and voltages resulting from resistivity changes. The four differences for each pair of probes were then averaged in such a way as to eliminate contributions to the Hall voltages which did not reverse with

field and contributions to the magnetoresistance voltages which did reverse. For the field dependence measurements, readings were taken at different electromagnet currents with θ set to 0° and 90°.

Because of the procedure of reversing the magnetic field, the angular dependence measurements were only made over 180° of rotation. However, viewed in retrospect, measurements over 360° might not have been superfluous because of possibilities such as the magnetic field direction not being exactly at right angles to the axis of rotation of the electromagnet.

Each set of measurements was made at room temperature and with the sample holder immersed in liquid air or liquid nitrogen.

The sample dimensions were measured with a micrometer and the spacing between the probes was determined with a travelling microscope.

5. EXPERIMENTAL RESULTS

In this section the experimental results are presented. The data covers well over a hundred experimental plots spread over some 25 figures (figures 8 to 32). To present this information on indium antimonide in a clear and convenient way it is treated in parts for the particular measurements involved and the results are described for the sets of samples within each part. The measurements on indium arsenide are given in a single part.

5.1 Angular Dependence of the Hall Effect

Values of the quantity $V_H t/IH$ in units of cm^3 $coulomb^{-1}$ were worked out at each value of θ for the Hall measurements on the indium antimonide samples using the averaged Hall voltage reading V_H, the sample current I, the magnetic field H and the thickness of the sample t. The thickness was the lateral sample dimension lying in the I, H plane. The quantity $V_H t/IH$ may be referred to as the reduced Hall voltage; it is equal to the Hall coefficient R_H when I and H are perpendicular to one another and for other angles it is equal ideally to $R_H \sin \theta$.

5.11 Crystal A Samples

For Samples A1a, A1b, A2 and A3 the variation of the reduced Hall voltage with θ is shown in figures 8, 9, 10, 11 and 12. For samples A1a and A1b the magnetic field was rotated in a (001) plane. For sample A2 it was rotated in both a (001) and a $(1\bar{1}0)$ plane and for sample A3 in a $(\bar{1}10)$ plane. All the measurements were done at a fixed field of 4,880 oersted in the six inch electromagnet except for sample A1b whose measurements were done in the four inch electromagnet at 4,350 oersted.

The reduced Hall voltage in all the figures appears to vary with angle as sin θ. The angles where the Hall effect passes through zero are usually within a few degrees of the origin. The largest deviation is about 7° for probe pair 1 on sample A2 at liquid air temperature (figure 11). The deviations can probably be taken as a measure of the error in alignment of the sample in the electromagnet.

At room temperature the Hall voltages on the two pairs of probes (separated on the average by about 0.15 cm) agree well with each other indicating no significant gradient of electron concentration at this temperature along the sample axes. However, at liquid air temperature the two Hall voltages differ from each other by amounts ranging from about 10 to 40%. Thus at this temperature there are gradients of extrinsic electron concentration along the samples of the order of 20% per mm.

5.12 Crystal B Sample

The variation of the reduced Hall voltage at 4,880 oersted with angle for the p-type sample B3 shown in figure 13 is regular and the average deviation of the Hall zeros from the origin amounts to about 3°. At room temperature the sample is intrinsic and the Hall voltage is characteristic of the electrons. Equality of the Hall voltages on the two pairs of probes indicates no measureable gradient of electron concentration at this temperature. This is to be expected for intrinsically excited carriers. At liquid air temperature, the Hall effect is characteristic both in sign and magnitude of the number of extrinsic holes. There is at this temperature again a difference between the Hall voltages at the two pairs of probes. As a percentage the difference is smaller

than in the A samples indicating a smaller gradient of extrinsic carriers.

5.13 Crystal C Samples

The plots of reduced Hall voltage against θ for samples C1a, C2 and C3 are given in figures 14, 15 and 16. The measurements were all made at a field of 4,350 oersted in the four inch electromagnet and the plane of rotation was $\{110\}$ for all three samples.

The figures show the same features observed with the previous samples namely an approximately sinusoidal variation with θ, small deviations of Hall zero from the origin (not exceeding 3° in these samples) and equality of the Hall voltages on the two probe pairs at room temperature. However, a difference from previous samples is that at liquid nitrogen temperature the Hall voltages on the two probe pairs agree with one another. At least this is true when I and H are mutually perpendicular. At smaller θ angles a small difference does exist with a maximum difference near $\theta = 0^{\circ}$. Thus no significant extrinsic carrier concentration gradients were evident in these samples so that crystal C had a more homogeneous distribution of impurity centres than crystals A and B.

Closer inspection of the liquid nitrogen curves shows small departures from sinusoidal behaviour which take the form of slope changes on either side of the origin.

5.2 Hall Coefficient and Conductivity Data for the Samples

The reduced Hall voltages at the maxima near $\theta = \pm 90^{\circ}$ obtained from the measurements given in the previous section were taken as the Hall coefficients. Table IV shows such Hall

coefficient values averaged for the two pairs of probes for each sample at two temperatures along with zero field conductivity (σ_o) values. The conductivities were obtained in each case from the zero field potential difference between the conductivity probes, the distance between the probes and the area of cross-section of the sample. The values in the table are the averages for the upper and lower probe pairs. The table also shows values of the Hall mobility $R_H \sigma_o$.

For a given crystal there are conductivity differences between the different samples. Such differences cannot arise from the particular crystal orientations of the sample axes because the cubic symmetry of the zinc blende structure requires the conductivity to be isotropic in the absence of external fields. The differences are due probably to conductivity inhomogeneity in the original crystals, to errors in the probe spacing measurement and departures of the sample shape from exact rectangular form.

5.3 Field Dependence of the Hall Coefficient

The variation of the Hall coefficient with magnetic field strength at room temperature and at liquid air or nitrogen temperature is shown in figure 17 for practically all the indium antimonide samples. There is, for the most part, no significant change in R_H from 1000 to 6,500 oersted. The only exception to this applies to sample B3 at liquid air temperature whose slight fall off in R_H with increasing field is attributed to the presence of light holes in addition to the normal heavy ones (Champness, 1958b).

5.4 Angular Dependence of Magnetoresistance

The magnetoresistance ratio $\Delta\rho/\rho_o$ was found for each θ angle setting from the conductivity probe potential difference readings. The ratio was measured as the increase of P.D. in the presence of the magnetic field to the steady P.D. in zero field with constant current through the source.

5.41 Crystal A Samples

The variation of magnetoresistance with angle θ is shown in figures 18, 19, 20, 21 and 22 for samples Ala, Alb, A2 and A3. The measurements were made at the same time as the Hall voltage measurements in figures 9, 10, 11 and 12 so that same conditions of field and rotation plane apply respectively.

The figures show that while the curves have roughly the shape of a $\sin^2\theta$ variation, which for weak fields would ideally correspond to spherical energy surfaces, there are considerable deviations. These deviations may be listed as follows.

(a) The $\frac{\Delta\rho}{\rho_o}$ minima deviate from the origin by angles which are much larger than those of the Hall zeros. In the largest case the angular deviation was about 25°. The large size of such angles and the fact that the deviations are not the same for both pairs of probes indicates that the effect is not directly due to misalignment of the sample.

(b) The magnetoresistance values at the minima or at $\theta = 0^\circ$ are not zero and differ in magnitude from one pair of probes to the other. There appears to be a tendency that the

larger the deviation of the minimum is from the origin, the greater is the absolute value of the magnetoresistance at the minimum.

(c) Negative values of $\frac{\Delta\rho}{\rho_o}$ occur for some of of the minima at room temperature and at liquid air temperature. However, negative values do not appear together on the two pairs of conductivity probes; if one pair gives a negative value, the other gives a positive one. This suggests some sort of inhomogeneity effect.

(d) The maxima near $\theta = \pm 90^{\circ}$ are in general displaced in the same direction as the corresponding minima. Most of the minima are displaced to the right of the origin. This apparent one-sidedness is probably not due to a personal error on the part of the observer in aligning the sample because of the much smaller Hall zero angular deviations.

(e) The values of $\frac{\Delta\rho}{\rho_o}$ at the minima for the [100] sample A1a are larger than for the other samples. In particular no negative magnetoresistance is observed either at room temperature or at liquid air temperature on this sample. However, the other [100] sample A1b shows a practically zero magnetoresistance at its minimum at room temperature although at liquid nitrogen temperature the

average longitudinal magnetoresistance is approximately the same as in sample A1a.

While none of the curves exhibits a subsidiary maximum near $\theta = 0^{\circ}$ at liquid air temperature such as was observed by Frederikse and Hosler (1957), some complex behaviour is seen to occur in sample A1b near the origin.

5.42 Crystal B Sample

Figure 23 shows the variation of $\Delta\rho/\rho_o$ with θ at room temperature and liquid air temperature for sample B3. As for the Hall measurements in figure 13 the rotation was in a $(\bar{1}\bar{1}2)$ plane and the field 4,880 oersted.

The curves are rather more regular than those for the A samples. The magnetoresistance minima lie nearer to $\theta = 0^{\circ}$ than for the A samples and the values at the minima are all positive. At room temperature the magnetoresistance is greater than that for the A samples at all angles and at $\theta = 0^{\circ}$ in particular. At liquid air temperature the magnetoresistance is characteristic of holes with their smaller mobility and cannot be compared with the results on the A samples. However it is noted that the magnetoresistance near $\theta = 0^{\circ}$ is appreciable considering the magnitude of the transverse effect in the sample. The fact that both pairs of probes give about the same longitudinal value means that the relatively large effect may have fundamental significance. The reason for the step in $\Delta\rho/\rho_o$ between $\theta = +5^{\circ}$ and $+10^{\circ}$ on the lower probe pair is not known.

5.43 Crystal C Samples

The variation of $\Delta\rho/\rho_o$ with θ for samples C1a, C2 and C3 is shown in figures 24, 25 and 26 which correspond respectively to the Hall voltage measurements as a function of θ in figures 14, 15 and 16.

Fixing attention on the room temperature measurements first, it may be noted that the curves are more regular than those found for the A samples. The minima lie closer to $\theta = 0^o$, no negative magnetoresistance values occur and the values on the two pairs of probes agree with each other much better than with the A samples. The nonzero values at the minima would appear to indicate the existence of a positive longitudinal magnetoresistance. The average $\Delta\rho/\rho_o$ value at the minima is slightly greater in the [100] sample C1a than in the [110] and [111] samples C2 and C3. The same tendency was found in the A samples. The difference in the C samples is, however, much smaller. The greater regularity of the magnetoresistance variation compared with the A samples is probably due to the absence of significant gradients of extrinsic carrier concentration or to the higher purity of crystal C.

At liquid nitrogen temperature the behaviour is more complex than at room temperature. For all three samples there appears to be a central maximum near $\theta = 0^o$ with at least one subsidiary minimum on either side of it. The subsidiary minima seem to occur at roughly the same angles as the points of inflection in the Hall curves referred to in 5.13. The two pairs of probes show approximately the same magnetoresistance variation.

Indeed inspection shows that even minor peaks on the curve for one pair of probes are reproduced peak for peak in the angular variation of the other. The liquid nitrogen behaviour is somewhat similar to that observed by Frederikse and Hosler (1957) on their unoriented n-type sample No. 3 except that in the present case the variations for the most part still leave a positive magnetoresistance.

5.5 Transverse and Longitudinal Magnetoresistance Data

In order to compare the measurements on the different samples, transverse and longitudinal magnetoresistance values are collected together in table V. The observed deviations of magnetoresistance near $\theta = 0^{\circ}$ indicate that the longitudinal magnetoresistance is often a somewhat uncertain quantity. Hence for the values given in table V longitudinal magnetoresistance was taken as the average $\Delta\rho/\rho_0$ value at the central minima of the two probe pairs. However, in the case of the C samples at liquid nitrogen temperature a single central minimum did not exist and the longitudinal value was taken as the average value at $\theta = 0^{\circ}$. For the transverse magnetoresistance each entry in the table represents the average $\Delta\rho/\rho_0$ value at the maxima near $\theta = \pm 90^{\circ}$.

The table shows more clearly some of the features previously mentioned. The [100] samples Ala and Cla both show at room temperature a greater longitudinal magnetoresistance than the other samples of their respective sets. Sample Alb is an exception in this trend. At liquid air temperature both [100] samples Ala and Alb give a longitudinal effect greater than the other A samples but the same trend is not followed in the

C samples. This effect appears to suggest anisotropy in the longitudinal magnetoresistance although the trend is not definite enough to be established with certainty. The largest room temperature longitudinal magnetoresistance in the table is shown by sample B3 which also shows the largest transverse effect.

Turning now specifically to the transverse case, it may be noted that the magnetoresistance values show no obvious evidence of anisotropy. Both the A and C sets of samples show the [111] samples A3 and C3 to give the smallest transverse magnetoresistance at liquid air or liquid nitrogen temperature but this may not be significant. Rupprecht (1961) has reported anisotropic effects associated with the direction of crystal growth. In n-doped indium antimonide crystals the transverse magnetoresistance was found to be greatest with the current in the sample parallel to the pull direction and smallest at right angles to it. No such trend is apparent in the present results due possibly to the lower doping levels.

5.6 Field Dependence of the Magnetoresistance Effect

The field dependence measurements were made with θ set to 90° (transverse) and 0° (longitudinal). It was not convenient to take measurements at the maxima of $\frac{\Delta\rho}{\rho_o}$ near $\pm 90^{\circ}$ and the minima near 0°. The results for the two temperatures are presented separately.

5.61 Room Temperature Results

The variation of the transverse and longitudinal magnetoresistance with magnetic field strength is shown in figure

27 (a), (b) and (c) for the A samples, figure 28 (a) for sample B3 and figure 29 (a), (b) and (c) for the C samples.

For the transverse effect there is fairly good agreement between the two pairs of probes. The variation with field is clearly shown and is approximately quadratic for all the samples. Detailed discussion of the room temperature transverse effect is, however, postponed until part II of the thesis where it is treated in conjunction with the high field measurements.

The longitudinal magnetoresistance is in general about an order of magnitude smaller than the transverse effect. It lies in a measurement range where at smaller fields it is barely detectable. The errors of measurement are therefore large especially at fields of about 1000 oersted. The two sets of probes give very different values, particularly in the case of sample B3 and in the A samples where negative values sometimes occur. Notwithstanding this, lines are drawn between the two sets of points in each case where possible, to ascertain the trend of the field variation. With the C samples the slope of the variation appears to fall off to a certain extent at the higher fields while in general all the samples show an average slope which is somewhat less than that of the transverse effect. It would thus appear that the measured longitudinal effect is not due, for the most part, to a stray component of the transverse effect resulting from misalignment of I and H (e.g. in a vertical plane). There may be an exception to this for the sample A1a where the slope of the longitudinal variation is approximately the same as that of the transverse effect in the other samples. The large size

of the longitudinal effect in this sample, however, suggests that if misalignment is the cause, it must be internal (inhomogeneity for example) rather than external. For sample B3 the difference in the longitudinal and transverse slopes suggests that here misalignment is not the cause of the large longitudinal effect.

5.62 Liquid Air Results

The field variation of magnetoresistance at liquid air temperature is shown in figure 30 (a), (b) and (c) for the A samples, in figure 28 (b) for sample B3 and at liquid nitrogen temperature in figure 31 (a), (b) and (c) for the C samples.

The transverse magnetoresistance does not increase with field as steeply as it does at room temperature. The variation for the A and C samples goes very roughly as $H^{1.2}$ but it will be noted that the curves for the C samples are slightly concave whereas those for the A samples are, if anything, slightly convex. The magnitude of the magnetoresistance in the C samples is about twice that in the A samples. The approximately linear increase with field in this range has been observed previously by Frederikse and Hosler (1957) and by Bate (Beer, 1961) and is attributed by these workers to the effect of Landau quantization on the conductivity. The magnitude and curvature of the transverse field variation in the p-type sample B3 is due to the combined conduction by light and heavy holes.

The longitudinal magnetoresistance is about an order of magnitude smaller than the transverse effect, as was the case at room temperature. This was also found to be true in the results

of Frederikse and Hosler (1957). As at room temperature also, there is a large difference in the longitudinal effect between the two probe pairs. The lines drawn between the points represent the average variation. No common trend is apparent in the results for the various samples. However, in general the shape is different from that for the corresponding transverse effect; the A samples show a steeper curve and the C samples show a slope which falls off at the higher fields to become less steep than the curve for the transverse effect.

The slope of the line for sample A1 is about the same as that for the transverse results on sample A1b. The remarks about sample A1a at room temperature therefore also apply here.

5.7 Magnetoresistance and Hall Coefficient Measurements in Indium Arsenide

The results of measurements of Hall coefficient, conductivity and transverse magnetoresistance on the two indium arsenide samples X1 and X3 are summarized in table VI.

Measurements of the field variation of the Hall coefficient and the transverse magnetoresistance at room and liquid air temperature are shown in figure 32 (a) and (b) for the two samples. With an extrinsic carrier concentration of about 6×10^{16} cm^{-3} there is little change in the Hall coefficient from liquid air to room temperature. Essentially no change is observed in R_H with field variation at room temperature and only a slight fall off with increase of field at liquid air temperature.

The transverse magnetoresistance at liquid air temperature is about five times that at room temperature while the variation with field is approximately the same at both temperatures, varying roughly as $H^{1.8}$. However, a slight fall off in slope at the higher fields is apparent in the field variation at liquid air temperature.

6. ANALYSIS OF RESULTS

The magnetoresistance measurements previously described were done on samples with different mobilities and sometimes different magnetic fields. To discuss them together the magnetoresistance values were reduced to an approximately common denominator by evaluating the quantity $\frac{\Delta\rho}{\rho_0 (R_H \sigma_0 H)^2}$. Weak field theory shows that the magnetoresistance is in general proportional to this quantity. However, the magnetic fields used in the experiments cannot be considered as weak since even at the lowest field of 1000 oersted, $\mu_n H$ for the electrons is of the order of unity. Furthermore, the conduction is not always due to one type of carrier; at room temperature, for instance, both electrons and holes contribute to conduction. Remembering such invalidations, values of the magnetoresistance coefficient $\frac{\Delta\rho}{\rho_0 (R_H \sigma_0 H)^2}$ at two fields, where possible, are given in Table VII. Theoretical weak field expressions for the coefficient from equation (8A) are also shown in the table for the particular directions of current and field.

6.1 Magnitude of the Transverse Magnetoresistance Coefficient

The average values of $\frac{\Delta\rho}{\rho_0 (R_H \sigma_0 H)^2}$ at the smaller fields for the transverse magnetoresistance are approximately 0.015 for the A and C samples at room temperature, 0.043 for the A samples at liquid air temperature and 0.011 for the C samples at liquid nitrogen temperature. Such magnitudes are very small considered on the basis of weak field theory and scattering mechanisms such as that by acoustic lattice modes. Fig.2 shows

that to get s values of the order of 10^{-2} the exponent q of the relaxation time energy dependence would have to be small. According to equation (2) the above values would in fact give $|q| < 0.3$. Such a weak dependence of the relaxation time on energy might occur in polar scattering or by the right combination of acoustic lattice scattering and ionized impurity scattering. When the two latter scattering mechanisms are combined by adding reciprocals of the relaxation times, the theoretical s value first decreases from a value of 0.38 as the impurity concentration is increased; it then goes through a minimum (Champness, 1958a) and finally rises to the value of 2.16. The fact that the coefficient for the A samples is four times that for the C samples at low temperatures could be due to the larger concentration of impurities in the A samples. Since the q value for impurity scattering is positive (= + 3/2), the direction of this change indicates that the effective q in the samples is also positive. Thus for the indium antimonide samples it would appear that $0 < q < 0.3$.

Table VI shows that the indium arsenide samples also exhibit small magnitudes for the coefficient $\frac{\Delta\rho}{\rho_o(R_H\sigma_o H)^2}$. Values are 0.011 at room temperature and 0.044 at liquid air temperature. Therefore a small q value would seem also to apply to this material.

The small value of q means that the Hall coefficient factor r (equation (3)) must be near to unity. In fact if $|q| < 0.3$ equation (4) gives $r - 1 < 0.04$. Since $R_H\sigma_o = r\mu_n$,

the Hall mobility $R_H \sigma_o$ for practical purposes is equal to the conductivity mobility μ_n. It should be noted that any contribution of the holes to the transverse magnetoresistance at room temperature means that the effective s value for the electrons is even smaller than the above values. In fact the indications from Part II are that mixed conduction effects do predominate at room temperature. This leads one to ask if the magnetoresistance at liquid air temperature is also not a result of mixed conduction. If the minority holes were to make a significant contribution in the n-type samples at liquid air temperature this would mean that

$$\left(\frac{\Delta\rho}{\rho_o}\right)_{mixed} > \left(\frac{\Delta\rho}{\rho_o}\right)_{electrons}$$

Using weak field equation (1) and equation (31B) from Part II, this becomes

$$\frac{p}{n}\mu_n\mu_p H^2 > s\mu_n^2 H^2$$

or

$$p > s\frac{\mu_n}{\mu_p} n$$

Putting in the relevant numbers this means $p > 10^{16}$ cm $^{-3}$ for the A samples and $p > 10^{15}$ cm $^{-3}$ for the C samples. At liquid nitrogen temperature the concentration of intrinsic holes would be smaller than these numbers by many orders of magnitude. Therefore the possibility of mixed conduction may be rejected as the cause of the magnetoresistance, at least as far as minority holes are concerned.

The value of the coefficient $\frac{\Delta\rho}{\rho_o(R_H\sigma_o H)^2}$ as a parameter for comparison purposes is brought out strongly in Table VII by the transverse values at liquid air temperature for the p-type

sample B3. While the values are only very approximate, they stand out in magnitude from the values on the other samples. The large effect is due, as mentioned previously, to the presence of light holes.

6.2 Examination for Anisotropic Effects

The transverse magnetoresistance coefficients $\frac{\Delta\rho}{\rho_o (R_H \sigma_o H)^2}$ given in Table VII show no strong evidence of directional dependence so that $b' \simeq s$ (equation (16)). The differences from sample to sample could, however, be accounted for (see eighth column) with a d' value which is somewhat smaller than b' in magnitude but of negative sign. The longitudinal magnetoresistance coefficients ought to be more sensitive to any nonzero values of the anisotropy parameter d'. Comparison with weak field theory (last column of Table VII), however, yields inconsistent values for d'. The C samples give values of differing sign and the A samples give positive values of differing magnitude. It is apparent that some of the differences in the longitudinal values are statistical rather than being associated with crystal direction.

Possibly a better method of examination of the longitudinal magnetoresistance is by synthesis rather than analysis. Accordingly in Table VIII theory and experiment are compared using ratios of longitudinal magnetoresistance coefficient in the three directions [100], [110] and [111]. The predictions of both the weak and the strong field theories when compared with the experimental results appear to rule out model (a) as a

possibility since the observed longitudinal magnetoresistance is not smallest in the [100] samples. Model (c) which predicts the largest effect in the [100] direction appears to accord more with the experimental results on the A samples. Model (b) with a K value between 0.1 and 0.5, giving the smallest magnetoresistance in the [110] direction, appears to be more consistent with the results on the C samples; to a lesser extent model (c) with a K value of 10 could also apply to the C samples.

Notwithstanding these remarks, the experimental ratios suggest that the longitudinal magnetoresistance may be greatest in the [100] direction and least in the [110] direction. This seems generally to point to model (b) for the conduction band.

The magnetoresistance subsidiary maxima observed at small θ angles at liquid nitrogen temperature in the C samples are now considered. The weak field equation (8) can be used to plot the variation of magnetoresistance as a function of angle in a $\{110\}$ plane for the three sample C orientations and for each of the three multi-spheroid models (a), (b) and (c). Such considerations show the possibility of obtaining subsidiary maxima centred at $\theta = 0°$ provided d' is comparable (or greater) in magnitude to b'. No maximum is possible for the situation in sample C1 with model (a) as has already been seen. Furthermore, no maximum is possible for the situation in sample C3 with model (c). This was not found experimentally. Thus weak field examination of the angular dependence again suggests model (b) for the conduction band.

7. DISCUSSION

The investigation shows the existence of a longitudinal magnetoresistance in indium antimonide. It is now necessary to answer the question: is the effect spurious or fundamental and if fundamental what is the mechanism? There are at least four possible causes for the longitudinal effect. These are:

a) anisotropy (consistent with cubic symmetry) in the effective mass or relaxation time,

b) conductivity inhomogeneity,

c) quantum transport,

d) geometrical misalignment.

In the writer's view the order given represents the order of likelihood. Each possibility is now discussed in turn.

7.1 Effective Mass or Relaxation Time Anisotropy

The experimental results, without giving any really clear cut evidence of anisotropy in the longitudinal magnetoresistance, do tend to support a model for the conduction band consisting of spherical energy surfaces at the centre of the reduced zone with the possibility of oblate spheroidal surfaces along $\langle 110 \rangle$ directions. To account for the magnitude and isotropy of the transverse magnetoresistance and the isotropy of cyclotron resonance, it must be supposed that most of the electrons reside in the central minimum, with the $\langle 110 \rangle$ minima at a slightly higher energy so as to be only partly populated.

However, according to Parmenter (1955) energy band minima (or maxima) along <110> directions are theoretically not possible for a zinc blende structure. If this is really so, the above model must be rejected in favour of the one with <111> subsidiary minima or alternatively to assume anisotropy in the relaxation time rather than the effective mass. The latter idea seems the more attractive and it could be supposed that the relaxation time has maximum values along <110> directions. This would seem to be equivalent to having the conductivity compounded from an array of conductivity tensors whose principal axes lie along <110> directions. Such a model might not be unrelated to the fact that cleavage occurs along {110} planes. These are electrically neutral planes containing equal numbers of indium and antimony atoms. One could readily understand if the conductivity were smaller normal to cleavage planes than at right angles to them; isotropy of the zero field conductivity would still presumably be maintained in such a situation. The anisotropy trend in the experimental longitudinal magnetoresistance such as it is, however, points to a conductivity greater parallel to a <110> direction than transverse to it.

The transverse room temperature magnetoresistance is mostly due to mixed conduction. This fact may help to explain the isotropy of the transverse effect; it also suggests that the longitudinal effect could be due to holes and valence band properties. The p-type sample B3, intrinsic at room temperature, does indeed show the largest longitudinal magnetoresistance. While this may be true at room temperature, it has been shown that

intrinsic holes do not contribute anything in the n-type material at liquid air temperature so that here the magnetoresistance effect is characteristic of the conduction band alone. The central subsidiary maxima observed in the C samples lend support to the ideas discussed above for the conduction band. The fact that the A samples do not show such maxima may be due to the higher impurity concentration in these samples.

7.2 Inhomogeneity Effects

The most noticeable features of the angular dependence experimental results on the A samples are inhomogeneity effects. These may have been due to the gradient of extrinsic carriers along the sample axes which were apparent from the Hall effect measurements at liquid air temperature. Bate and Beer (1961) have considered the influence of such a gradient on the transverse magnetoresistance with two different probe orientations. They did not, however, consider the influence on the longitudinal magnetoresistance. It seems that the negative effects could result from conductivity inhomogeneity. The two pairs of probes on either side of the sample could be in contact with regions of different conductivity. Any difference of magnetoresistance between regions would cause a redistribution of current when the magnetic field is present. It is possible to think of simple models for the inhomogeneity where such a redistribution of current could lead to increases of potential gradient in some regions of the sample and to decreases in other parts; if probes were present such changes would be interpreted as apparent positive and negative magneto-

resistance effects. The type of "see-saw" effect (see 5.41(c)) observed on the A samples wherein the two pairs of probes gave effects of opposite sign, could possibly be explained along such lines.

Inhomogeneity effects were less in evidence in the C samples showing no "see-saw" effect and no negative magneto-resistance at room temperature. This was due, no doubt, to the absence of an extrinsic carrier concentration gradient. Therefore, it is assumed that the subsidiary minima observed at liquid nitrogen temperature are not due to inhomogeneity effects. It is significant that the effects did not occur in the more inhomogeneous A samples. The asymmetry in the angular variation at liquid nitrogen temperature for the C samples cannot, however, be fundamental. A regular asymmetry in the results for sample C3 might have been acceptable since in a $\{110\}$ plane a $\langle 111 \rangle$ direction is not an axis of two-fold symmetry like $\langle 110 \rangle$ and $\langle 100 \rangle$ directions but such was not observed. Therefore despite the other indications some inhomogeneity would seem to be present. Some of the asymmetry may be due to a mixing up of Hall effect and magnetoresistance. The method of separating the two effects by magnetic field reversal may be invalid in inhomogeneous material where a Hall effect might arise depending on an even power of H and a magnetoresistance on an odd power.

Bate, Bell and Beer (1961) found that in samples containing abrupt changes of conductivity, the Hall coefficient field dependence showed large anomalies and the transverse magneto-

resistance could be negative. No such anomalies were found in the present measurements so that while the A and B crystal samples contained concentration gradients, they did not contain discontinuities of conductivity. In addition to the above mentioned work, galvanomagnetic effects arising from stratification of conductivity in indium antimonide samples have been discussed by Weiss (1961) using a theoretical treatment due to Herring (1961).

7.3 Quantum Transport

Nonzero longitudinal magnetoresistance can result from a dependence of the relaxation time on magnetic field arising from orbital quantization. As indicated in 2.2 explicit calculations at weak fields are only available for acoustic lattice scattering, which from the apparently small q values would seem not to be entirely applicable in the samples. With a value of $\xi = \frac{\hbar\omega_c}{kT} = 0.2$ for the electrons, corresponding approximately to a field of 5,000 oersted, an effective mass ratio of 0.01 and room temperature, the formula of Omar and Miller equation (20) gives $\frac{\Delta\rho}{\rho_o} = -0.08$. In view of the fact that the experimental results show for the most part a positive longitudinal magnetoresistance, it may be concluded that this mechanism is not the important one. Whether other scattering mechanisms could give a positive effect at weak fields is not known. The quantum treatment has been suggested for explaining the approximately linear field dependence of the transverse effect in n-type material at liquid nitrogen temperature, where at 5,000 oersted, ξ approaches unity. However, the only really definite evidence of Landau quantization effects in the magnetoresistance of indium antimonide has been at liquid helium

temperatures (e.g., Frederikse and Hosler, 1957).

7.4 Sample Misalignment

An important question is whether the nonzero longitudinal magnetoresistance is a result of misalignment of field and sample axes in a vertical plane. Alignment in a horizontal plane is checked by the angular dependence measurements. These show only small deviations in the Hall zeros and in such symmetrical magnetoresistance minima as occur in the C samples at room temperature. Suppose that when θ is set to zero there is still a nonzero angle ϕ between I and H in a vertical plane. A rough estimate of the magnitude of this angle ϕ can be made from the observed variation of magnetoresistance with θ by supposing all the magnetoresistance at the minimum to be due to misalignment. Values of ϕ estimated in this way for the C samples at room temperature in figs.24, 25 and 26, are from 14° to 17°. Such angles are too big to go undetected. Hence it is believed that lack of perfection in aligning the magnetic field to the sample axis is not responsible for the larger part of the observed longitudinal magnetoresistance. Internal misalignment is another matter, although even here the small Hall zero deviation angles suggest that the current flows, for the most part, parallel to the axis of the sample. Furthermore, the field variation of the longitudinal magnetoresistance has, in general, a somewhat different character from the transverse effect.

An effect thought to be due to misalignment was found in the angular dependence measurements on sample C1$_a$ at 77°K. At $\theta = -20°$, it was found that the potential difference between one

pair of conductivity probes was negative with the magnetic field on in one direction but had a normal positive potential difference with the field reversed. This apparent reversal of current near the probes in the first case could be explained as an inhomogeneity effect and in fact a similar effect was observed by Bate, Bell and Beer (1961) in a sample containing an abrupt conductivity change. However, in the present case the relative uniformity of the sample indicates that a more likely explanation could arise from the axis of rotation of the electromagnet not being exactly at right angles to the sample plane containing the probes. In this situation if the probes were not exactly in line with the sample axis, the magnetic field would be able to "see" a component of current between the conductivity probe pairs, and as a result a Hall voltage could be developed between them. If this voltage is sufficiently large and negative, it could exceed the normal conductivity voltage and give a resultant negative potential difference. In other words, the effect was due to a large inclination of the equipotentials across the "thickness" of the sample. Not enough information is available for estimating the angular deviation of the sample causing this effect.

For completeness, it should be mentioned that, besides inhomogeneity and misalignment, spurious effects could also arise from surface conduction and contamination and from the small but finite area of the potential probe contacts. However, there is no indication that such influences were important in the samples investigated.

The trends reported in this part of the thesis will have to be studied further before their certainty can be established. While further work on p-type material could be undertaken with profit, it seems that at the present moment there is little point, from a fundamental aspect, in repeating the work on n-type samples unless these are of extreme uniformity and purity. These two requirements for the material do not necessarily go together. Uniformity is required to avoid spurious effects and purity is required to reduce or even eliminate the impurity band which may be masking fundamental properties of the conduction band.

P A R T II

HIGH FIELD

TRANSVERSE MAGNETORESISTANCE

MEASUREMENTS

8. PRELIMINARY SURVEY FOR PART II

The technique of obtaining high transient magnetic fields by capacitor discharge through a solenoid offers the possibility of measuring galvanomagnetic effects in semiconductors in a field range never yet investigated. Indium antimonide, apart from its brittleness, is an excellent material for study, particularly because the magnetoresistance effect in it is so large. Some high field studies on the material have already been made but these have mostly been below room temperature.

Busch, Kern and Lüthi (1957) made transverse measurements on n-type material up to 100 kilo-oersted from 4.2° to 80°K and found oscillatory effects at the lowest temperatures. Haslett and Love (1959) made measurements of longitudinal magnetoresistance up to 170 kilo-oersted at 3.9°, 14° and 78°K and observed large resistance changes but no oscillations with field variation. Measurements at 77°K were carried out by Amirkhanov, Bashirov and Zakiev (1960) up to about 500 kilo-oersted for longitudinal magnetoresistance and up to 900 kilo-oersted for the transverse case but no oscillatory effects were found. These workers examined one of their samples (No. 2 with $N_D - N_A = 10^{16}$ cm^{-3}) up to room temperature where it had a transverse magnetoresistance of about 9. The only other transverse measurements reported at room temperature were obtained by Haslett (1959) who found the magnetoresistance to have an approximately quadratic dependence on field and at 170 kilo-oersted to have a value approaching 120.

In the present investigations, transverse magnetoresistance at room temperature was measured up to 300 kilo-oersted in intrinsic indium antimonide and extrinsic indium arsenide. For the possible observation of effects arising from the discreteness of the Landau levels it might have been better to have used degenerate extrinsic indium antimonide since in such material the Fermi level is sharply defined and conduction is predominantly by the electrons. However, it appears that heavily doped material presently available suffers from being very inhomogeneous and so measurements on it might have been of doubtful value. Because of difficulties of alignment of magnetic field and sample axis in the high field solenoids, longitudinal magnetoresistance was not measured. Hence, hereafter whenever the word magnetoresistance occurs by itself it is understood to mean transverse magnetoresistance.

A new feature of the present measurements is that they were carried out in a field range which has for the most part not previously been investigated. A more important feature however is that the measured variation with field was subjected to a quantitative comparison with theory arising from the knowledge of the conduction parameters of the individual samples investigated.

9. THEORY FOR ISOTROPIC SEMICONDUCTORS

This section contains the theory of the transverse magnetoresistance in an isotropic nondegenerate semiconductor specially pertinent at high magnetic fields. It deals primarily with the classical two band conduction model but results for a single band quantum treatment are also given.

9.1 Classical Two Band Theory

As mentioned in 2.11 transverse magnetoresistance in a single band of electrons only appears if $q \neq 0$ (where the scattering relaxation time $\tau \propto \varepsilon^q$); when $\mu_n H >> 1$ it saturates at a value equal to $\frac{1}{\alpha} - 1$. If q is of the order of unity, positive or negative, as occurs for many scattering mechanisms, figure 2 shows that $\frac{1}{\alpha} - 1$ is also of the order of unity. Hence in such a case the increase of resistance at very high fields would be expected to be of the order of the zero field resistivity ρ_o itself. When two systems of carriers are present, such as electrons and holes however, the magnetoresistance can be very much larger due to the Lorentz force being able to exert a greater effect on the carriers. This comes about because of a reduction in the transverse Hall field. Equilibrium can be maintained by separate but equal transverse current components of the holes and electrons flowing in opposite directions across the sample. Formal treatment by the Lorentz theory of conduction (see Wilson, 1953) in the notation of Champness (1957) gives for the two carrier case of electrons and holes:

$$\frac{\Delta\rho}{\rho_o} = \frac{(n\mu_n X_n + p\mu_p X_p)(n\mu_n + p\mu_p)}{(n\mu_n X_n + p\mu_p X_p)^2 + H^2(n\mu_n{}^2 Y_n - p\mu_p{}^2 Y_p)^2} - 1 \quad , \quad \ldots\ (21)$$

where

$$X_n = \frac{1}{(q+\frac{3}{2})!}\int_0^\infty \eta^{\frac{3}{2}+q} e^{-\eta}\left[\frac{q\pi}{16}\left(\frac{\mu_n H}{(q+\frac{3}{2})!}\right)^2 \eta^{2q} + 1\right]^{-1} d\eta \quad , \quad \ldots\ (22)$$

$$X_p = X(\mu_p) \quad , \quad \ldots\ (23)$$

$$Y_n = \frac{3\pi^{\frac{1}{2}}}{4[(q+\frac{3}{2})!]^2}\int_0^\infty \eta^{\frac{3}{2}+q} e^{-\eta}\left[\frac{q\pi}{16}\left(\frac{\mu_n H}{(q+\frac{3}{2})!}\right)^2 \eta^{2q} + 1\right]^{-1} d\eta \quad \ldots\ (24)$$

and

$$Y_p = Y(\mu_p) \quad . \quad \ldots\ (25)$$

9.11 Energy Independent Relaxation Time

Great simplification results if it is assumed that the relaxation time is independent of energy by putting q = 0. The integrals (22), (23), 24) and (25) then reduce to

$$X_n = Y_n = \left[1 + (\mu_n H)^2\right]^{-1} \quad \ldots\ (26)$$

and

$$X_p = Y_p = \left[1 + (\mu_p H)^2\right]^{-1} \quad \ldots\ (27)$$

Substituting these into equation (21) gives after some algebraic rearrangement

$$\frac{\Delta\rho}{\rho_o} = \frac{np\mu_n\mu_p H^2(\mu_n + \mu_p)^2}{(n\mu_n + p\mu_p)^2 + H^2\mu_n^2\mu_p^2(n-p)^2} \quad \ldots\ (28)$$

This equation holds, under the assumptions made, at all fields from weak ($H \ll \frac{1}{\mu_n}, \frac{1}{\mu_p}$) to strong ($H \gg \frac{1}{\mu_n}, \frac{1}{\mu_p}$). It can also be derived in an elementary way without the use of Lorentz conduction theory by treating the motion of the electrons and holes under the influence of electric and magnetic fields, supposing only that the drift velocities are proportional to the applied fields through the mobilities μ_n and μ_p. The formula corresponds to that of MacDonald and Sarginson (1952) where relaxation times rather than mobilities were used.

If $$\mu_n^2\mu_p^2 H^2 \gg \left(\frac{n\mu_n + p\mu_p}{n-p}\right)^2 , \quad \ldots\ (29)$$

equation (28) shows that the magnetoresistance saturates to obtain

$$\left(\frac{\Delta\rho}{\rho_o}\right)_{sat} = \frac{np(\mu_n+\mu_p)^2}{(n-p)^2\mu_n\mu_p} \qquad \ldots\ (30)$$

With inequality (29) reversed, the magnetoresistance well below saturation from equation (28) is given by

$$\frac{\Delta\rho}{\rho_o} = \mu_n\mu_p\, np\left(\frac{\mu_n+\mu_p}{n\mu_n+p\mu_p}\right)^2 H^2 \qquad \ldots\ (31)$$

Thus below saturation a quadratic field dependence holds down to the smallest fields.

In an intrinsic semiconductor where $n \gg n-p$, equation (31) becomes

$$\frac{\Delta\rho}{\rho_o} = \mu_n\mu_p H^2 \qquad \ldots\ (31A)$$

and the saturation magnetoresistance (equation (30)) can be extremely large.

In an extrinsic semiconductor where $n \gg p$, if also $\mu_n \gg \mu_p$ (which is approximately true in indium antimonide and indium arsenide), the saturation magnetoresistance is just

$$\left(\frac{\Delta\rho}{\rho_o}\right)_{sat} = \frac{p}{n}\frac{\mu_n}{\mu_p} \qquad \ldots\ (30A)$$

which from inequality (29) occurs when $\mu_p H \gg 1$. This is the same condition as for magnetoresistance saturation of the lowest mobility carriers by themselves. When $\mu_p H \ll 1$, equation (31) gives

$$\frac{\Delta\rho}{\rho_o} = \frac{p}{n}\mu_n\mu_p H^2 \qquad \ldots\ (31B)$$

9.12 Energy Dependent Relaxation Time

If $q \neq 0$ the integrals (22), (23), (24) and (25) have, in general, to be computed. For acoustic lattice scattering in which $q = -\frac{1}{2}$, $X = K$ and $Y = \frac{3\pi L}{8}$ where K and L are expressable in terms of tabulated functions (Willardson, Harman and Beer, 1954). However, some simplification occurs at high fields. If

$$\mu_n H >> 1 \quad \ldots\ (32)$$

and

$$\mu_p H >> 1 \ , \quad \ldots\ (33)$$

then integrals (22), (23), (24) and (25) become

$$X_n = \frac{1}{\alpha} \frac{1}{(\mu_n H)^2} \quad \ldots\ (34)$$

$$X_p = \frac{1}{\alpha} \frac{1}{(\mu_p H)^2} \quad \ldots\ (35)$$

$$Y_n = \frac{1}{(\mu_n H)^2} \quad \ldots\ (36)$$

$$Y_p = \frac{1}{(\mu_p H)^2} \quad \ldots\ (37)$$

Substitution into equation (21) gives

$$\frac{\Delta\rho}{\rho_0} = \frac{\frac{1}{\alpha}\left(\frac{n}{\mu_n} + \frac{p}{\mu_p}\right)(n\mu_n + p\mu_p)H^2}{\frac{1}{\alpha^2}\left(\frac{n}{\mu_n} + \frac{p}{\mu_p}\right)^2 + H^2(n-p)^2} - 1 \quad \ldots\ (38)$$

The condition corresponding to inequality (29) requires in general a stronger field than conditions (32) and (33). This enables us to obtain expressions from equation (38) not only for the magnetoresistance at saturation but also for the approach to saturation in the case of a near intrinsic semiconductor.

(a) Saturation Region. If the following inequality holds (note the difference from (29))

$$\alpha^2 \mu_n^2 \mu_p^2 H^2 \gg \left(\frac{n\mu_p + p\mu_n}{n-p} \right)^2 , \qquad \text{.... (39)}$$

equation (38) shows that the magnetoresistance attains a saturation value

$$\left(\frac{\Delta\rho}{\rho_o} \right)_{sat} = \frac{(n\mu_p + p\mu_n)(n\mu_n + p\mu_p)}{\alpha \mu_n \mu_p (n-p)^2} - 1 , \qquad \text{.... (40)}$$

which after some algebraic manipulation becomes

$$\left(\frac{\Delta\rho}{\rho_o} \right)_{sat.} = \frac{np}{\alpha(n-p)^2} \frac{(\mu_n + \mu_p)^2}{\mu_n \mu_p} + \frac{1-\alpha}{\alpha} . \qquad \text{.... (41)}$$

The second term on the right hand side is just the saturation magnetoresistance for a single band $\left(\frac{\Delta\rho}{\rho_o} \right)_{\text{sat. 1 band}}$ so that equation (41) can be written as

$$\left(\frac{\Delta\rho}{\rho_o} \right)_{sat.} = \left(\frac{\Delta\rho}{\rho_o} \right)_{\substack{sat. \\ 2 \text{ band}}} + \left(\frac{\Delta\rho}{\rho_o} \right)_{\substack{sat. \\ 1 \text{ band}}} \qquad \text{.... (41A)}$$

If $q = 0$ then $\alpha = 1$ and equation (41) is identical with equation (30). In an intrinsic semiconductor $n \gg n-p$, $\left(\frac{\Delta\rho}{\rho_o} \right)_{\text{sat 1 band}}$ would be negligible compared with $\left(\frac{\Delta\rho}{\rho_o} \right)_{\substack{sat. \\ 2 \text{ band}}}$ and therefore

$$\left(\frac{\Delta\rho}{\rho_o} \right)_{sat.} = \frac{1}{\alpha} \left(\frac{n}{n-p} \right)^2 \frac{(\mu_n + \mu_p)^2}{\mu_n \mu_p} . \qquad \text{.... (41B)}$$

If $\mu_n / \mu_p \gg 1$ this is just

$$\left(\frac{\Delta\rho}{\rho_o} \right)_{sat.} = \frac{1}{\alpha} \left(\frac{n}{n-p} \right)^2 \frac{\mu_n}{\mu_p} \qquad \text{.... (41C)}$$

To see the magnitude of the effect suppose $\alpha = 1$, $\mu_n = 6.5 \times 10^{-4}$ gauss^{-1}, $\mu_p = 7.5 \times 10^{-6}$ gauss^{-1}, $n = 1.89 \times 10^{16}$ cm^{-3} and $p = 1.54 \times 10^{16}$ cm^{-3}. The saturation magnetoresistance is then about 2,500, which from inequality (39) occurs approximately when H is much greater than 10^6 oersted. For an extrinsic semiconductor $n \gg p$, and with $\mu_n \gg \mu_p$ it follows that

$$\left(\frac{\Delta\rho}{\rho_o}\right)_{sat} = \frac{1}{\alpha}\,\frac{p}{n}\,\frac{\mu_n}{\mu_p} + \frac{1-\alpha}{\alpha} \quad ; \qquad \ldots\ldots (41\,D)$$

which according to inequality (39) holds if

$$\alpha\mu_p H \gg \frac{\mu_p}{\mu_n} + \frac{p}{n}$$

Since $\frac{\mu_p}{\mu_n}, \frac{p}{n} < 1$ and $\alpha \sim 1$, the above condition is necessarily true by condition (33) for the holes.

Taking $\alpha = 1$, $n = 5.85 \times 10^{16}$ cm^{-3}, $p = 6.9 \times 10^{15}$ cm^{-3}, $\mu_n = 1.69 \times 10^{-4}$ gauss^{-1} and $\mu_p = 4.6 \times 10^{-6}$ gauss^{-1}, the extrinsic saturation magnetoresistance from equation (41D) is found to be about 4.3. It is thus smaller than in an intrinsic semiconductor. However, it is still likely to be larger than in single band saturation where for examole with $q = -\frac{1}{2}$,

$$\left(\frac{\Delta\rho}{\rho_o}\right)_{\substack{sat \\ 1\,band}} = \frac{\alpha - 1}{\alpha} \simeq 0.13 \quad .$$

(b) Presaturation Region. It has just been shown that for an extrinsic semiconductor the condition $\mu_p H \gg 1$ for the high field approximation also ensures saturation. Therefore equations (35) and (37) and hence (38) are invalid below saturation and

an equation corresponding to (31B) cannot readily be found. However, this state of affairs does not prevail for an intrinsic semiconductor.

Suppose that inequalities (32) and (33) hold and also that (if possible)

$$\alpha^2 \mu_n^2 \mu_p^2 H^2 \ll \left(\frac{n\mu_p + p\mu_n}{n-p}\right)^2 \qquad \ldots\ (42)$$

Since usually $\mu_n > \mu_p$, the condition (33) that $\mu_p H \gg 1$ is more stringent than condition (32), $\mu_n H \gg 1$. Combining (33) with condition (42) gives

$$1 \ll \mu_p H \ll \frac{n}{\alpha(n-p)} \frac{\mu_p}{\mu_n} + \frac{p}{\alpha(n-p)}$$

This means that inequality (42) is only possible if $p \gg n-p$ (assuming α is near unity) i.e. for an intrinsic semiconductor.

Proceeding now to apply inequality (42) to equation (38) this yields

$$\frac{\Delta\rho}{\rho_o} = \alpha \mu_n \mu_p \frac{n\mu_n + p\mu_p}{n\mu_p + p\mu_n} H^2 - 1 \qquad \ldots\ (43)$$

which apart from the -1 term indicates a quadratic field dependence. In any case because of inequalities (32) and (33) $\mu_n \mu_p H^2 \gg 1$ so that with only small error

$$\frac{\Delta\rho}{\rho_o} = \alpha \mu_n \mu_p \frac{n\mu_n + p\mu_p}{n\mu_p + p\mu_n} H^2 \qquad \ldots\ (43A)$$

In an intrinsic semiconductor $n = p$ and then it becomes simply

$$\frac{\Delta\rho}{\rho_o} = \alpha \mu_n \mu_p H^2 - 1 \qquad \ldots\ (43B)$$

or with sufficient accuracy

$$\frac{\Delta\rho}{\rho_o} = \alpha \mu_n \mu_p H^2 \qquad \ldots\ (43C)$$

Another way of expressing condition (42) using equations (40) and (43) is seen to be just

$$\left(\frac{\Delta\rho}{\rho_o}\right)_{\text{non sat}} \ll \left(\frac{\Delta\rho}{\rho_o}\right)_{\text{sat}}, \text{ as might be expected.}$$

Summarizing the previous analysis it may thus be said that the approach to saturation would be expected to have a quadratic field dependence for (a) an intrinsic semiconductor at fields above $1/\mu_p$ and (b) for any semiconductor and any fields sufficiently below saturation provided $q = 0$.

At weak fields when $\mu_n H$, $\mu_p H \ll 1$, equation (21) for an intrinsic semiconductor can be shown to lead to

$$\frac{\Delta\rho}{\rho_o} = s\mu_n^2 H^2 + (r^2 - s)\mu_n \mu_p H^2 , \qquad \ldots\ (44)$$

which is just the single band magnetoresistance plus a two band term. The two band term involves the familiar $\mu_n \mu_p H^2$ product which occurs at higher fields.

9.2 Quantum Treatment

A quantum mechanical treatment of the transverse magnetoresistance of a single band of electrons at high fields leads to monotonic increases with no saturation. Adams and

Holstein (1959) have worked out field and temperature dependencies for the transverse resistivity ρ_T in the so-called extreme quantum limit when all the electrons are in the lowest Landau quantum level. Thus occurs for a semiconductor when $\xi = \frac{\hbar\omega_c}{kT} \gg 1$. Omitting the dependence on temperature, the approximate field dependence results for the various scattering mechanisms considered by Adams and Holstein are reproduced below in table IX.

TABLE IX

Scattering Mechanism	Magnetic Field Dependence of ρ_T
Low temp. acoustical	$H^{5/2}$
High temp. acoustical	H^2
Point defect	H^2
Low temp. piezoelectric	$H^{3/2}$
High temp. piezoelectric	H
High temp. optical	H
Ionized impurity	H^0

The table shows that only with ionized impurity scattering would saturation be at all possible. An extension to two bands can be done formally but the detailed implications have not yet been worked out. However, in general, it might be expected that the variations would be superimposed on the classical two band effect. Thus where two-carrier saturation would be expected to take place, the fields would be well into the quantum regime and either no saturation, or only a tendency to saturate, would occur. However, the magnitude of the classical two band

magnetoresistance is so large at high fields, even before saturation, that Landau quantization effects would have to be large to show up clearly. No oscillation component would be expected in the field variation unless the material was degenerate enough so that $\zeta/kT \gg 1$ (in addition to the requirement of $\hbar\omega_c \gg kT$) . This condition is not readily met at room temperature and was in fact not met in the samples used in the experiments described in the following sections.

For the electrons in indium antimonide, $\xi = 1$ in a field of about 25 kilo-oersted at room temperature whereas for the holes, the field required for the same condition is about 500 kilo-oersted. Thus any quantum effects which occur up to fields presently attainable in the laboratory would be likely to be due to the electrons rather than the holes.

10. EXPERIMENTAL METHOD

10.1 Experimental Techniques

10.11 Arrangement

Measurements of transverse magnetoresistance were made on five indium antimonide and two indium arsenide samples. Four of the indium antimonide samples were n-type (A2, A3, C1b and C3) and one p-type (B3) but at room temperature all were practically intrinsic. The two indium arsenide samples (X1 and X3) were n-type and still extrinsic at room temperature. Details of crystals and samples are discussed in part I and their properties summarized in tables III to VII.

The measurements were made by charging up a 2,000 μF bank of capacitors to a definite voltage and discharging through a high field solenoid containing the sample. The probe holders for the samples were the same as those used for the medium field measurements except that in each case the sample and probes were embedded in epoxy resin. This was to minimize the effect of mechanical disturbance during the discharges, since in earlier experiments before encapsulation was tried, the sample had been shaken out of the holder. The sample in the holder was transverse to the solenoid axis so that the magnetic field was normal to the two sample faces carrying the probe wires. In this respect it differed from the transverse orientation in the medium field work where the magnetic field was in the plane of these faces.

The magnetoresistance was measured by observing the potential change on one or other of the two pairs of probes

with a type 551 Tektronix dual beam oscilloscope and type D pre-amplifiers (figure 33 shows the circuit arrangement). The traces were photographed with an attached type 1245 Beattie Oscillotron-Polaroid camera. Current through the sample was maintained normally at 30 mA supplied from a constant current source consisting of 0 - 400 V D.C. power supply with series rheostats. A reversing switch was also included in the current circuit. Plots of the variation of the zero field probe potential difference were made on all the samples from 0 to 50 mA. In all cases the variation with current was linear indicating that no appreciable joule heating of the sample was taking place.

The capacitor bank could be charged to any desired voltage up to a maximum of 3,000 volts, although in the present measurements 1,800 volts was the largest voltage employed. Reversal of the initial current, and therefore the magnetic field in the solenoid, was done by opposite charging of the condenser bank.

10.12 Stray Electromagnetic Pickup

In the initial stages of the work one of the biggest problems was the very large stray pickup voltage which appeared between the sample probes. This was due to e.m.f's induced by the changing magnetic field in stray loops in the probe circuit despite the efforts made in making the holder to minimize this possibility. The oscilloscope trace of the pickup voltage showed it to be the differential coefficient of the field trace. While it was repeatable from one discharge to another at the same condenser voltage, it was often one or two orders of

magnitude larger than the magnetoresistance voltage changes, at least with small sample currents of around 30 mA.

The first attempt to buck out the pickup voltage using a many turn coil located just outside the solenoid was unsuccessful. Neither by axially moving the compensating coil or using it with a potentiometer was it possible to balance out sufficiently the unwanted voltage due apparently to differences of wave form and phase. However success was obtained with a bucking out coil located inside the solenoid near the centre. This coil consisted of two turns of fine wire wound on the sample holder near the sample itself, cemented in position and connected to an external low resistance potentiometer to give an adjustable opposing emf in the probe circuit. By making a number of low voltage discharges and observing the oscilloscope, the potentiometer was adjusted until as near balance as possible was obtained, progressively increasing the oscilloscope sensitivity in the process. Any remaining pickup signal after this was small and could in any case be clearly distinguished from the magnetoresistance effect by its nondependence on sample current.

10.2 High Field Solenoid

The high field solenoid used was similar in design to that employed by Foner and Kolm (1956). It consisted of a ten turn helix with an inner diameter of 3/8 inch and an outer diameter of 1½ inches turned out of a solid rod of Berylco 25, each turn being about 1/16 inch in thickness. Before use the helix was heat-treated for maximum hardness. The turns were insulated from each other by discs of impregnated teflon and

the helix was compressed between end plates of brass and steel by means of six insulated bolts. The outer diameter of the helix was embedded in Sauereisen cement and left to harden. A few turns of copper wire were wound in the Sauereisen to restrict its violent breakup in the event of deformation or explosion of the solenoid. More details of the solenoids and the care necessary in their construction are given by Stevenson (1961).

The measurements were carried out mostly in one solenoid (No. 1) which, however, fractured eventually in an 1,800 volt discharge. After this, another similar solenoid (No. 2) was used. The breakage in solenoid No. 1 occurred after many discharges at lower voltages and appeared to be due to excessive heat developed at a particular point where perhaps some non-uniformity existed. The fracture split the solenoid into two parts with no swelling or other evidence of distortion. Solenoid No. 2 was used for the measurements on the indium arsenide samples and was only taken up to 1,400 volts. Some internal sparking between turns which first occurred in this solenoid was later prevented by coating the inner surface of the helix with a layer of epoxy resin.

A check on the variation of field along the axis of solenoid No. 2 was made using a pickup coil at different positions during a number of 1,000 volt discharges. The variation of the maximum field with distance is shown in figure 34. While the field changes rapidly along the axis, the variation over the width of the sample (about 1m.m.) at the centre of the solenoid is less than 1%. The field variation in solenoid No. 1 is expected to be somewhat less, since it was longer than solenoid

No. 2. The radial variation was not measured but calculation indicates (Montgomery and Terrell, 1956) that it amounts to a deviation of less than 1% over the inner diameter of the solenoid.

10.3 Magnetic Field Measurement

The magnetic field in the solenoid was measured with a pickup coil connected to the second input of the oscilloscope through an R.C. integrator. The pickup coil consisted of five turns of fine wire wound on a paper tube large enough for the sample holder to pass through and inserted in the solenoid so that the coil encircled the sample at the centre. The magnetic field at any instant was obtained from the height of the oscilloscope trace, knowing the total area-turns of the pickup coil and the time constant of the integrator (1 millisecond). The initial voltage rise from the pickup coil and integrator was used to trigger the two oscilloscope traces (field and probe signals) simultaneously. The field trace showed the usual damped sinusoidal variation with time and had a half period of approximately 100 microseconds. Usually during the measurements the trace sweep speed was set at 20 microseconds per cm. so that only the first two half cycles appeared on the oscilloscope screen as shown in figures 37 and 38.

At the higher discharge voltages, damage was caused to the pickup coils. Above 1,500 volts a coil would start to lose its circular shape and become irregular with a smaller inductive area and thus to give a smaller voltage for a given field. No doubt this distortion was due to the magnetic forces

and the weakness of the paper tube in being unable to withstand them. Unfortunately the size of the solenoid and sample holder used did not permit a coil former of thicker material to be used. Successive destruction resulted in eight pickup coils being used in the measurements. Errors due to distortion were carefully watched for by comparison of one coil with another. Plotting the measured maximum field against discharge voltage as in figures 35 and 36 showed a clear and definite relationship characteristic of the solenoid concerned. So much so in fact that discharge voltage was used to give the maximum field in doubtful cases where distortion had evidently taken place.

10.4 Measurement Procedure

For measuring the magnetoresistance the following experimental routine was adopted. At a given voltage a discharge was made with a sample current of 30 mA. Then another discharge was made at the same voltage with no sample current and finally a third discharge was made with a reverse current of 30 mA. The three discharges were recorded on a single photograph which showed three coincident field traces and three probe signal traces. Next a second photograph was obtained showing three more single traces taken during reversed discharges at the same voltage. Figure 37 shows such a pair of oscilloscope photographs at a discharge voltage of 500 volts and figure 38 shows another pair at 800 volts. The middle zero current trace in each photograph shows the residue of the stray pickup voltage left after the balancing out process. The difference between this curve and the other two is due to stray Hall effect and magnetoresistance.

The stray Hall effect component appearing on the conductivity probes arose probably because the probes were not exactly in line with the sample axis. With the magnetic field normal to the probe carrying sample faces, this can have a larger effect than in the medium field orientation. However, just as in the medium field work, the effect can be eliminated by reversal of the magnetic field. Accordingly at a given field the average voltage difference, between the middle trace and the upper and lower traces, was measured on one of the photographs. Suppose this was $\frac{1}{2}(\Delta V_{I,H} + \Delta V_{-I,H})$. The same measurement was then made at an equal but opposite field on the second photograph to get $\frac{1}{2}(\Delta V_{I,-H} + \Delta V_{-I,-H})$. The magnetoresistance increase was taken as the algebraic average of these two voltages $\frac{1}{4}\left[(\Delta V_{I,H} + \Delta V_{-I,H}) + (\Delta V_{I,-H} + \Delta V_{-I,-H})\right]$ in which only components depending on an even function of H were retained. At the smaller fields in some cases the Hall voltage exceeded that of magnetoresistance but in most cases the magnetoresistance was predominant. To determine the sign of the voltages, it was helpful to identify the same current direction on the two photographs. This was done by making one of the traces thicker using increased spot brilliancy on the oscilloscope during the discharge with current in a certain direction.

The magnetoresistance ratio $\Delta\rho/\rho_o$ was obtained at each field from the ratio of the average probe voltage increase to the steady zero field voltage measured between the probes with a high resistance galvanometer.

11. EXPERIMENTAL RESULTS

Fig.39 shows a pair of photographs for sample C1b taken with 600 volt discharges at a number of sample currents. The change of voltage in the presence of the magnetic field is shown clearly to depend on current. A plot of the maximum voltage increases against sample current (Fig.40) taken from these two photographs and from two others obtained in a second experiment (with a different oscilloscope) shows the relation to be linear. In other words, the observed magnetoresistance effect was independent of sample current at least up to 50 mA. It will be noted in Fig.39 that the thicker traces are uppermost in both photographs and in both half cycles as well indicating that the sign of the probe signal was the same for the two field directions. However, the difference of magnitude on reversal in the trace displacements is due to the presence of a stray Hall voltage.

It might be expected that a single pair of photographs would give magnetoresistance values over a large range of fields below the maximum. However, in practice, only a few values covering less than a decade in magnitude could be obtained with any accuracy at one discharge voltage. Hence to get a sufficiently large range of values it was necessary to obtain photographs at many different discharge voltages. In fact, in the present measurements some 350 photographs were taken on the seven samples, with discharge voltages ranging from 100 to 1,800 volts corresponding to maximum fields of roughly 10^4 to 3×10^5 oersted.

The transverse magnetoresistance plotted against field strength is shown in figs.41, 42, 43, 44 and 45 for the indium antimonide samples, and in figs.46 and 47 for the two indium arsenide samples. The experimental points below 7,000 oersted were taken from the medium field measurements in Part I and appear to line up well with the pulsed field measurements. This shows in particular that the different arrangements of field direction and probes did not produce any significant difference in the magnetoresistance effect. Differences, however, can apparently arise in the two arrangements in samples with axial concentration gradients (Bate and Beer, 1961). The gradients of extrinsic carriers in the samples A2, A3 and B3 (see figs .10, 11, 12 and 13) were thus not important enough at room temperature to cause differences in the transverse magnetoresistance.

Another satisfactory feature of the results is that the magnetoresistance is essentially the same on the two pairs of probes in all the samples except C1b. This sample showed some anomalous values on the upper pair of probes at lower pulsed fields.

Considerable scatter is shown in the pulsed field values at the lower fields where the method is not very accurate. Below about 200 volts in indium antimonide for example the magnetoresistance voltage increases were of the order of millivolts compared with very nearly one volt at the highest fields.

Particulars of the results on the two materials are now given separately.

11.1 Indium Antimonide

The indium antimonide results in figs.41 to 45 are collected together in fig.48 which shows an average line obtained from the experimental points for each sample. The curves show the following features:

1) Very large increases of resistance occur at the highest fields. In sample C1b for example, there appears to be more than a four hundred-fold increase at 300 kilo-oersted.

2) The variation with H is approximately quadratic for all the samples over nearly five decades of resistance change.

3) Although no marked tendency towards saturation is shown at the highest fields, a slight bending over seems to occur in samples A2 and A3.

4) The magnitude of the magnetoresistance does not differ so very much from one sample to another. However, the B3, C3 and C1b samples do have somewhat higher values than the two A samples.

5) The lines for the samples A2 and A3 are nearly coincident showing no anisotropy of the transverse effect up to the highest fields.

6) There is no evidence of oscillations of magnetoresistance with field strength at the higher fields.

Measurement of the slopes of the lines at 10^5 oersted gives field dependencies of $H^{1.8}$ for samples A2, A3 and C3 and $H^{1.96}$ for samples B3 and C1b. The curves for the last two samples bend up slightly at the highest fields. This could have been due to heating up of the solenoid and sample. Some heating of these two samples was apparently taking place because of increases observed in the zero field probe voltages just after each high voltage discharge. Possibly this heating was due to deterioration of the solenoid prior to its final fracture with sample B3. The order in which the measurements were done on the samples in solenoid No.1 was A3, C3, A2, C1b and B3.

The already mentioned anomalously large magnetoresistance on the upper pair of probes of sample C1b was disregarded in drawing the average experimental line in fig.48.

Some room temperature results on a sample 29H obtained by Haslett (1959) are also shown in fig.48. They agree essentially with the present measurements.

11.2 Indium Arsenide

Average lines drawn through the experimental points in figs.46 and 47 are reproduced together in fig.49. The results show the following special features:

1) The magnetoresistance is much smaller than in indium antimonide with approximately a five-fold increase near 300 kilo-oersted.

2) The scatter of the experimental points is larger than in indium antimonide. This is a result of the relative smallness of the effect which is barely detectable at the lower fields with the pulsed technique.

3) The two samples show no significant difference in their field variations except possibly at the highest fields where sample X1 has a higher magnetoresistance than sample X3.

4) At the lowest fields there appears to be a tendency to a quadratic dependence while above this there is gradual curvature of the variation with a suggestion of saturation at the highest fields.

5) No oscillations of magnetoresistance with field variation are apparent.

12. COMPARISON WITH THEORY

To compare the experimental results with theory it is first desirable to calculate the magnetoresistance on the two band classical model from equation (21). The simplest way of doing this is to assume q = 0 and then to use equation (28). This was done and in fig.50 the theoretical variation of magnetoresistance with field is shown for all the samples on which high field measurements were made except C1b (which should be similar to C3). The curves were calculated using room temperature values of n, p and μ_n obtained from the Hall and conductivity data given in table IV, taking p to be n - (N_D -N_A). The quantity N_D -N_A is the difference between the donor and acceptor concentrations and was taken to be equal to the extrinsic carrier concentration at liquid air temperature. The values for μ_p were taken as 7.5×10^2 and 4.6×10^2 cm^2 volt $^{-1}$ sec $^{-1}$ (Hilsum and Rose-Innes, 1961) for indium antimonide and indium arsenide respectively.

As expected from algebraic considerations, the curves exhibit two carrier saturation at the highest fields and a quadratic variation at fields below this. The range of fields used in the measurements is indicated in the figure. It is clear that for the indium antimonide samples the magnetoresistance remains practically quadratic over the whole range and is given approximately by $\mu_n \mu_p H^2$ (equation (31A)). Furthermore, saturation would not be approached with any presently available laboratory high field. For the indium arsenide samples the magnetoresistance in the experimental range is given approximately by $\frac{p}{n} \mu_n \mu_p H^2$ (equation

(31B)) at the lower fields but shows a tendency towards saturation at the higher fields. In this case saturation would seem to be possible at fields near 10^6 oersted. These theoretical lines are shown separately with the corresponding experimental points in figs.41 to 47. The comparison with theory is now treated separately for the two semiconductors.

12.1 Indium Antimonide

Considering the simplicity of the theory the measure of agreement with the theoretical lines over such a large range of magnitudes is remarkable. The best agreement occurs for sample B3. All the samples show deviations from the theoretical curves at the lower fields and in the case of samples A2, A3 and C3 at the higher fields as well.

At the lower fields the experimental points lie slightly above the theoretical lines. This could be due to the magnetoresistance of the electrons alone which should exceed the two carrier effect at low fields if $q \neq 0$. To see how important this is a calculation was made for sample A2 using equation (21) taking $q = -\frac{1}{2}$ (corresponding to acoustic lattice scattering). This value of q was chosen not because it was particularly appropriate, but because the integrals (22), (23), (24) and (25) in this case come out to be expressions involving tabulated functions. Fig.51 shows the resultant magnetoresistance variation together with the appropriate theoretical $q = 0$ curve for sample A2. At small fields, the $q = -\frac{1}{2}$ curve lies higher than the $q = 0$ curve and is characteristic mainly of the conduction band. It shows a

saturation tendency around 5×10^3 oersted where $\mu_n H$ is about 3, after which it merges into the q = 0 curve, crosses below it and finally recrosses it again to saturate at a slightly higher value. Most of these features can be shown from the algebraic treatment of special cases already given. For instance with $q = -\frac{1}{2}$, fig.2 gives s = 0.38 and $\alpha = 0.883$, so that $\frac{\Delta\rho}{\rho_o}$ is equal to 0.38 $(\mu_n H)^2$ at low fields, 0.132 at single carrier saturation, $0.883\ \mu_n\mu_p H^2$ at higher fields and is 1.132 times the corresponding q = 0 value at saturation. The theoretical $q = -\frac{1}{2}$ curve is shown again in fig.41 (broken line) for comparison with the experimental points for sample A2. It is clear that below 10^4 oersted the $q = -\frac{1}{2}$ line gives values which are too high. Hence if single carrier magnetoresistance is responsible for the experimental points being above the q = 0 line, the effective q value must be nearer to 0 than to $-\frac{1}{2}$. In Part I, q was in fact estimated to be between 0 and 0.3. The α value corresponding to q = 0.3 from fig.2 is 0.95 which is sufficiently near unity to explain the agreement of the experimental points with the q = 0 line at the fields just greater than 10^4 oersted.

It is important to realize that the vertical position of the theoretical q = 0 line is particularly dependent on the values chosen for μ_n and μ_p. If the values used were too small it would cause the curve to be lower than it should be. However, considering the constancy of the Hall coefficient with field (from which the mobility was obtained) and the small q value, this is an unlikely possibility so far as μ_n is concerned. The two μ_p values, on the other hand, were not ones measured on the

samples concerned and error could be possible here.

At the higher fields the experimental points fall somewhat below the q = 0 line for samples C3, A2 and A3. The amount by which the theoretical q = $-\frac{1}{2}$ line falls below the q = 0 line for sample A 2 (fig.41) is not sufficient to account for this discrepancy. Hence energy dependent scattering mechanisms and also any possible associated variation of hole mobility with field ($\mu_p H$ approaches unity at 10^5 oersted) can be ruled out as likely causes for the deviation. Another explanation is that two carrier saturation is occurring earlier than expected. This would arise for example if the n - p value used for the calculated curve was too small. However, for sample C3 an error of something like two orders of magnitude in n - p would be required to obtain such an early tendency to saturation. A third and more plausible possibility is that it is due to quantum processes since at 300 kilo-oersted $\xi = \frac{\hbar \omega_c}{kT}$ is about 12.

In fig.52 the average deviation expressed as the ratio $\gamma = \left(\frac{\Delta\rho}{\rho_o}\right)_{exp} \Big/ \left(\frac{\Delta\rho}{\rho_o}\right)_{theor}$ is plotted against field strength for the three samples C3, A2 and A3. The variation is somewhat similar in shape and magnitude in all three cases. This leads to speculation that the deviation might be due to a change of the electron mobility with field arising from quantum effects. In the range of fields concerned the magnetoresistance should be given by equation (43) or more approximately by $\propto \mu_n \mu_p H^2$ (equation (43c)). The last expression may alternatively be written as $\mu_{sn} \mu_p H^2$ where μ_{sn} is the saturation electron mobility equal

to $\propto \mu_n$. Thus the variation of γ could correspond to a variation of μ_{sn} with field. With Landau quantization in mind, a scale in units of $\xi = \frac{\hbar\omega_c}{kT}$ for the electrons is also given in fig.52. If μ_{sn} is taken to be proportional to γ then the resistivity ρ_T of the electrons alone is proportional to $\frac{1}{\gamma}$. Fig.53 shows a double log plot of $\frac{1}{\gamma}$ against H. The slope of the plots indicates that on the average $\frac{1}{\gamma}$ is proportional to $H^{0.4}$. While this field dependence does not correspond with any of those predicted by Adams and Holstein (1959), a mixture of scattering mechanisms could presumably yield the form of dependence observed.

12.2 Indium Arsenide

The theoretical curves assuming q = 0 fall well below the experimental points (figs.46 and 47) in both indium arsenide samples. Nevertheless, the theoretical curve is nearer to the experimental results than would be the case assuming the conduction either to be completely intrinsic or to be due to the conduction band alone. In the latter case for example if a q value of $-\frac{1}{2}$ is assumed, the magnetoresistance at the lowest fields would be more than an order of magnitude larger than the observed values. Therefore the smaller magnetoresistance in the indium arsenide compared with indium antimonide is due, not only to its smaller mobilities, but more particularly to its extrinsic condition. This point regarding extrinsic material is brought out more strongly in the measurements of Amirkhanov, Bashirov and Zakiev (1960) on an indium antimonide sample (No.2) with $N_D - N_A = 10^{16}$ cm $^{-3}$ where the magnetoresistance was found to be only about 9.

The difference between the theoretical curve and the experimental points may be due in part to the use of too small a value of p, the hole concentration. This quantity was obtained from a rather small difference between the electron concentrations at room and liquid air temperatures. An upward displacement of the theoretical curve to produce agreement at the higher fields would therefore not be out of order, particularly for sample X3. Doing this would still leave the theoretical curve below the experimental points at the lower fields. However, this deviation could then be explained by a magnetoresistance contribution from the electrons alone arising from a small but finite q value, probably less than 0.3 (see Part I). With an average electron mobility of 1.7×10^4 cm^2 volt $^{-1}$ sec $^{-1}$ ($= 1.7 \times 10^{-4}$ gauss $^{-1}$) a so-called weak field in the indium arsenide is one less than $\frac{1}{1.7} \times 10^4 \simeq 6{,}000$ oersted. Hence weak field theory would be applicable below this value where a tendency to a quadratic dependence is in fact observed.

It thus seems that while the effective q value is as low as it is in indium antimonide, its effect is much greater in the extrinsic indium arsenide. For comparison with the results at intermediate fields, computed theoretical curves with small q values are therefore necessary, since simplified theoretical treatments such as that in 9.12(b) for $q \neq 0$ do not apply to an extrinsic semiconductor below saturation.

13. DISCUSSION

The treatment in the previous section shows that the classical two band theory accounts well for the observed transverse magnetoresistance in the intrinsic indium antimonide and fairly well in the intrinsic indium arsenide. However, the agreement requires a weak dependence of the relaxation time on energy with a q value probably less than 0.2. Thus in indium antimonide the observed magnetoresistance is almost entirely the result of two carrier conduction. Put another way, the results corroborate the conclusion reached by Weiss (1961) from an analysis of Hall effect measurements at high magnetic fields that the magnetoresistance effects of a single band alone have not yet definitely been detected in indium antimonide at room temperature.

The results and the calculations (particularly in indium arsenide) demonstrate the important role played by the holes in magnetoresistance. It might be thought that in an n - type extrinsic high mobility semiconductor the magnetoresistance would be characteristic of the electrons and would give small saturation values around unity or less. While at very low fields the holes can probably be neglected they have a very profound effect at higher fields, where despite their inferiority in number and mobility, they can enhance the magnetoresistance considerably above that for electrons alone. One is therefore lead to wonder if a two carrier model would not also explain the magnetoresistance in other situations such as in indium antimonide at liquid nitrogen temperature where quantum effects have been suggested to explain

the observed results (Bate, Willardson and Beer, 1959).

The success of the two band model would suggest that high field transverse magnetoresistance could be useful as a tool for determining unknown conduction parameters of semiconductors. In intrinsic material for example μ_p could be determined in the quadratic region if μ_n and α are known and in extrinsic material p can be found if α, n, μ_n and μ_p are known. If the two carrier saturation plateau can be reached and if α, n and μ_n/μ_p are known, then p and hence $n - p = N_D - N_A$ can be determined.

The reasonable agreement with the classical theory is surprizing when looked at from a quantum point of view. At 300 kilo-oersted ξ is about 12 for the electrons at room temperature. The Landau levels thus have a separation of 0.3eV which is greater than the intrinsic energy gap in indium antimonide and the thermal broadening only accounts for $\frac{1}{12}$ of the spacing. A calculation of the collision broadening puts this at only $\frac{1}{200}$ of the spacing between the levels. Why then are quantum effects not more pronounced? The reason is probably connected with the weak energy dependence of the scattering process. For example, any change in the energy of the electrons resulting from quantization would lead apparently to no change in the conductivity if τ were independent of energy. The observed deviation of the experimental results from the q = 0 line at high fields could well be due to Landau quantization effects. It would indeed be interesting if a theoretical treatment using a hypothetical scattering mechanism with a relaxation time proportional to $\varepsilon^{0.2}$ would give a mobility

variation for the electrons proportional to $H^{-0.4}$ as was found experimentally for γ. The quantum explanation however must be regarded with reserve not only because of the slight possibility of earlier saturation being the cause of the deviation but because of the relative inaccuracy of the pulsed field method.

The question of the observed magnetoresistance being a result of spurious effects such as inhomogeneity and short circuiting by the end contacts is now raised. If such effects were present they were either very small or very regular because of the following facts: (a) the relative voltage changes on the two pairs of probes were the same, (b) the magnetoresistance was not very different from one indium antimonide sample to another and (c) the lining up of the medium and pulsed field results was good despite a difference of probe-field orientation. Short circuiting by end electrodes would cause an enhancement of the magnetoresistance and would make the curves bend up rather than down so that this cannot be the cause of the high field deviation already referred to in samples C3, A2 and A3. A slight bending up at the highest fields occurred in samples C1b and B3 as was already mentioned in 11.1.

The possible existence of Landau quantization effects and the examination of the validity of the classical two band theory suggests that work at much higher fields would be worth while on indium antimonide. The use of smaller samples and the further miniturization of the sample holder necessary for insertion in a $\frac{1}{4}$" or even a 3/16" solenoid could probably be done. Heavily doped

degenerate material would be more likely to show up quantum effect oscillations provided such material was uniform and the mobility was not too much reduced. Such measurements could be made at room temperature but work at lower temperatures is likely to be more fruitful.

GENERAL CONCLUSIONS

The main results and conclusions of the whole study may now be summarized. For the medium field work in Part I these may be stated as follows:

(1) In n-type indium antimonide at room and liquid air temperature there is nonzero longitudinal magnetoresistance which is not predominantly due to misalignment of sample and magnetic field.

(2) The possibility that the nonzero longitudinal magnetoresistance is due to inhomogeneity in the electrical properties within the sample cannot be entirely ruled out.

(3) Negative longitudinal magnetoresistance at room and liquid air temperature observed in some samples is almost certainly due to conductivity inhomogeneity.

(4) There are indications of a tendency for the longitudinal magnetoresistance to be greatest in a $\langle 100 \rangle$ direction and least in a $\langle 110 \rangle$ direction. This anisotropic effect is not definite enough to be established with certainty.

(5) At liquid nitrogen temperature, the purer and more uniform C samples all show a subsidiary maximum near $\theta = 0°$ in the magnetoresistance variation with angle θ between I and H.

(6) The anisotropic effect, if it exists, and the subsidiary maxima just mentioned could be accounted for by cubically symmetrical $\langle 110 \rangle$ anisotropy in the electron effective mass or relaxation time.

(7) The transverse magnetoresistance at liquid air temperature shows no definite evidence of anisotropy. This indicates that any deviations from spherical symmetry for the conduction band must be small and the anisotropic effects referred to in (6) can only apply to some of the electrons. Another reason for the transverse isotropy could be the domination of mixed conduction over single band conduction at room temperature.

(8) Small values of the coefficient $\frac{\Delta\rho}{\rho_0 (R_H \sigma_0 H)^2}$ for the transverse effect in n-type material indicate a very weak dependence of the relaxation time τ on energy. It would appear that if $\tau \propto \varepsilon^q$, q lies between 0 and 0.3 in both indium antimonide and indium arsenide. The purer material C gave a smaller q than the more impure material A at liquid air temperature.

(9) The transverse value of $\frac{\Delta\rho}{\rho_0 (R_H \sigma_0 H)^2}$ for the p-type material at liquid air temperature is about a hundred times that for the n-type material. This is due to the presence of light holes.

(10) At liquid air temperature the p-type material has a longitudinal $\frac{\Delta\rho}{\rho_0 (R_H \sigma_0 H)^2}$ value of about a hundred times that

for the n-type samples. It also has the largest ratio of longitudinal to transverse magnetoresistance. This suggests that the longitudinal effect may, like the transverse effect, involve mixed conduction processes.

(11) The available theoretical quantum treatments of longitudinal magnetoresistance at weak fields cannot explain the observed results.

From the high field work in Part II, the following main results and conclusions may be stated:

(12) The transverse magnetoresistance in the indium antimonide and indium arsenide can be largely accounted for by the combined classical motion of electrons and holes over the range 10^3 to 3×10^5 oersted. In particular in the intrinsic indium antimonide the field variation is given approximately by $\mu_n \mu_p H^2$.

(13) Very large magnetoresistance increases of several hundredfold can occur in intrinsic material at high fields while in extrinsic material increases of about an order of magnitude are possible.

(14) In indium antimonide no significant contribution from the electrons (or holes) alone is found down to the lowest fields of 10^3 oersted in agreement with analysis of Weiss (1961). The weak dependence of the scattering processes on energy appears to be the reason for this.

(15) Discrepancies from classical theory appear to occur at the highest fields in indium antimonide. This could be explained by supposing the electron mobility to have a field variation proportional to $H^{-0.4}$ as might arise in quantum transport in a magnetic field. Other explanations for the discrepancy however also exist.

(16) The absence of more pronounced Landau quantization effects on the magnetoresistance is surprizing considering that at 300 kilo-oersted the spacing between adjacent Landau levels is some 12 times kT. The reason for this may be the weak energy dependence of the scattering process and also the preponderance of classical two band conduction.

(17) Spurious influences such as those due to inhomogeneity, end contacts, probes etc. are apparently not responsible for the observed magnetoresistance effects at high fields.

REFERENCES

Abeles, B. and Meiboom, S. 1954. Phys. Rev., 95, 31.

Adams, E. N. and Holstein, T. D. 1959. J. Phys. Chem. Solids, 10, 254.

Allgaier, R. S. 1958. Phys. Rev., 112, 828.

Allred, W. P. and Bate, R. T. 1961. J. Electrochem. Soc. 108, 258.

Amirkhanov, Kh. I., Bashirov, R. I. and Zakiev Yu. E., 1960. Doklady Akademii Nauk SSSR, 132, 793.
[Translation: Soviet Physics - Doklady 5, 556, 1960.]

Appel, J. 1956. Zeit. f. Naturf., 11a, 892.

Argyres, P. N. and Adams, E. N. 1956. Phys. Rev., 104, 900.

Argyres, P. N. 1958. J. Phys. Chem. Solids, 4, 19.

Barrie, R. 1959. Can. J. Phys. 37, 893.

Bate, R. T., Willardson, R. K. and Beer, A. C. 1959. J. Phys. Chem. Solids, 9, 119.

Bate, R. T. and Beer, A. C. 1961. J. App. Phys., 32, 800.

Bate, R. T., Bell, J. C. and Beer A. C. 1961. J. App. Phys. 32, 806.

Broom, R. F. 1958. Proc. Phys. Soc. 71, 500.

Burstein, E., Picus, G. S. and Gebbie, H. A. 1956. Phys. Rev. 103, 825.

Busch, G., Kern, R. and Lüthi, B. 1957. Helv. Phys. Acta, 30, 471.

Champness, C. H. 1957. Metropolitan Vickers Research Report No.5135.

Champness, C. H. 1958a. J. Electronics and Control 4, 201.

Champness, C. H. 1958b. Phys. Rev. Lett., 1, 439.

Conwell, E. M. and Weisskopf V. F. 1946. Phys. Rev. 69, 258; Ibid. 1950. 77, 388.

Dresselhaus, G., Kip, A. F., Kittel, C. and Wagoner, G. 1955. Phys. Rev., 98, 556.

Frederikse, H. P. R. and Hosler, W. R. 1957. Phys. Rev., 108, 1136.

Glicksman, M. 1958. Progress in Semiconductors, 3, 2.

Haslett, J. C. 1959. A.E.C. Report No.4 (Contract AT (11-1)-377), University of Colorado.

Haslett, J. C. and Love, W. F. 1959. J. Phys. Chem. Solids, 8, 518.

Herman, F. 1955. J. Electronics 1, 103.

Herring, C. 1955. Bell Syst. Tech. J. 34, 237.

Herring, C. 1961. J. App. Phys., 31, 395.

Hilsum, C. and Rose-Innes, A. C. 1961. Semiconducting III-V Compounds, (Pergamon Press).

Keyes, R. W. and Sladek, R. J. 1956. J. Phys. Chem. Solids, 1, 143.

Keyes, R. J., Zwerdling, S., Foner, S., Kolm, H. H. and Lax, B. 1956. Phys. Rev., 104, 1804.

Mansfield, R. 1955. J. Electronics, 1, 175.

Miller, S. C. and Omar, M. A. 1961. Phys. Rev., 123, 74.

Parmenter, R. H. 1955. Phys. Rev., 100, 573.

Pearson, G. L. and Suhl, H. 1951. Phys. Rev., 83, 768.

Pearson, G. L. and Tanenbaum, M. 1953. Phys. Rev., 90, 153.

Potter, R. F. 1957. Phys. Rev. 108, 652.

Rupprecht, H., Weber, R. and Weiss, H. 1960. Zeit. f. Naturf. 15a, 783.

Rupprecht, H. 1961. Zeit. f. Naturf. 16a, 395.

Seitz, F. 1950. Phys. Rev., 79, 372.

Shibuya, M. 1954. Phys. Rev., 95, 1385.

Sosniak, J. 1961. Thesis. University of Western Ontario.

Stevenson, R. 1961. Can. J. Phys. 39, 367.

Tanenbaum, M., Pearson, G. L. and Feldman, W. L. 1954. Phys. Rev., 93, 912.

Weiss, H. 1961. J. App. Phys., 32, 2064.

Willardson, R. K., Harman, T. C. and Beer, A. C. 1954. Phys. Rev., 96, 1512.

Wilson, A. H. 1953. The Theory of Metals (Cambridge University Press), Ch.8.

APPENDIX

NONSYSTEMATIC MEASUREMENT ERRORS

Part I Errors

The accuracy of the tabulated figures in Part I as limited by random measurement errors is now discussed. These errors are estimated in general to be as follows.

Hall Coefficient	R_H	$\pm$ 3%		
Conductivity	σ_o	$\pm$ 4%		
Hall Mobility	$R_H \sigma_o$	$\pm$ 5%		
Transverse Magnetoresistance	$\frac{\Delta\rho_\perp}{\rho_o}$	$\pm$ 2%	room temp.	At 5000 Oer.
		$\pm$ 1%	liq. N_2 temp.	
Longitudinal Magnetoresistance	$\frac{\Delta\rho_\parallel}{\rho_o}$	$\pm$ 6%	room temp.	
		$\pm$ 4%	liq. N_2 temp.	
	$\Delta\rho_\perp / [\rho_o (R_H \sigma_o H)^2]$	$\pm$ 11%		
	$\Delta\rho_\parallel / [\rho_o (R_H \sigma_o H)^2]$	$\pm$ 11%		

For R_H and σ_o (and hence $R_H \sigma_o$), the errors in the potentiometer and sample current readings can be neglected in comparison with errors in determining the sample dimensions and the magnetic field H. For example, the Hall voltage, V_H can be measured to within an error of $\pm$ 0.3% which is reduced to $\pm \frac{0.3}{\sqrt{16}}\% \simeq \pm$ 0.1% in averaging over the sixteen readings taken each time; this figure is negligible in comparison with a uniformity error in the sample thickness t of $\pm$ 2% and an error in measuring H of $\pm$ 2.5%. Since R_H is equal to $V_H t/IH$, the error in R_H is therefore given by

$$\frac{\Delta R_H}{R_H} = \pm \sqrt{\left(\frac{\Delta V_H}{V_H}\right)^2 + \left(\frac{\Delta t}{t}\right)^2 + \left(\frac{\Delta I}{I}\right)^2 + \left(\frac{\Delta H}{H}\right)^2}$$

$$= \pm \sqrt{(0.1)^2 + (2)^2 + (0.5)^2 + (2.5)^2}\ \%$$

$$= \pm 3.2\ \%$$

Relative errors in R_H and σ_o measured on the same sample are smaller than the above values.

The errors in the $\Delta\rho/\rho_o$ values arise mainly from the error in measuring the magnetoresistance potential change, which in some cases only amounts to a few microvolts. Averaging over eight or sixteen readings reduces the error by a factor between about three and four. The accuracy is sufficient, at least at the higher fields of around 5000 oersted, to justify the analytical discussion in sections 6 and 7. The largest measurement error occurs in the quantity $\Delta\rho/[\rho_o(R_H\sigma_o H)^2]$ where the main contribution comes from the $(R_H\sigma_o H)^2$ term due to the separate errors in R_H, σ_o and H.

The measurement errors in the longitudinal magnetoresistance are probably smaller than deviations which arise from conductivity inhomogeneity in the samples. For example, a calculation from the formula given by Weiss (1961) can be made of the spurious magnetoresistance effect in a sample containing stratified conductivity variations. This shows that the observed average room temperature longitudinal magnetoresistance could be obtained in such a sample having a 20% conductivity variation from one layer to the next and the plane of the layers inclined at an angle of 20° to the plane normal to the sample axis.

Part II Errors

The high pulsed field magnetoresistance values show a large amount of scatter even though they are plotted against field on logarithmic scales. The scatter is particularly large at the smaller fields. Nonsystematic errors in H can arise from such causes as movement of the sample and the pickup coil in the inhomogeneous solenoid field from one discharge to another, changes in the area of the

pickup coil and to errors associated with measuring the pickup coil voltage on the oscilloscope. These errors altogether could amount to an error in H of between ± 5% and ± 8%. The errors in measuring $\Delta\rho_\perp/\rho_o$ explicitly would arise from noise, drift and trace height measuring errors in the determination of the potential change on the probes using the oscilloscope. This could amount in indium antimonide to an error of about ± 12% at a discharge voltage of 200V, where $\Delta\rho_\perp/\rho_o$ is relatively small, and ± 3% at 1500V. This error in general would be larger than that resulting from angular error in the transverse setting of the sample in the solenoid. Assuming $\Delta\rho_\perp/\rho_o \propto H^2$ approximately, the errors combine to give a total error in $\Delta\rho_\perp/\rho_o$ of about ± 18% at 200V and ± 12% at 1500V in indium antimonide. The former figure is about half and the latter figure about equal to the vertical deviation of the experimental points from the average values.

For indium arsenide the errors arise mainly from the measurement of the small magnetoresistance changes and amount to about ± 50% and ± 10% at 200V and 1500V respectively. This is in rough agreement with the observed vertical scatter about the average values.

TABLE II

LONGITUDINAL MAGNETORESISTANCE

Direction of I & H	Model (a) <100> Spheroids		Model (b) <110> Spheroids		Model (c) <111> Spheroids	
	Weak Field $\frac{\Delta\rho}{\rho_0 (R_H \sigma_0 H)^2}$ $(d' < 0)$	Saturation $\frac{\Delta\rho}{\rho_0}$	Weak Field $\frac{\Delta\rho}{\rho_0 (R_H \sigma_0 H)^2}$ $(d' > 0)$	Saturation $\frac{\Delta\rho}{\rho_0}$	Weak Field $\frac{\Delta\rho}{\rho_0 (R_H \sigma_0 H)^2}$ $(d' > 0)$	Saturation $\frac{\Delta\rho}{\rho_0}$
[100]	0	0	$2d'$	$\frac{(K-1)^2}{K(K+5)}$	d'	$\frac{2(K-1)^2}{9K}$
[110]	$-\frac{d'}{2}$	$\frac{(K-1)^2}{K(K+5)}$	$\frac{3d'}{2}$	$\frac{3(K-1)^2}{K^2+20K+3}$	$\frac{d'}{2}$	$\frac{(K-1)^2}{3K(K+2)}$
[111]	$-\frac{2d'}{3}$	$\frac{2(K-1)^2}{9K}$	$\frac{4d'}{3}$	$\frac{(K-1)^2}{3K(K+2)}$	$\frac{d'}{3}$	$\frac{2(K-1)^2}{3(7K+2)}$

TABLE III

DETAILS OF THE SEMICONDUCTOR CRYSTALS

Material and Crystal Designation	Conductivity Type	Carrier Concentration (cm^{-3}).		Mobilities (cm^2/volt sec)		Doping Material	Direction of Growth	Concentration of Ionized Impurity Centres (estimated from mobilities) (cm^{-3})	Source of Crystal
		Room Temp	Liq. Air or liq. N_2 Temp	Room Temp	Liq. Air or liq. N_2 Temp				
InSb A	n	1.85×10^{16}	2.87×10^{15}	6.4×10^4	9.4×10^4	?	?	10^{16}	Minneapolis Honeywell (T.J. Davies)
InSb B	p	1.69×10^{16} (electrons)	1.87×10^{14} (holes)	6.7×10^4 (electrons)	$\sim 3 \times 10^3$ (holes)	undoped	<111>	10^{16}	Canadian Marconi (M. Gransden)
InSb C	n	1.91×10^{16}	6.65×10^{14}	6.8×10^4	2.7×10^5	T_e	<110>	$10^{15} - 10^{16}$	Lincoln Laboratory (A.J. Strauss)
InAs X	n	5.68×10^{16}	5.21×10^{16}	1.71×10^4	1.91×10^4	?	?	10^{17}	Lincoln Laboratory (A.J. Strauss)

TABLE IV

AVERAGE CONDUCTIVITY AND HALL COEFFICIENT OF THE InSb SAMPLES

Sample	Cond Type	Current Direction	Faces on which probes were placed	Conductivity σ_o (Ω^{-1} cm^{-1})			Hall Coefficient R_H (10^2 cm^3/coulomb)			Magnetic Field for Hall Coeff.		Hall Mobility $R_H\sigma_o$ (10^4 cm^2/volt sec).		
				Room Temp	Liq. Air Temp	Liq. N_2 Temp.	Room Temp	Liq. Air Temp	Liq. N_2 Temp	Strength (oersted)	Direction	Room Temp	Liq. Air Temp	Liq. N_2 Temp
A1a	n	[100]	(001)	164	28		-3.7	-32		4880	[010]	6.1	9.0	
A1b	n	[100]	(001)	196		38	-2.7		24	4350	[010]	5.4		8.9
A2	n	[110]	(001)	199	55		-3.3	-17.9		4880	[1$\bar{1}$0]	6.6	9.9	
			(1$\bar{1}$0)	197	53		-3.3	-17.7		4880	[001]	6.5	9.4	
A3	n	[111]	($\bar{1}$10)	209	53		-3.2	-17.7		4880	[$\bar{1}\bar{1}$2]	6.6	9.4	
B3	p	[111]	($\bar{1}\bar{1}$2)	181	(0.1)		-3.7	+340		4880	[$\bar{1}$10]	6.7	(0.33)	
C1a	n	[100]	(011)	209		32	-3.5		-94	4350	[0$\bar{1}$1]	7.2		30
C2	n	[110]	(1$\bar{1}$0)	189		26	-3.3		-99	4350	[001]	6.3		26
C3	n	[111]	($\bar{1}$10)	227		29	-3.0		-89	4350	[$\bar{1}\bar{1}$2]	6.9		26

Measurement Errors: σ_o ± 4% R_H ± 3% $R_H\sigma_o$ ± 5%

TABLE V

AVERAGE MAGNETORESISTANCE VALUES

Sample	Current Direction	Magnetic Field Strength (oersted)	Transverse Magnetoresistance* $\Delta\rho/\rho_o$			Magnetic Field Direction	Longitudinal Magnetoresistance** $\Delta\rho/\rho_o$		
			Room Temp	Liq. Air Temp	Liq. N_2 Temp		Room Temp	Liq. Air Temp	Liq. N_2 Temp
A1a	[100]	4880	0.116	0.46		[010]	0.028	0.061	
A1b	[100]	4350	0.089		0.41	[010]	0.00		0.058
A2	[110]	4880	0.117	0.51		[1$\bar{1}$0]	0.005	0.01	
			0.110	0.41		[001]	0.008	-0.02	
A3	[111]	4880	0.105	0.30		[11$\bar{2}$]	-0.006	0.008	
B3	[111]	4880	0.149	0.034		[$\bar{1}$10]	0.032	0.0070	
C1a	[100]	4350	0.127		0.74	[01$\bar{1}$]	0.016		0.18
C2	[110]	4350	0.106		0.68	[001]	0.008		0.11
C3	[111]	4350	0.106		0.63	[11$\bar{2}$]	0.014		0.20
Measurement Errors			$\pm$0.002	$\pm$ 0.005 B3 $\pm$ 0.0005			$\pm$ 0.001	$\pm$ 0.001 B3 $\pm$0.0005	C1a, C2, C3 $\pm$ 0.005

* Average values taken at the maxima near $\pm$ 90°.

** Average values taken at the minima except for samples A1b, C1a, C2 and C3 which were taken at θ = 0°.

TABLE VI

CONDUCTIVITY AND GALVANOMAGNETIC DATA
FOR THE N-TYPE InAs SAMPLES

Sample	Current Direction	Face on which probes were placed	Magnetic Field Direction for R_H and Transverse $\frac{\Delta\rho}{\rho_o}$	Temp	Zero Field Conductivity $\sigma_o (\Omega^{-1}cm^{-1})$	Hall Coeff. R_H at 3040 oersteds (cm^3/coulomb)	Hall Mobility $R_H\sigma_o$ (10^4 cm^2/volt sec)	Transverse Magnetoresistance Coefficient $\frac{\Delta\rho}{\rho_o(R_H\sigma_o H)^2}$ at 3040 oersted
InAs X1	[100]	(011)	[0$\bar{1}$1]	Room	154	-110	1.7	1.3×10^{-2}
				Liq. Air	152	-124	1.9	4.2×10^{-2}
InAs X3	[111]	($\bar{1}$10)	[$\bar{1}\bar{1}$2]	Room	156	-110	1.7	1.1×10^{-2}
				Liq. Air	167	-116	1.9	4.6×10^{-2}

Measurement Errors: σ_o ± 4% R_H ± 3% $R_H\sigma_o$ ± 5% $\frac{\Delta\rho}{\rho_o(R_H\sigma_o H)^2}$ ± 10%

TABLE VII

VALUES OF $\frac{\Delta\rho}{\rho_o (R_H \sigma_o H)^2}$

Sample and Current Direction	Magnetic Field Strength (oersted)	TRANVERSE					LONGITUDINAL***			
		Magnetic Field Direction	$\frac{\Delta\rho_t}{\rho_o (R_H \sigma_o H)^2}$				$\frac{\Delta\rho_{\parallel}}{\rho_o (R_H \sigma_o H)^2}$			
			Room Temp	Liq. Air Temp	Liq. N_2 Temp	Weak Field* Theory Coeff.	Room Temp	Liq. Air Temp	Liq. N_2 Temp	Weak Field* Theory Coeff.
A1a [100]	4880 1510	[010]	0.013	0.024		b'	0.0029 0.0055	0.0029 0.0095		$b' + c' + d'$
A1b [100]	6625 1560	[010]	0.015 0.028		0.018 0.047		-0.00026 0.00045		0.0038 0.0073	
A2 [110]	4880	[1$\bar{1}$0]	0.011	0.022		$b' + \frac{d'}{2}$	0.00044	0.00043		
	4880 1260	[001]	0.011 0.014	0.020 0.045		b'	0.0011 0.0012	0.0028 0.0043		$b' + c' + \frac{d'}{2}$
A3 [111]	4880 1260	[$\bar{1}$12]	0.010 0.012	0.014 0.037		$b' + \frac{d'}{3}$	0.0006 0.00041 (1990 oer.)	0.0010 -0.00022		$b' + c' + \frac{d'}{3}$
B3 [111]	4880 1260	[$\bar{1}$10]	0.014 0.018	2.6** 1.3			0.0042 0.0088 (1990 oer.)	0.3** 0.4		
C1a [100]	6625 1560	[011]	0.011 0.017		0.0033 0.011	b'	0.0011 0.0031		0.00052 0.0018	$b' + c' + d'$
C2 [110]	6625 1560	[001]	0.013 0.016		0.0042 0.012	b'	0.00070 0.0023		0.00072 0.00092	$b' + c' + \frac{d'}{2}$
C3 [111]	6625 1560	[$\bar{1}$12]	0.011 0.014		0.0038 0.011	$b' + \frac{d'}{3}$	0.0013 0.0030		0.00080 0.0023	$b' + c' + \frac{d'}{3}$

* See equation (8A)

** Mobility not known accurately

*** Measured at $\theta = 0^\circ$

Measurement error in transverse and longitudinal $\Delta\rho / [\rho_o (R_H \sigma_o H)^2]$ values $\pm$ 10%

TABLE VIII

LONGITUDINAL MAGNETORESISTANCE
[100] : [110] : [111] DIRECTIONAL DEPENDENCE RATIOS

Theoretical

Weak Field $\frac{\Delta\rho}{\rho_o(R_H\sigma_o H)^2}$ ratios			Strong field $\left(\frac{\Delta\rho}{\rho_o}\right)_{sat}$ ratios			K
Model (a)	Model (b)	Model (c)	Model (a)	Model (b)	Model (c)	
0 : 0.75 : 1	1.5 : 1.125 : 1	3 : 1.5 : 1	0 : 0.88 : 1	1.24 : 0.38 : 1	9 : 6.43 : 1	0.1
			0 : 0.82 : 1	1.36 : 0.85 : 1	3.66 : 2.2 : 1	0.5
			0 : 0.64 : 1	1.71 : 1.53 : 1	2.66 : 1 : 1	2
			0 : 0.30 : 1	2.4 : 3.56 : 1	2.4 : 0.30 : 1	10

Experimental

Samples	Magnetic Field (oersted)	$\frac{\Delta\rho}{\rho_o(R_H\sigma_o H)^2}$ ratios	
		Room Temp	Liq. air or N_2 Temp.
A	4880	4.9 : 1.9 : 1	2.8 : 2.7 : 1
	1260	15 : 3.2 : 1	48 : 19 : -1
C	6625	0.86 : 0.55 : 1	0.65 : 0.89 : 1
	1560	1.02 : 0.77 : 1	0.75 : 0.40 : 1

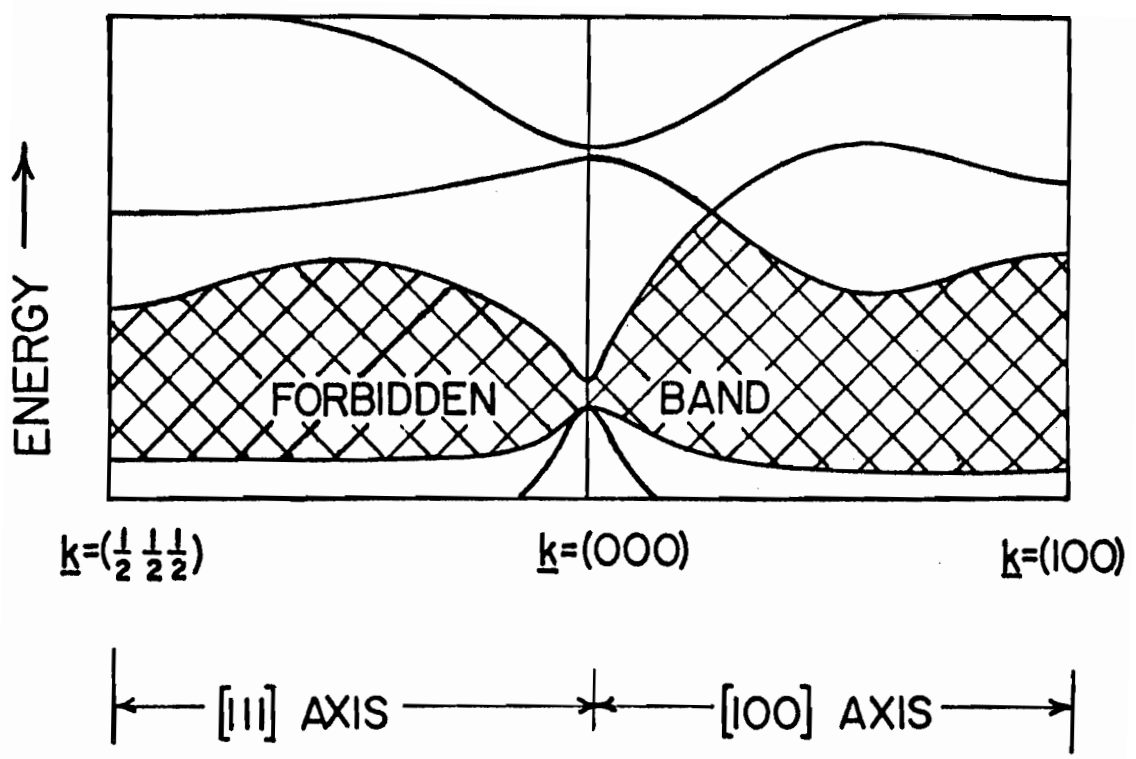

Figure 1 Schematic energy band diagram for indium antimonide (after Herman 1955).

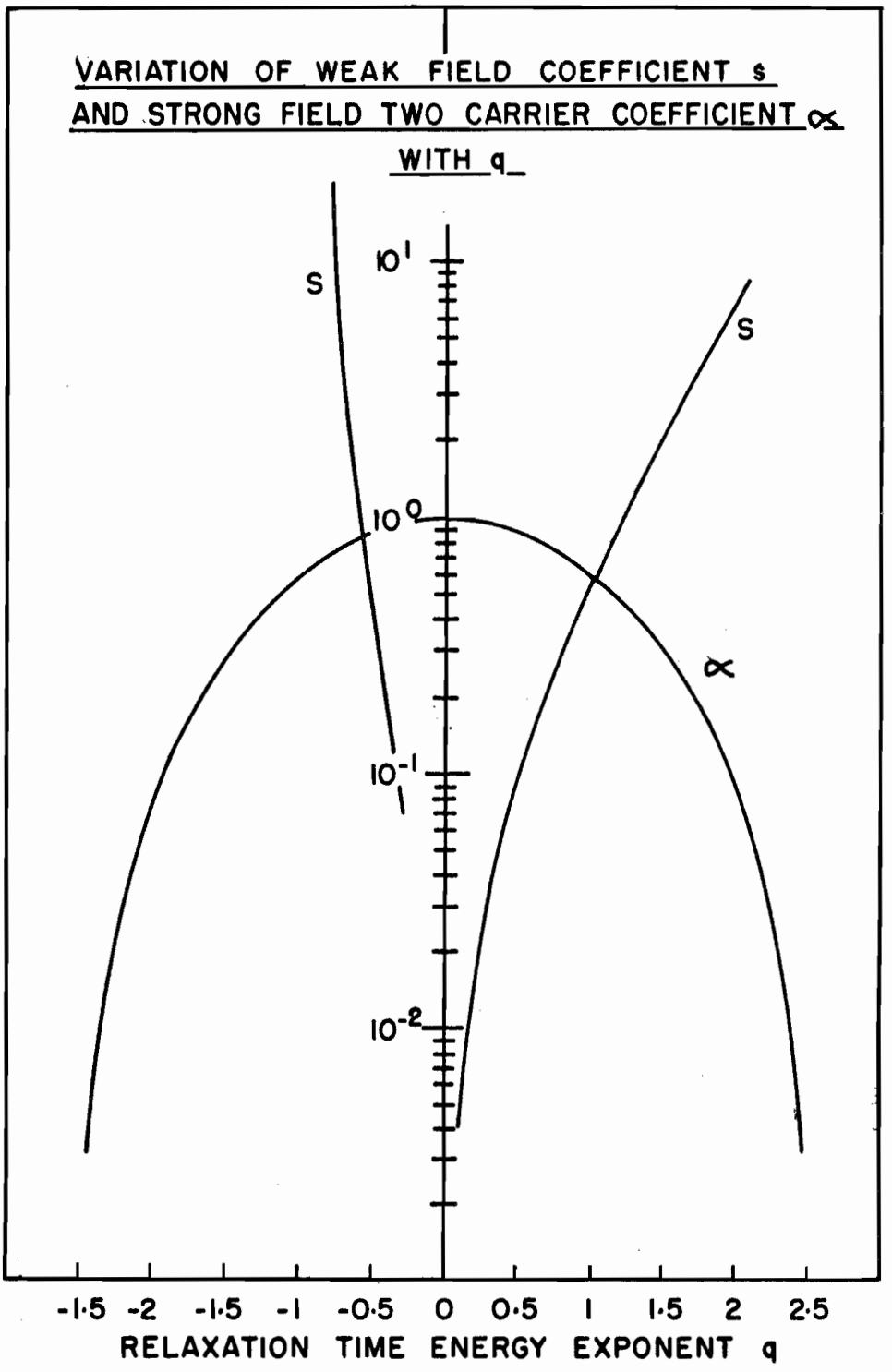

Fig. 2 Variation of the weak field magnetoresistance coefficient s and the strong field two-band magnetoresistance coefficient α (see section 2.11).

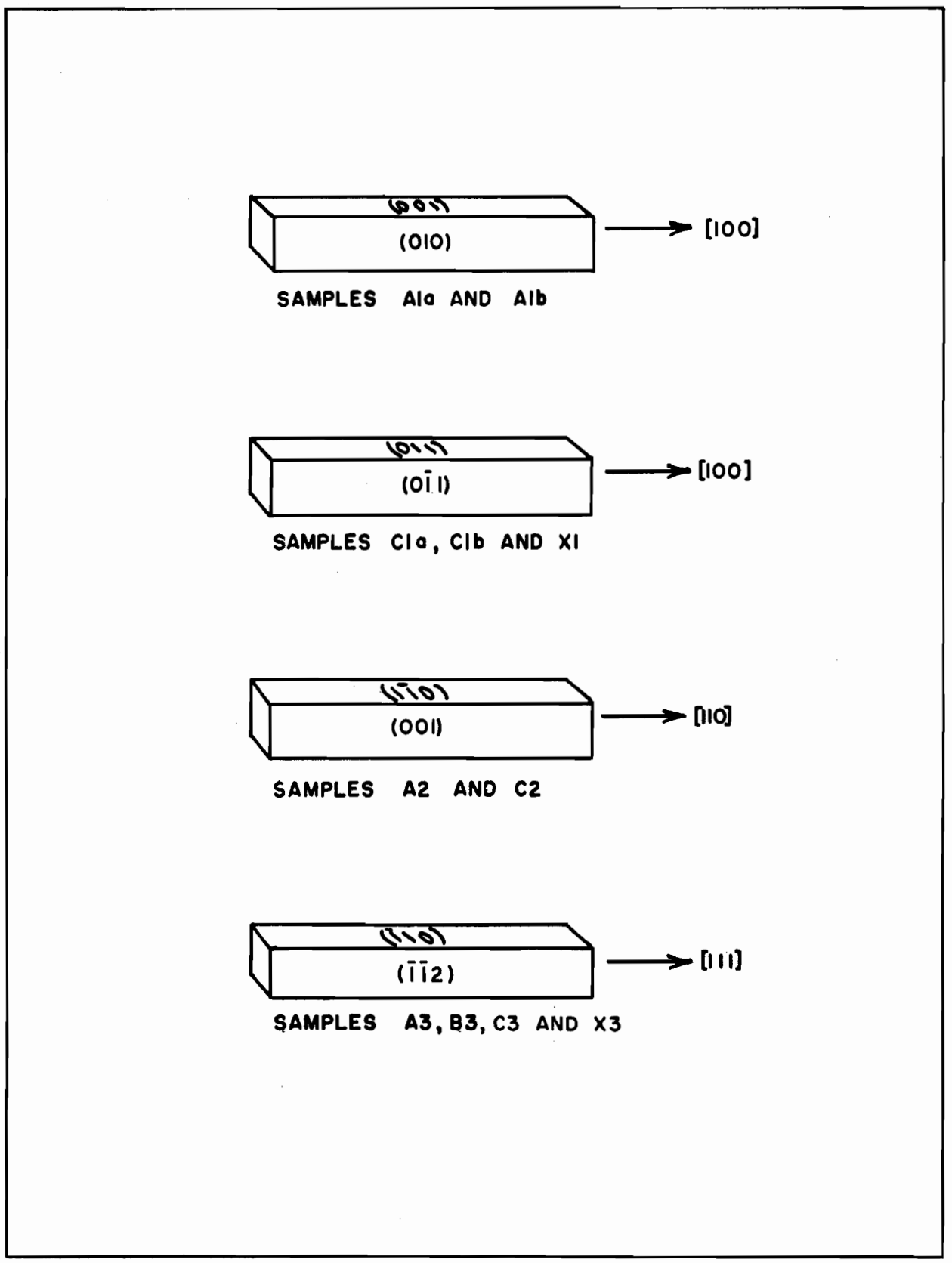

Fig. 3 The orientations of the samples used in the measurements.

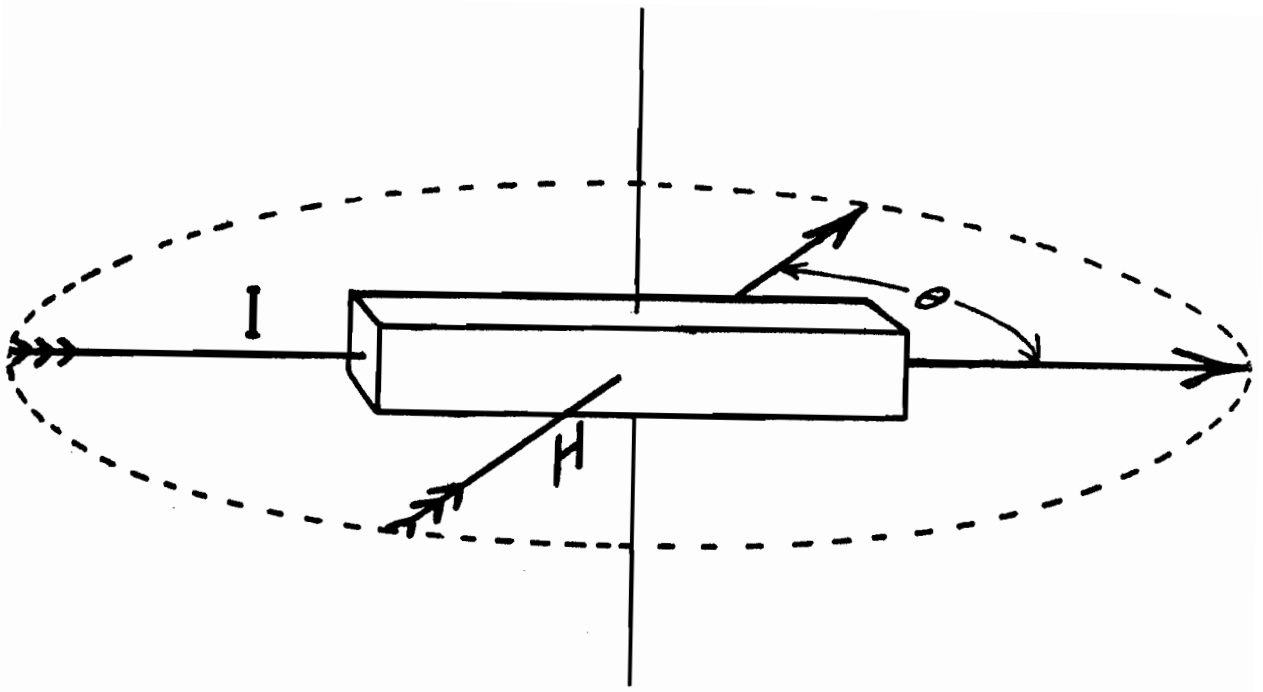

Fig. 4 Schematic diagram showing the angle of rotation of the magnetic field.

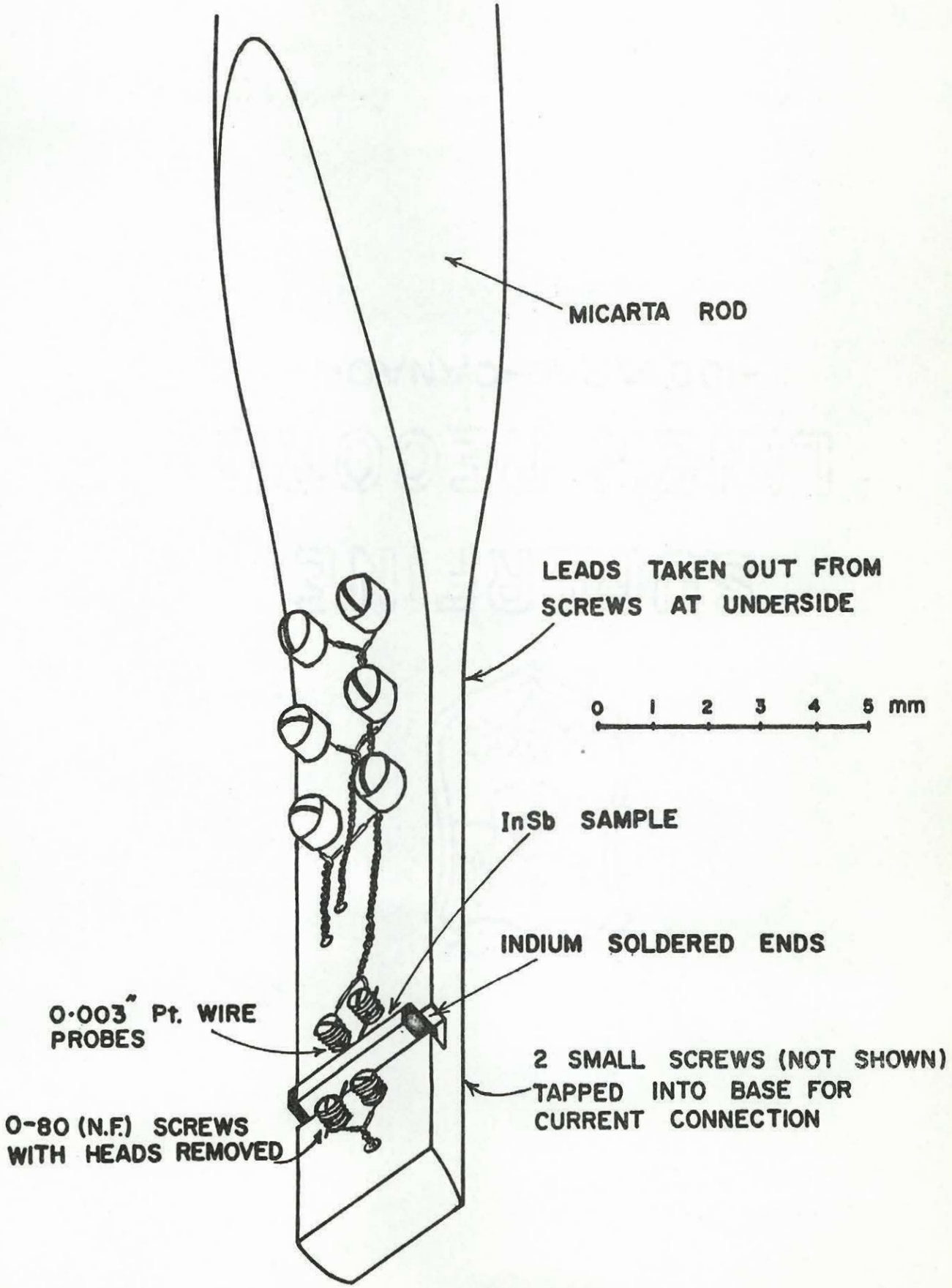

Fig. 5 Sample holder used in the measurements.

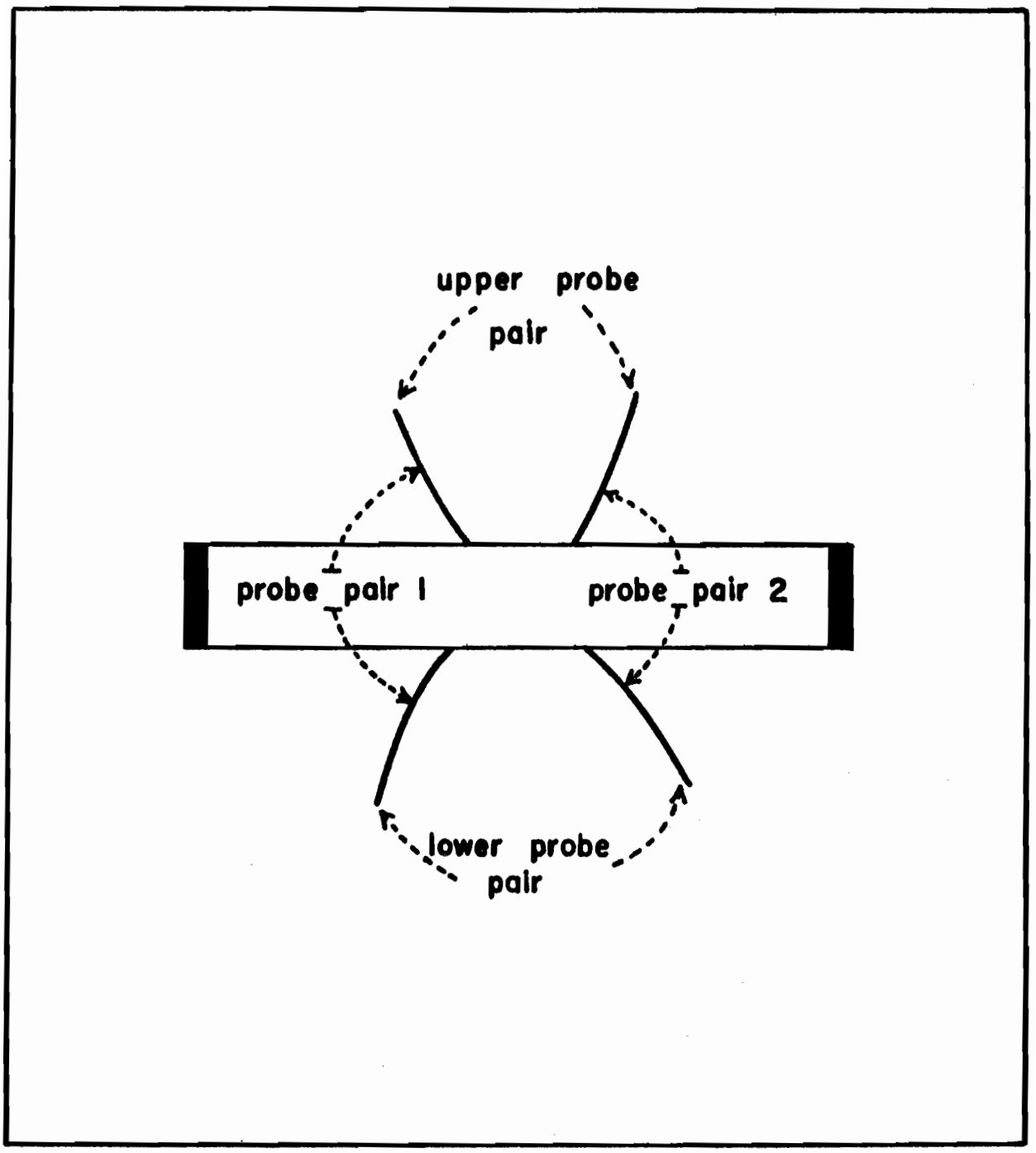

Fig. 6 The arrangement of the four probes on each sample.

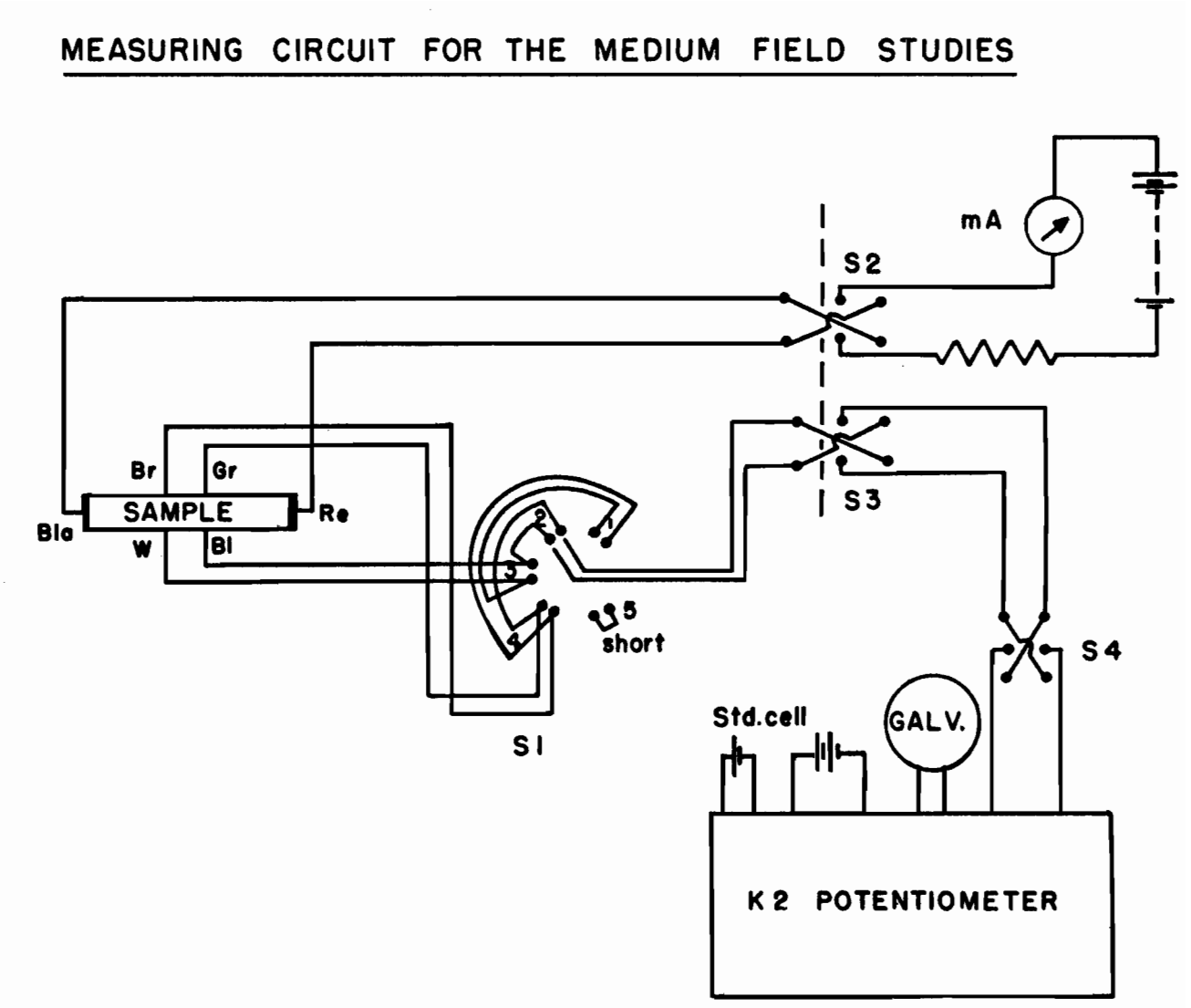

Fig. 7 Measuring circuit used for the medium field galvano-magnetic measurements.

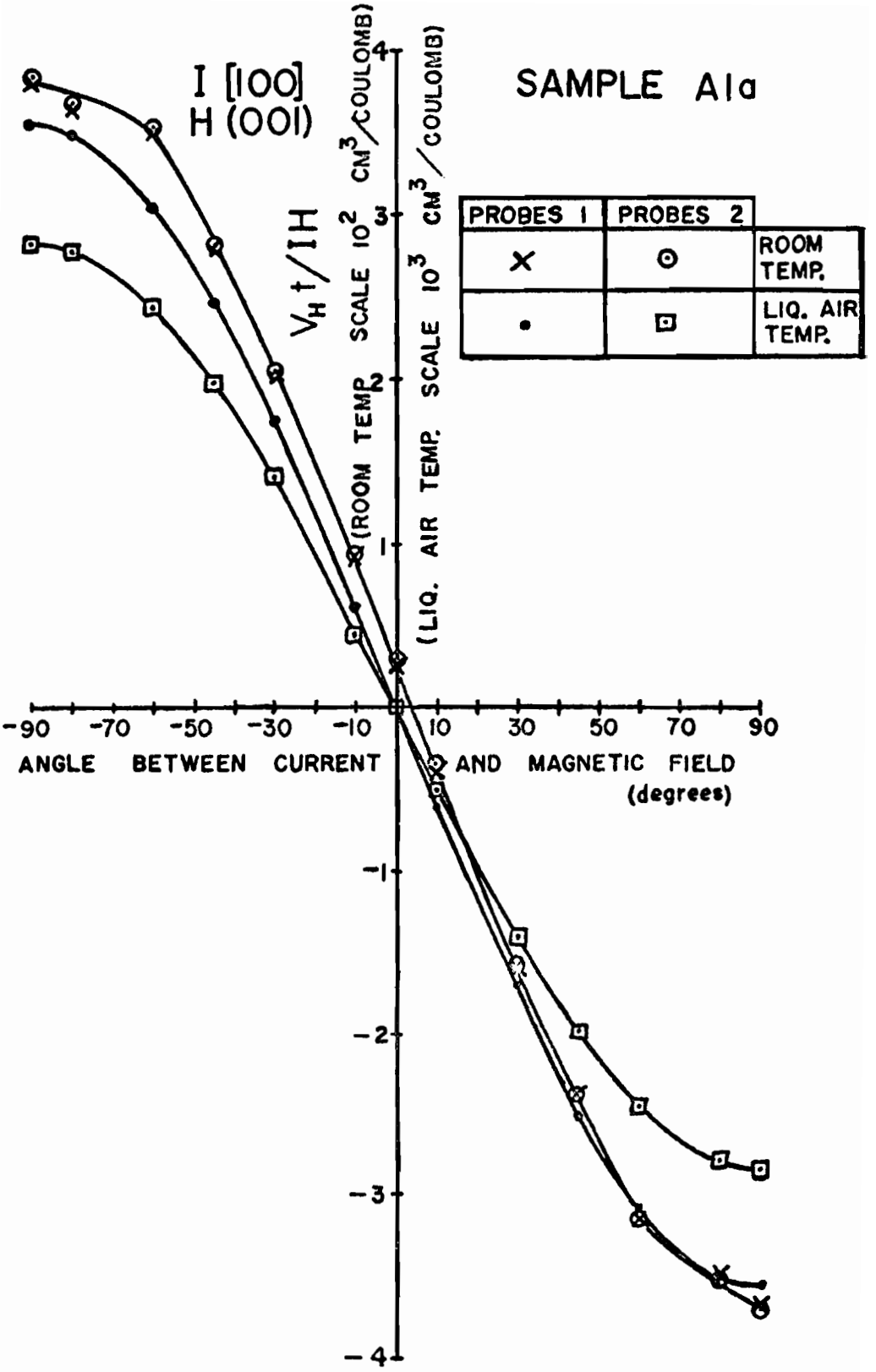

Fig. 8 Variation in sample Ala of the reduced Hall voltage $10^8 V_H t/IH$ for current in the [100] direction with rotation of the magnetic field (4880 gauss) in an (001) plane.

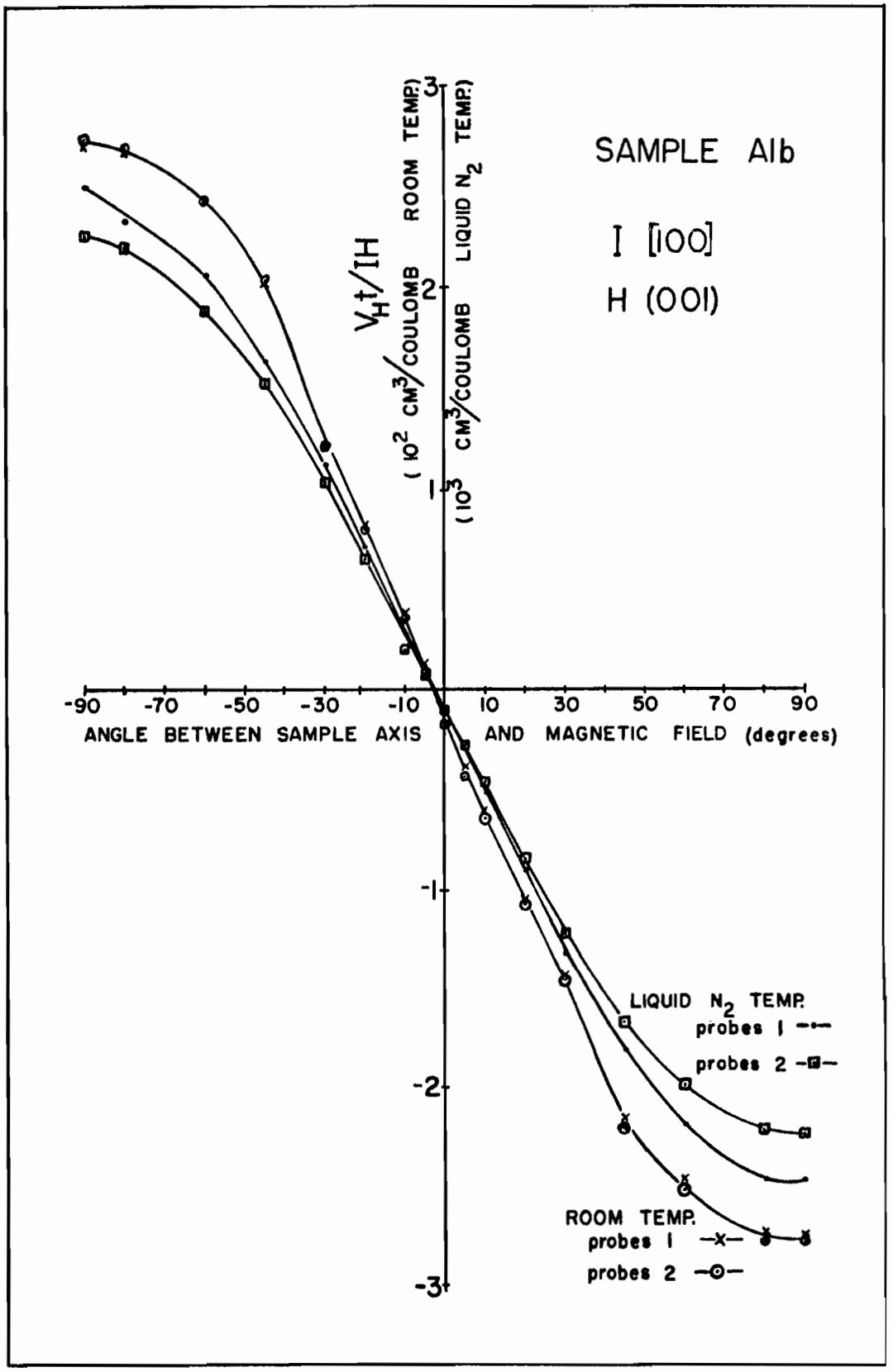

Fig. 9 Variation in sample Alb of the reduced Hall voltage $10^5 V_H t/IH$ for current in the [100] direction with rotation of the magnetic field (4350 gauss) in an (001) plane.

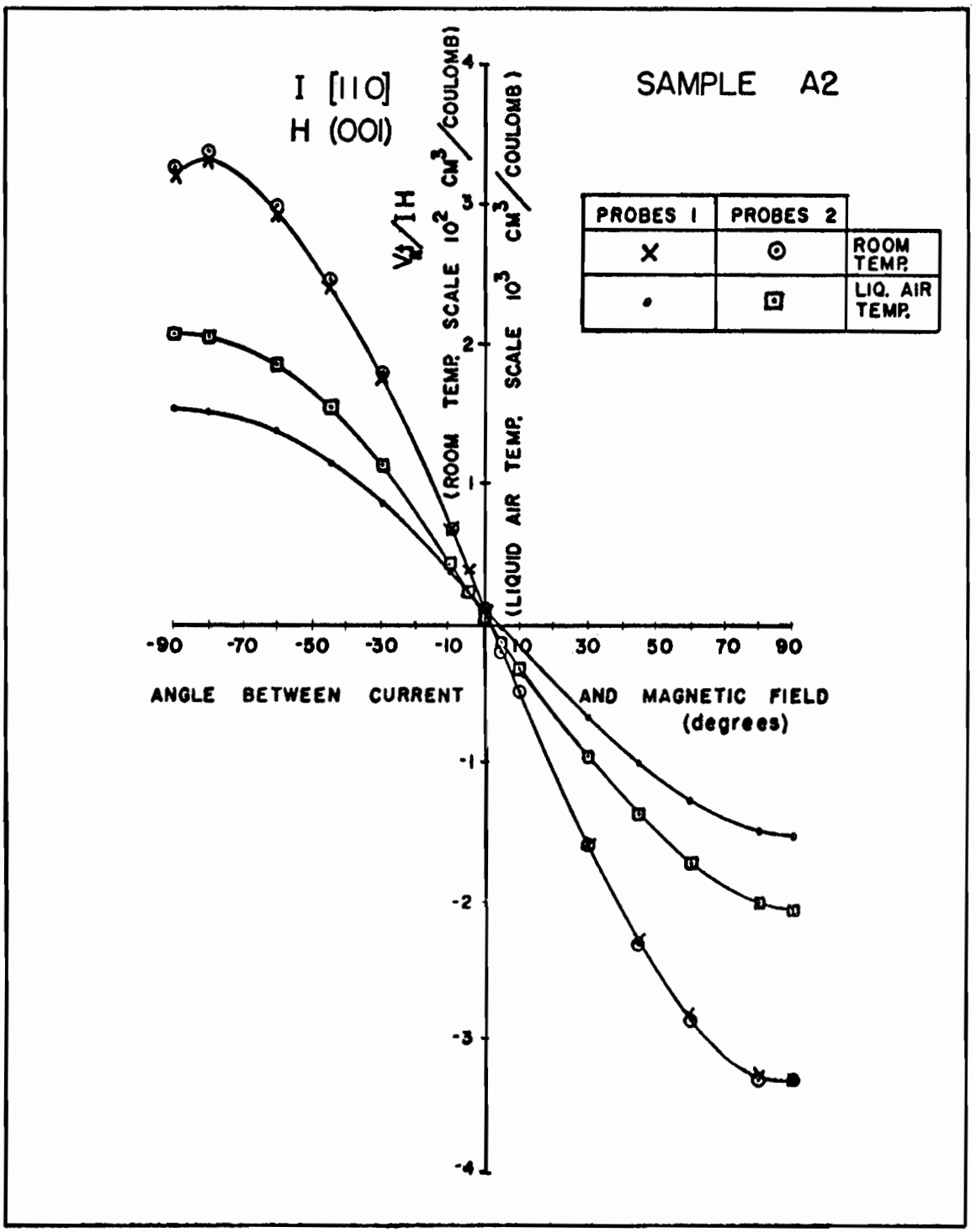

Figure 10 Variation in sample A2 of the reduced Hall voltage $10^8\ V_H t/IH$ for current in the [110] direction with rotation of the magnetic field (4800 gauss) in an (001) plane.

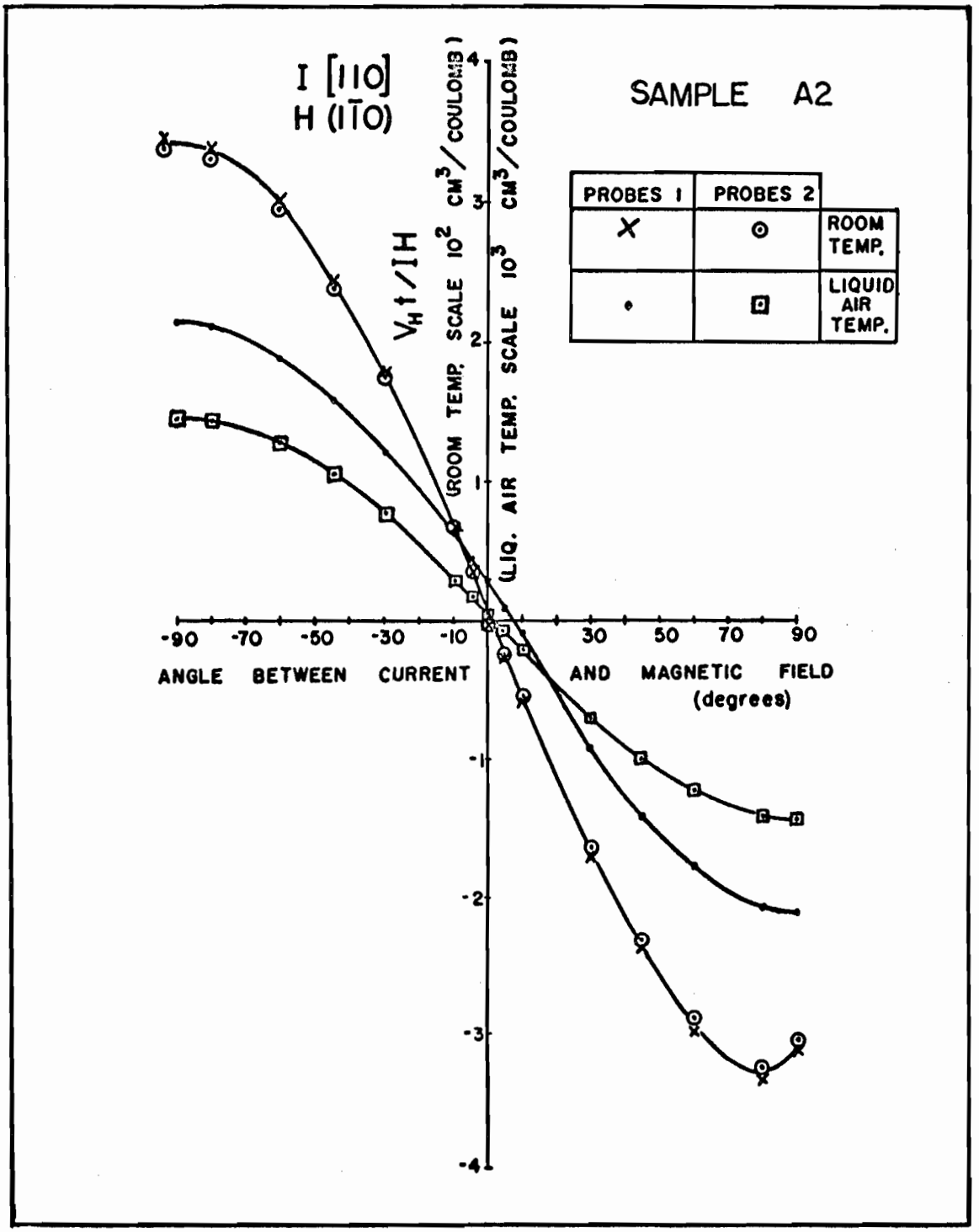

Figure 11 Variation in sample A2 of the reduced Hall voltage 10^8 $V_H t/IH$ for current in the [110] direction with rotation of the magnetic field (4880 gauss) in a (1$\bar{1}$0) plane.

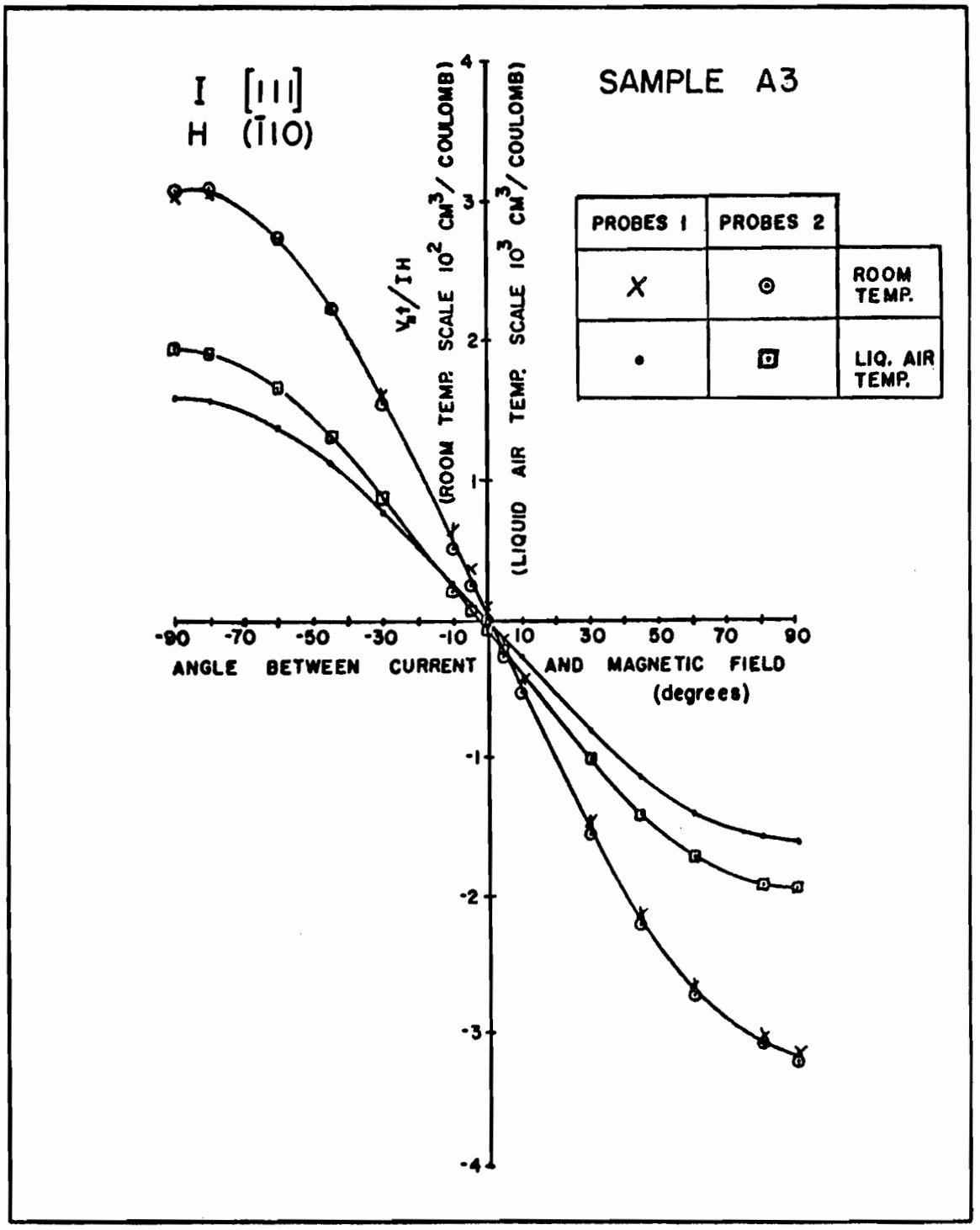

Figure 12 Variation in sample A3 of the reduced Hall voltage 10^8 $V_H t/IH$ for current in the [111] direction with rotation of the magnetic field (4880 gauss) in a ($\bar{1}$10) plane.

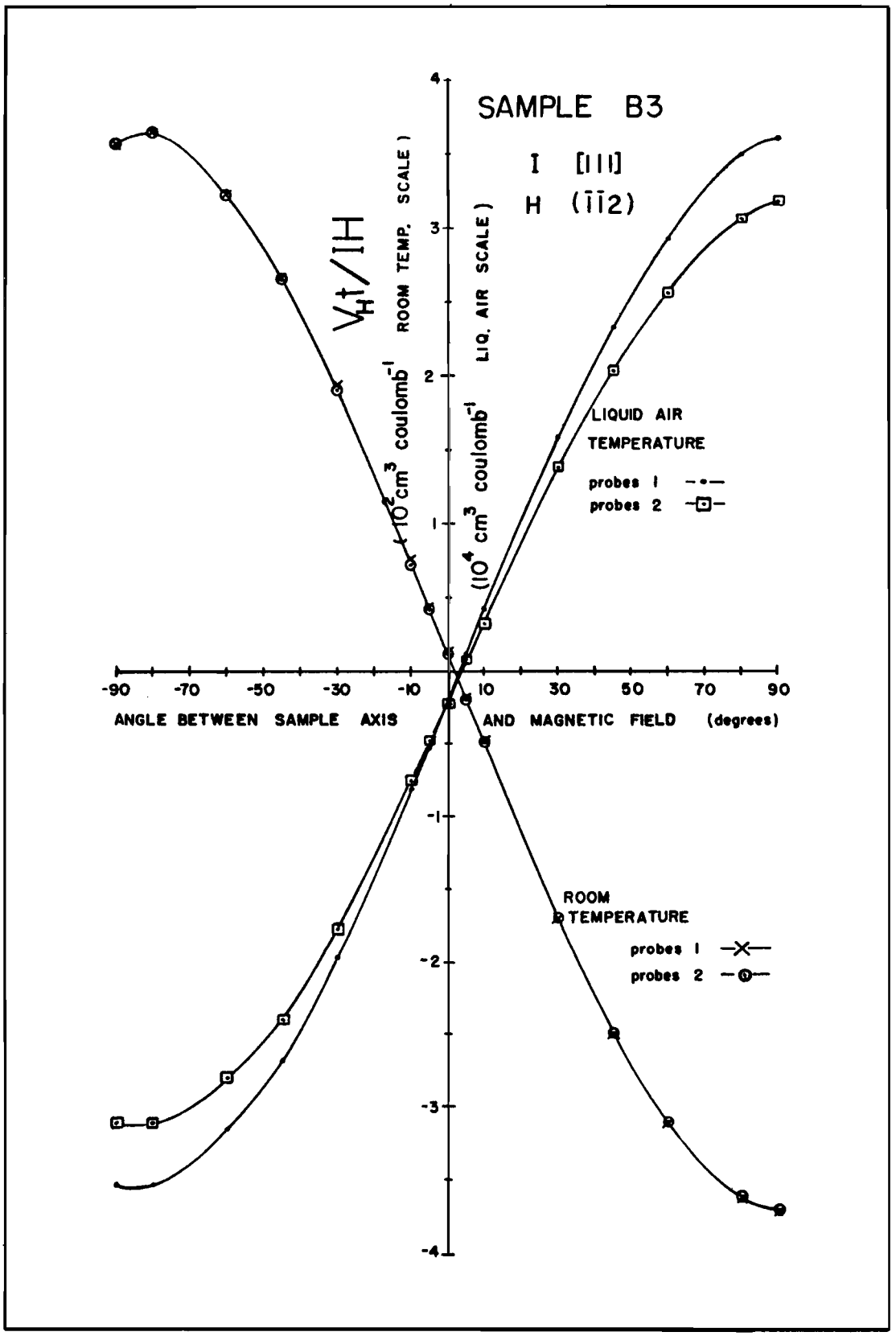

Fig. 13 Variation in sample B3 of the reduced Hall voltage $10^8 v_H t/IH$ for current in the [111] direction with rotation of the magnetic field (4880 gauss) in a $(1\bar{1}2)$ plane.

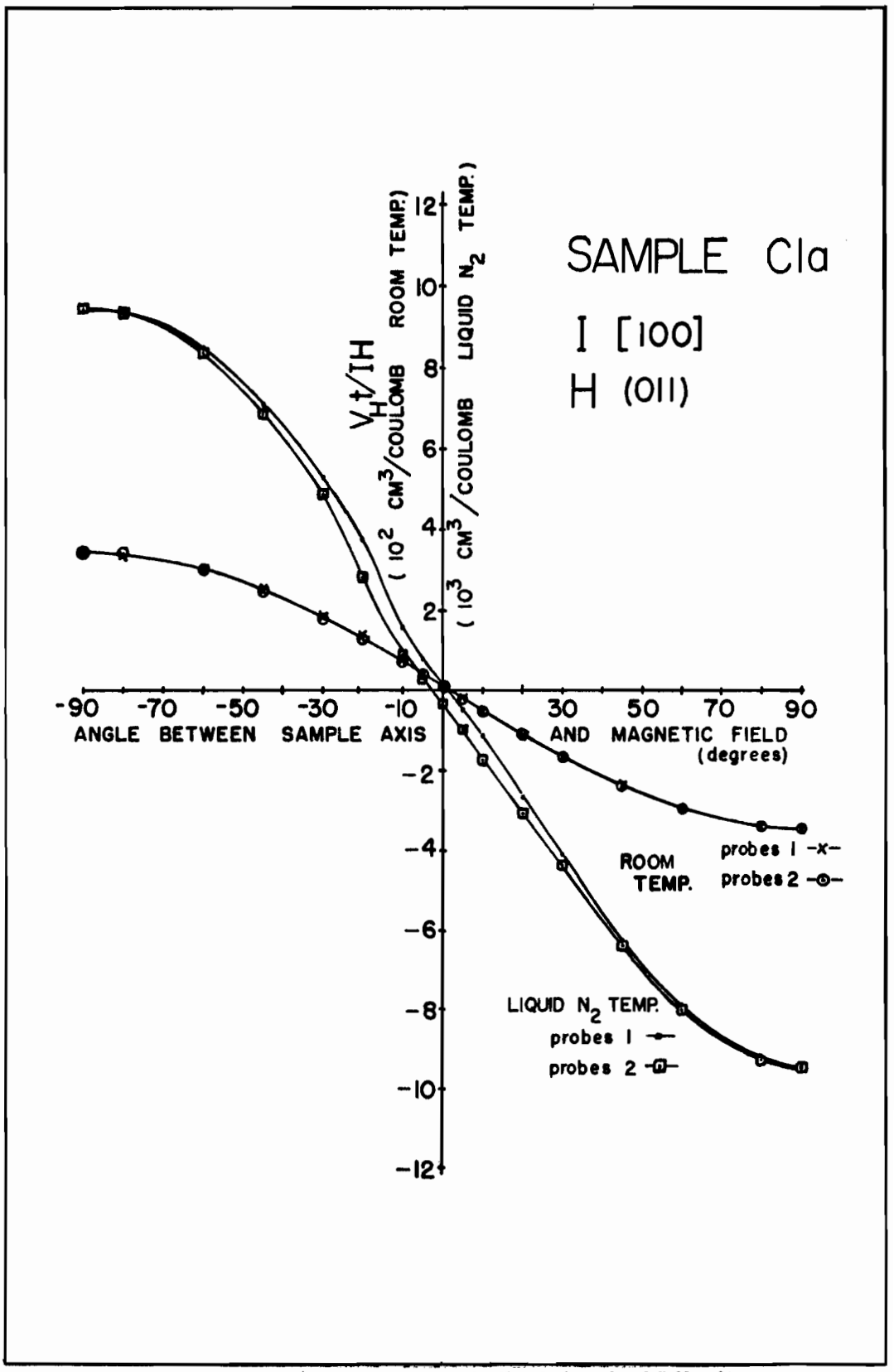

Fig. 14 Variation in sample Cla of the reduced Hall voltage $10^8 V_H t/IH$ for current in the [100] direction with rotation of the magnetic field (4350 gauss) in an (011) plane.

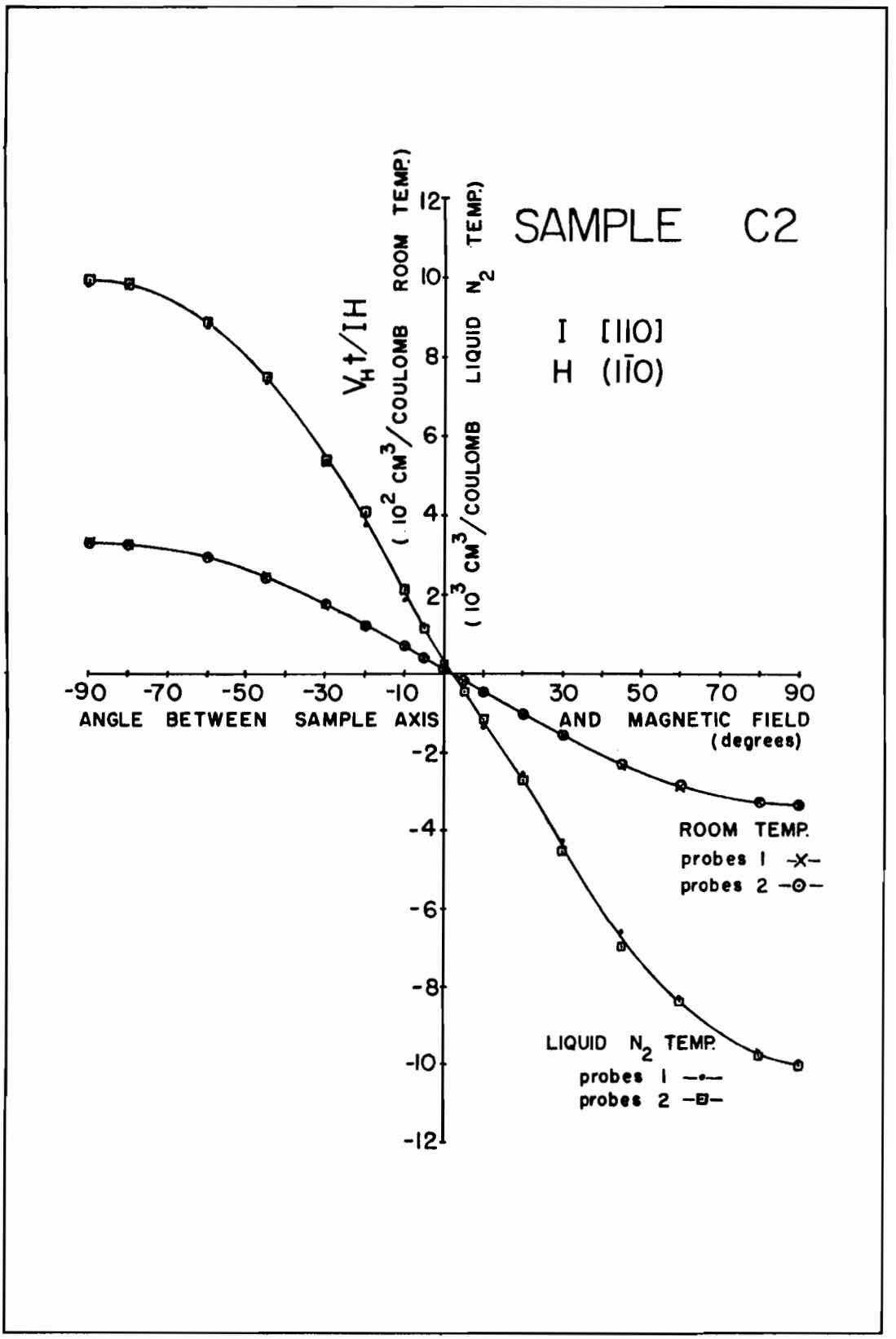

Fig. 15 Variation in sample C2 of the reduced Hall voltage $10^8 V_H t/IH$ for current in the [110] direction with rotation of the magnetic field (4350 gauss) in a $(1\bar{1}0)$ plane.

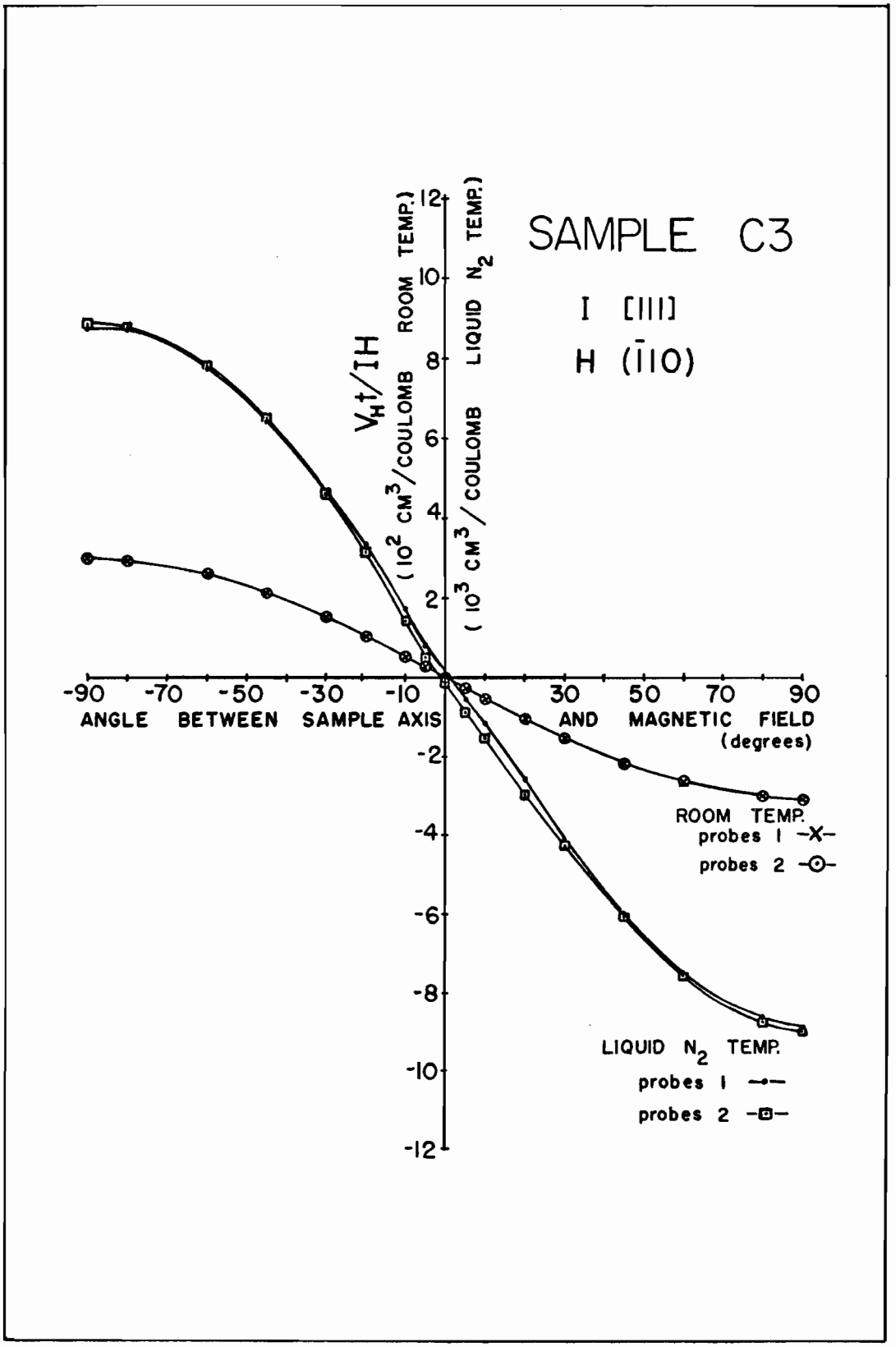

Fig. 16 Variation in sample C3 of the reduced Hall voltage $10^8 V_H t/IH$ for current in the [111] direction and rotation of the magnetic field (4350 gauss) in a (1̄10) plane.

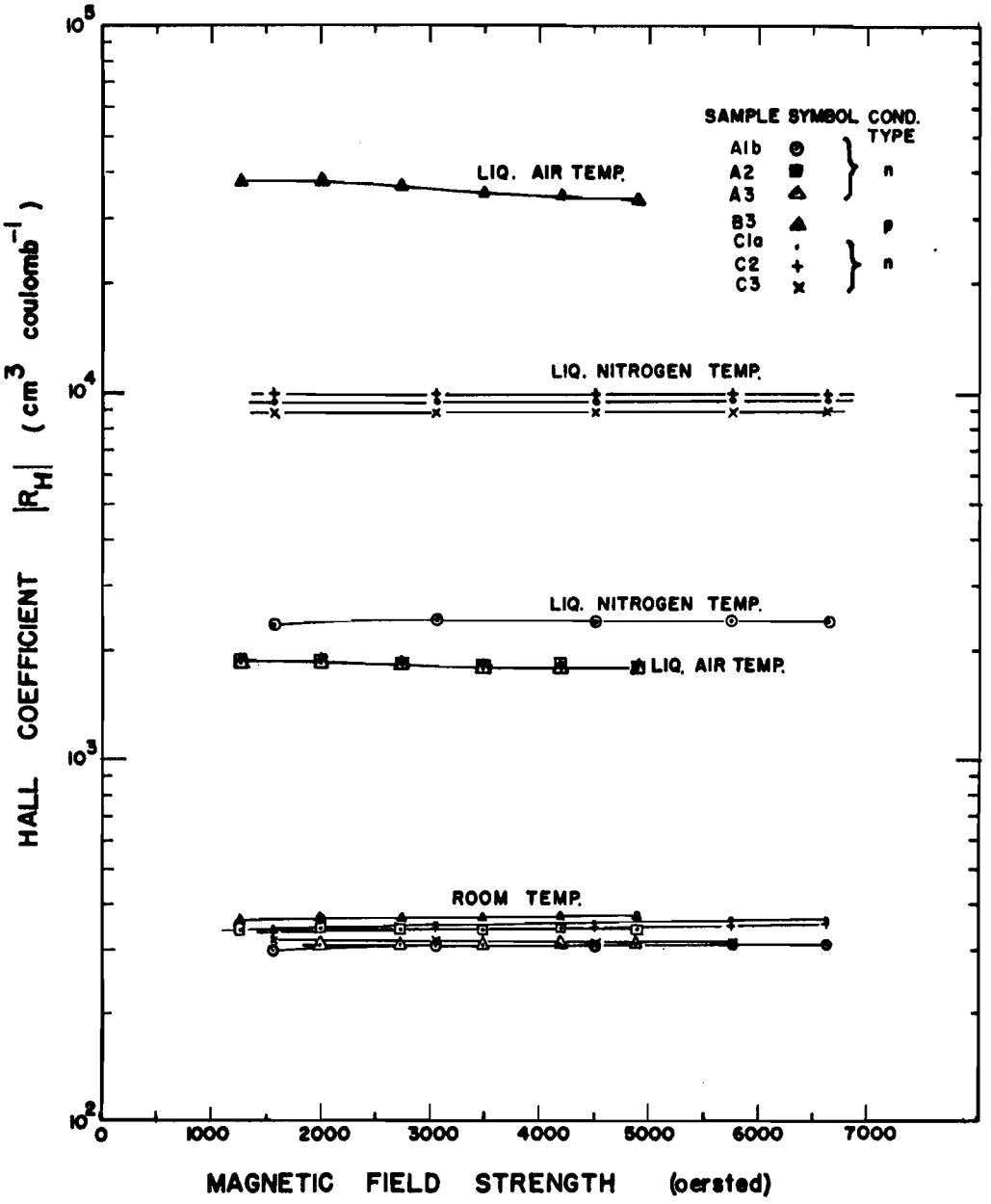

Fig. 17 Variation of Hall coefficient with magnetic field strength for the various indium antimonide samples.

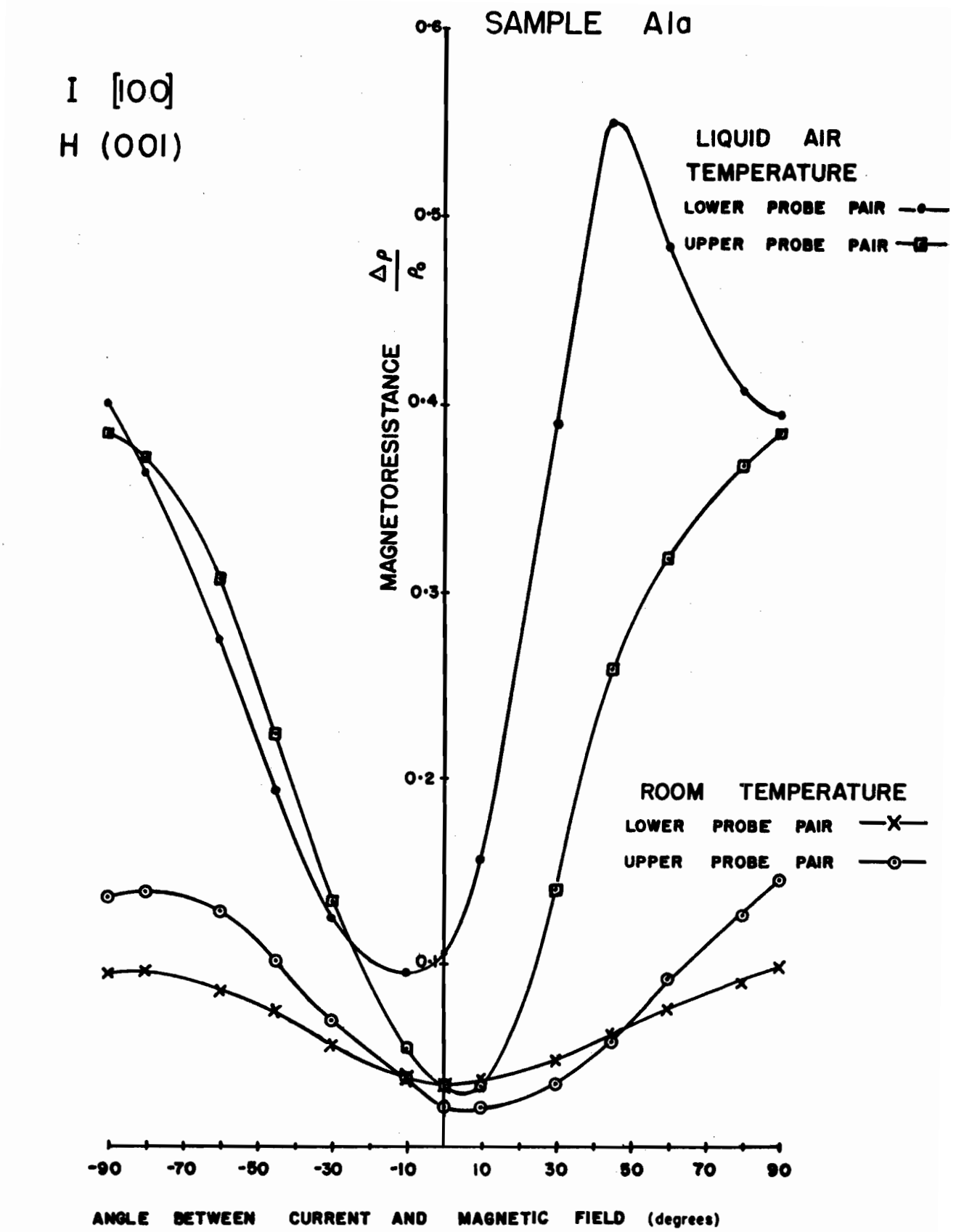

Fig. 18 Variation of the magnetoresistance in the [100] direction of sample Ala with rotation of the magnetic field (4880 gauss) in an (001) plane.

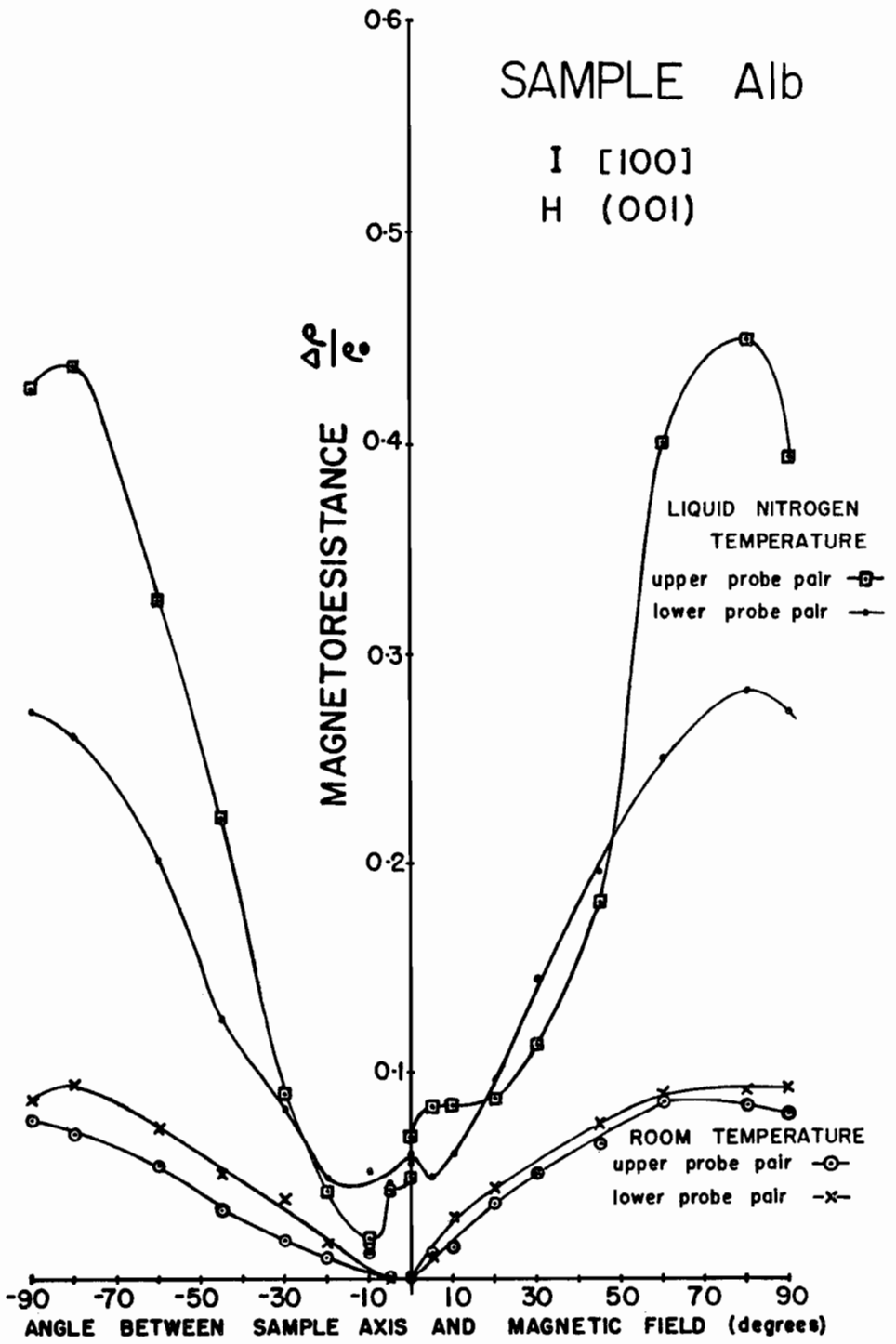

Fig. 19 Variation in sample Alb of the magnetoresistance for current in the [100] direction with rotation of the magnetic field (4350 gauss) in an (001) plane.

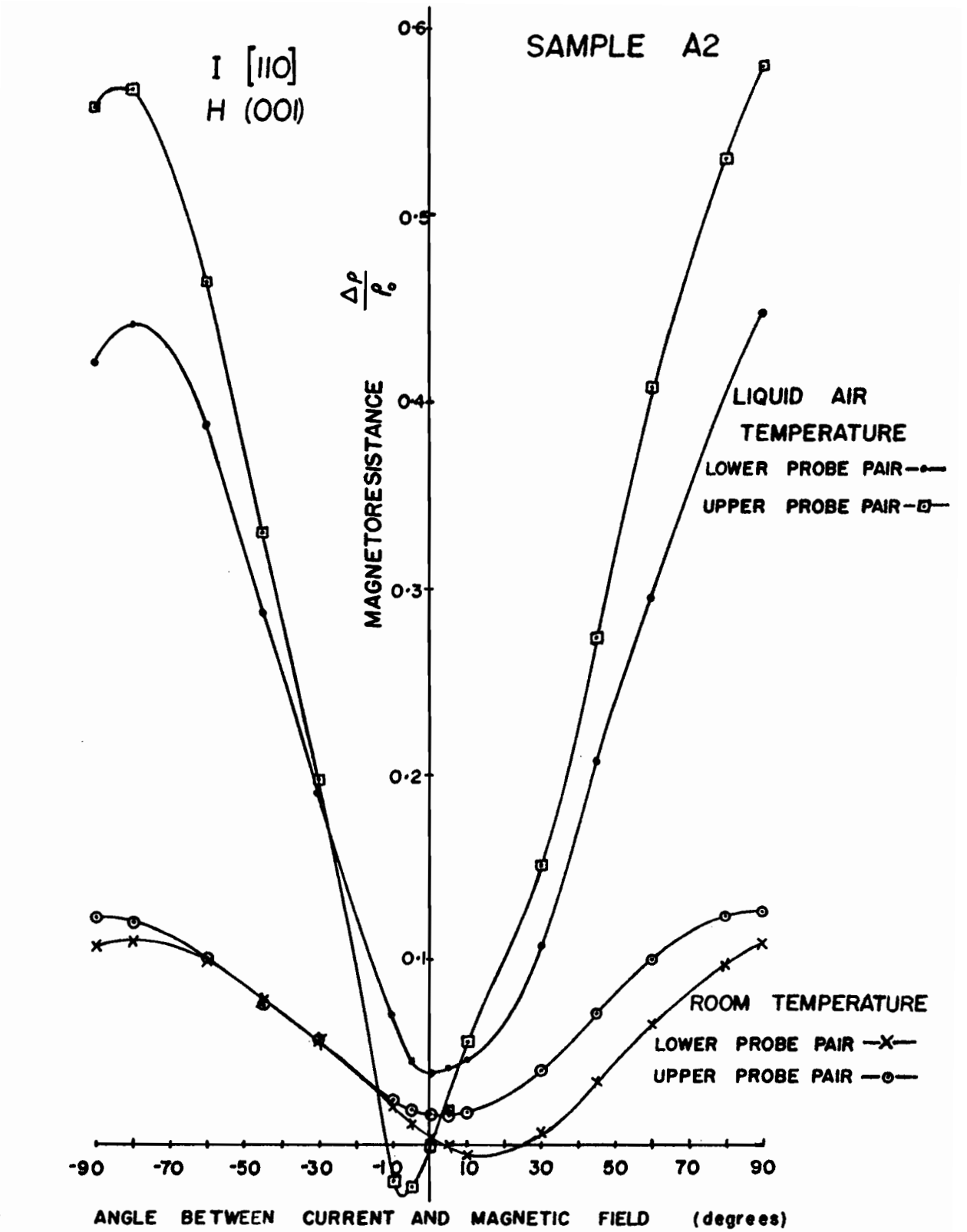

Fig. 20 Variation of the magnetoresistance in the [110] direction of sample A2 with rotation of the magnetic field (4880 gauss) in an (001) plane.

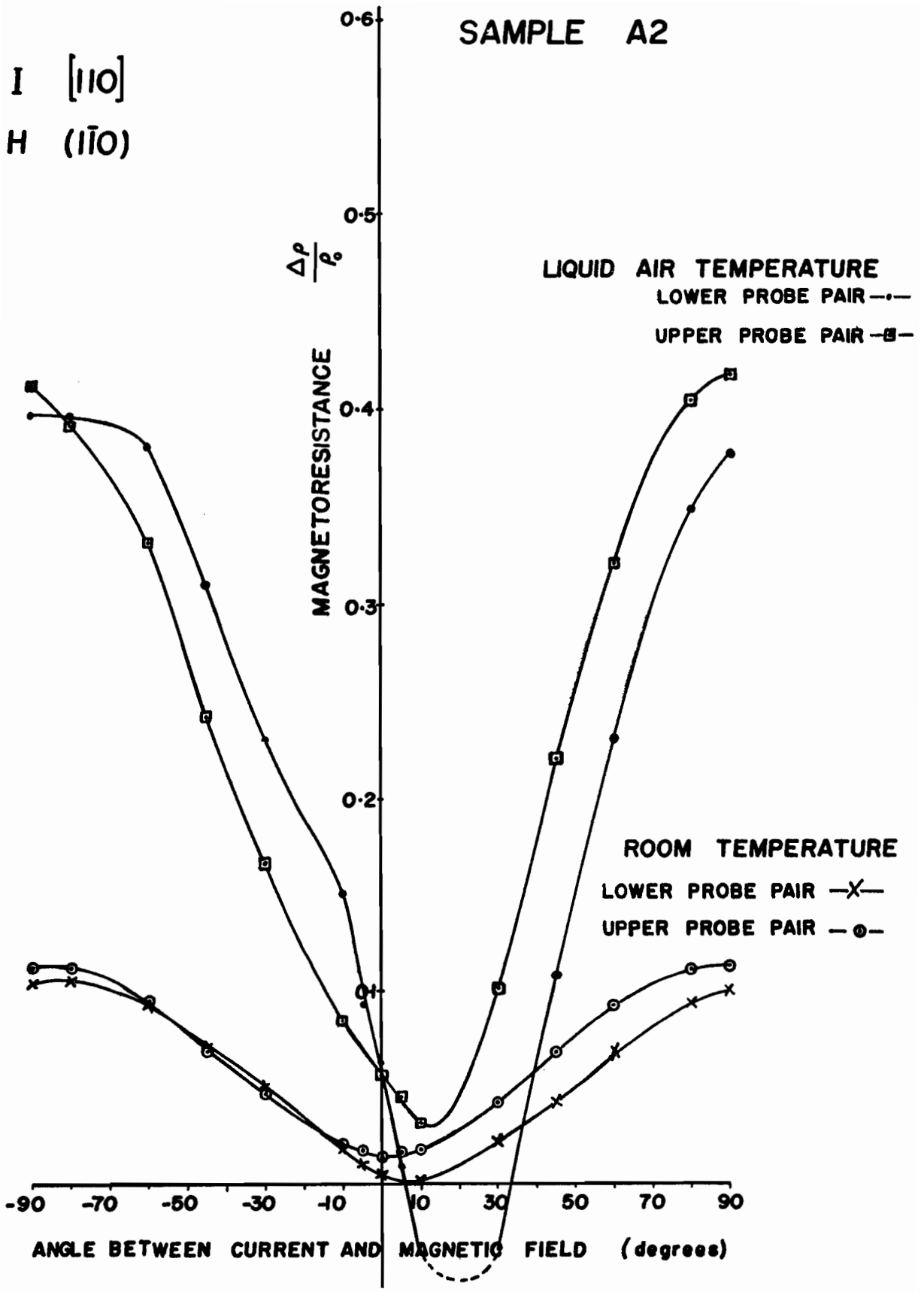

Fig. 21 Variation of the magnetoresistance in the [110] direction of sample A2 with rotation of the magnetic field (4880 gauss) in a (1$\bar{1}$0) plane.

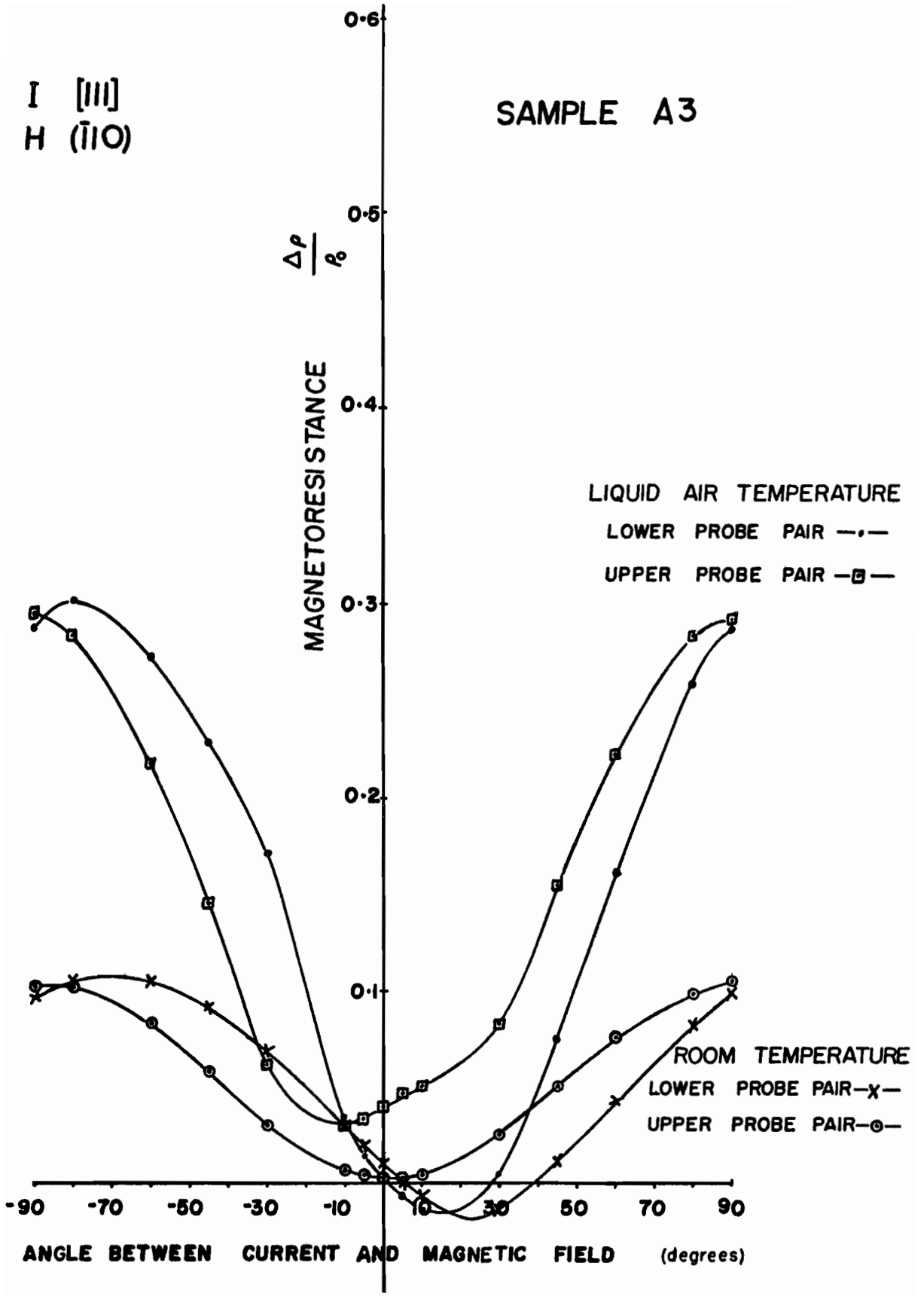

Fig. 22 Variation of the magnetoresistance in the [111] direction of sample A3 with rotation of the magnetic field (4880 gauss) in a (1̄10) plane.

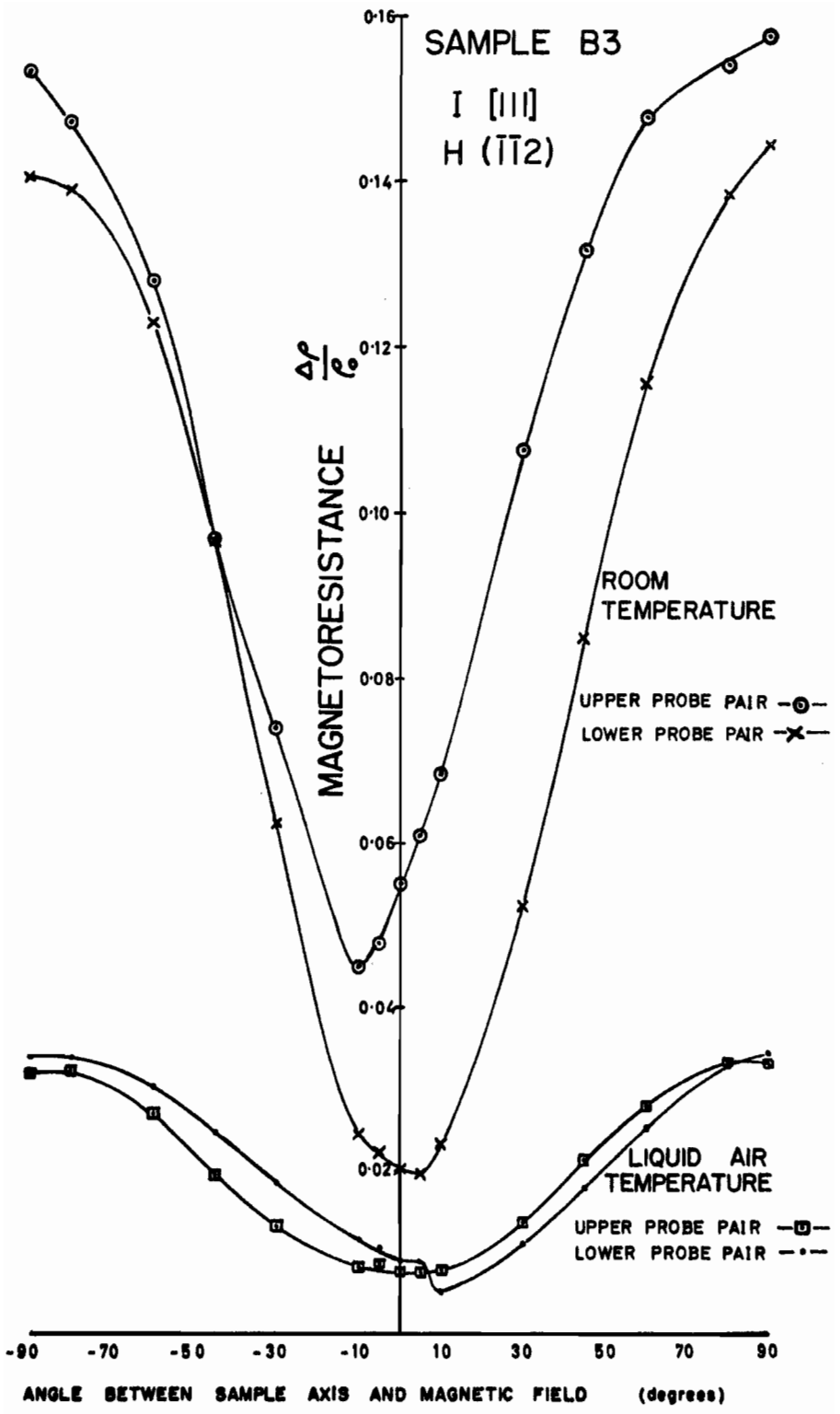

Fig. 23 Variation of the magnetoresistance in the [111] direction of sample B3 with rotation of the magnetic field (4880 gauss) in a (1̄1̄2) plane.

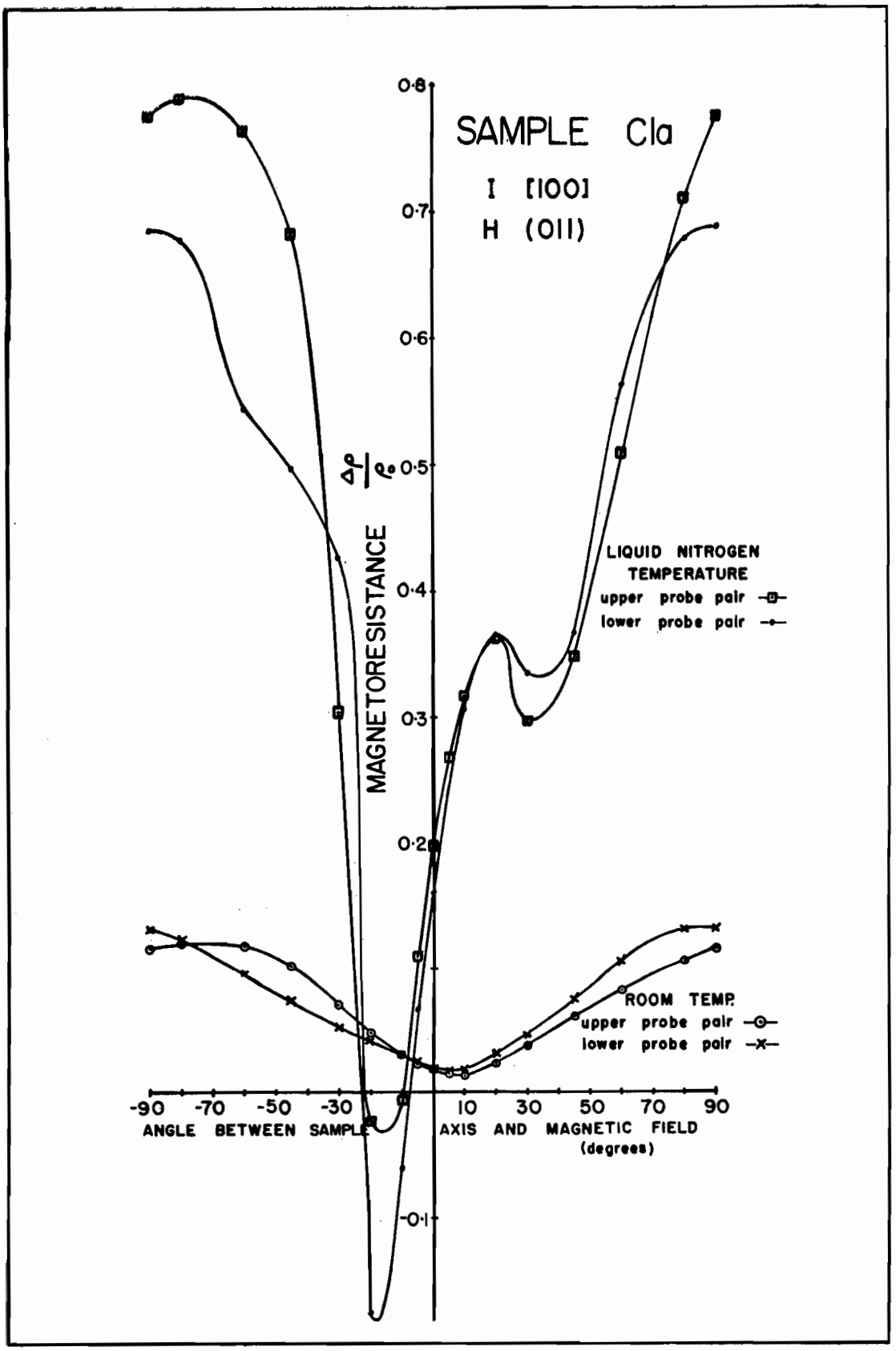

Fig. 24 Variation in sample Cla of the magnetoresistance for current in the [100] direction with rotation of the magnetic field (4350 gauss) in an (011) plane.

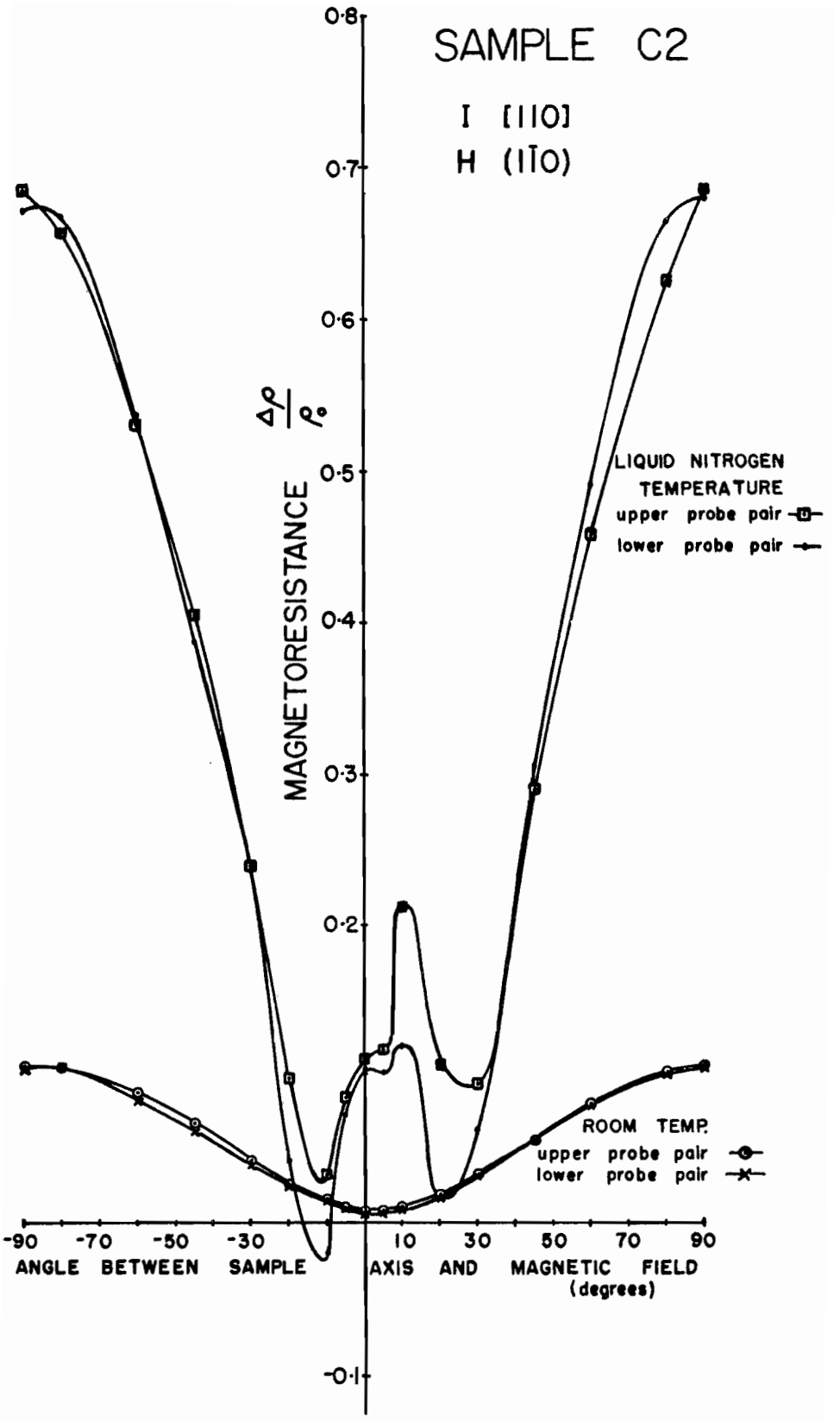

Fig. 25 Variation in sample C2 of the magnetoresistance for current in the [110] direction with rotation of the magnetic field (4350 gauss) in a (1$\bar{1}$0) plane.

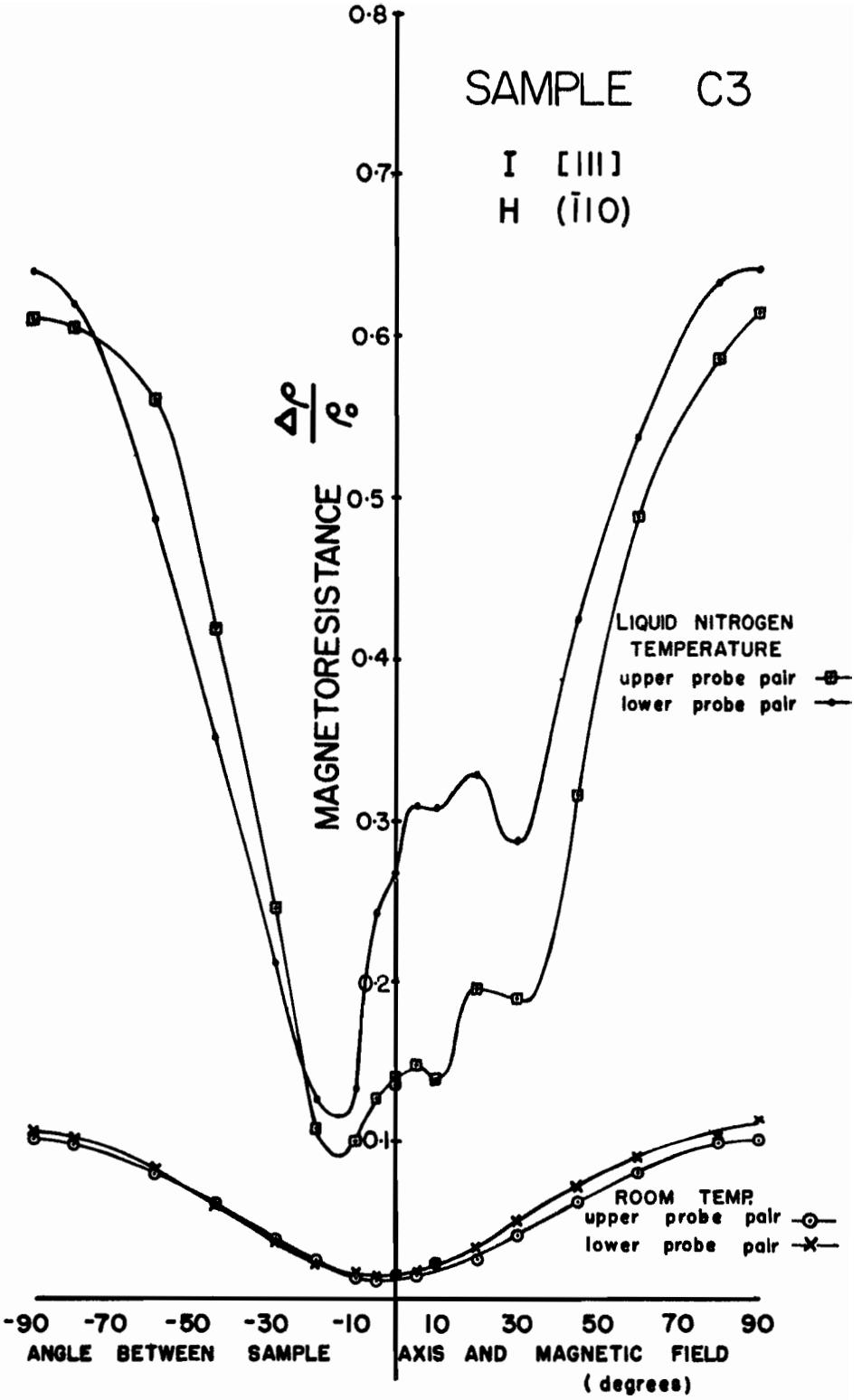

Fig. 26 Variation in sample C3 of the magnetoresistance for current in the [111] direction with rotation of the magnetic field (4350 gauss) in a (1̄10) plane.

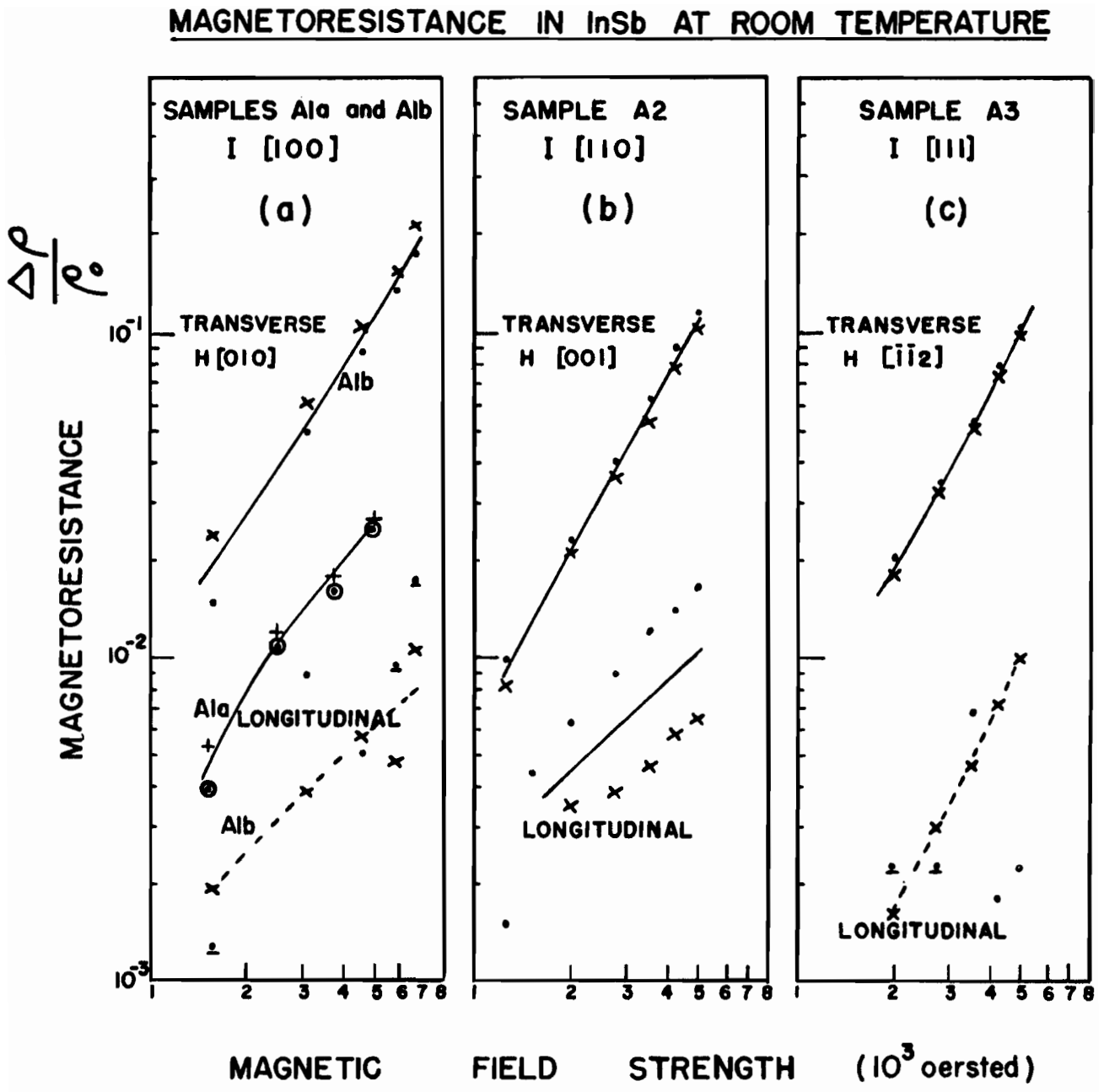

Fig. 27 Magnetic field dependence of the transverse and longitudinal magnetoresistance in indium antimonide samples Ala, Alb, A2 and A3 at room temperature where the points • and ⊙ refer to the upper pairs of probes and X and + to the lower probe pairs. Underlined points represent negative values.

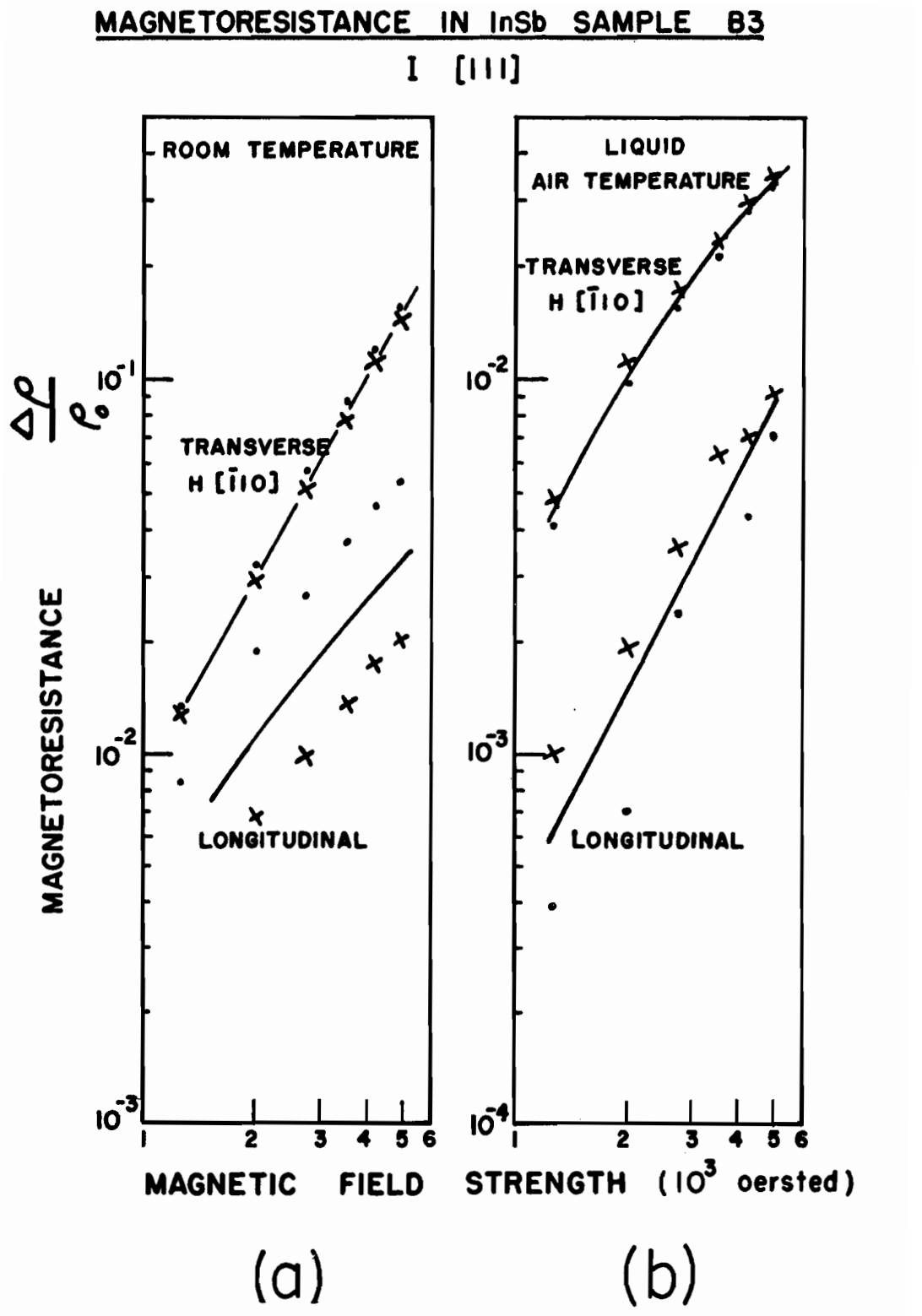

Fig. 28 Magnetic field dependence of the transverse and longitudinal magnetoresistance in sample B3 at room and liquid air temperature where the points • refer to the upper probe pair and × to the lower probe pair.

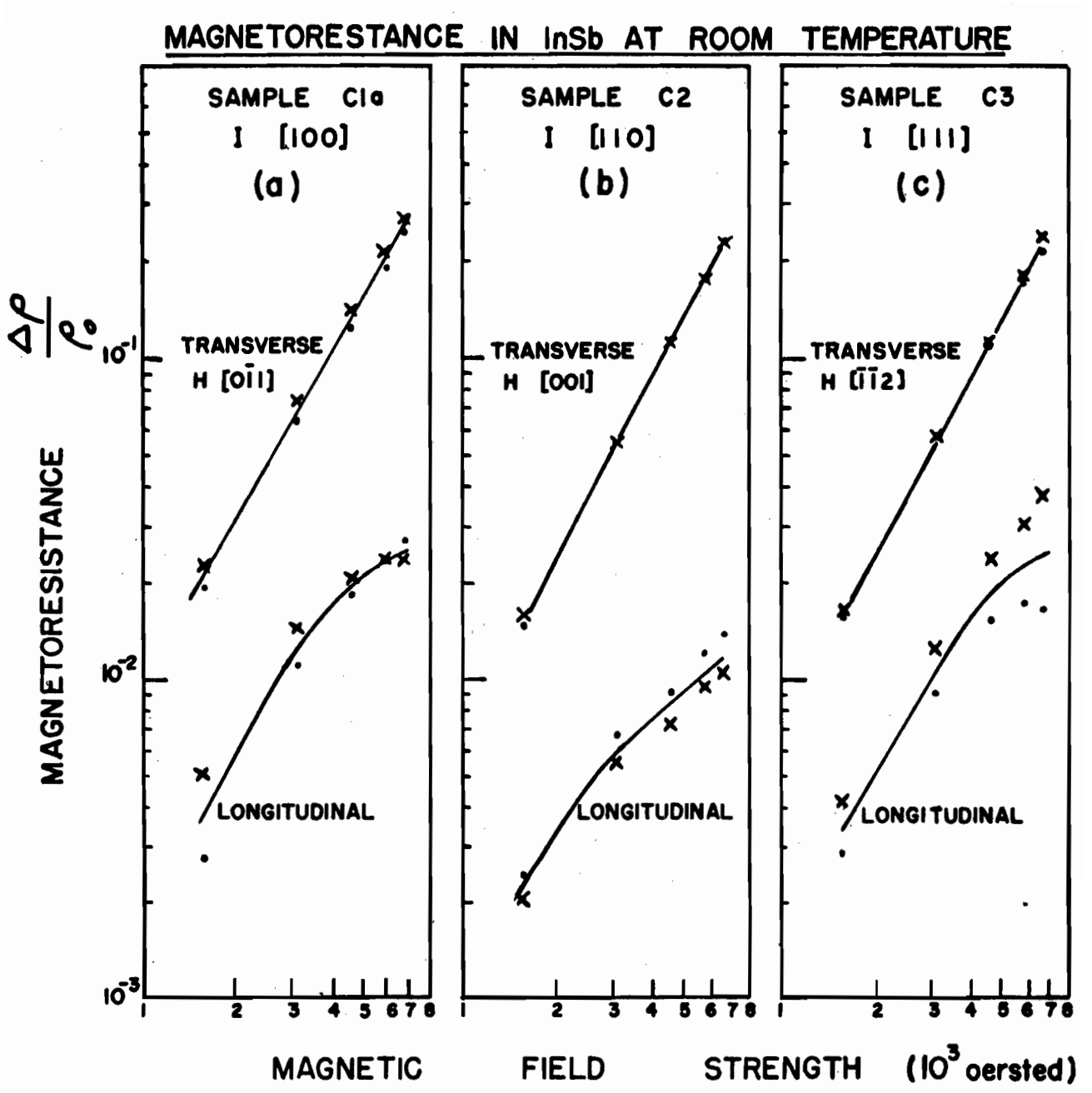

Fig. 29 Magnetic field dependence of the transverse and longitudinal magnetoresistance in the indium antimonide samples C1a, C2 and C3 at room temperature where the points • refer to the upper probe pairs and × to the lower probe pairs.

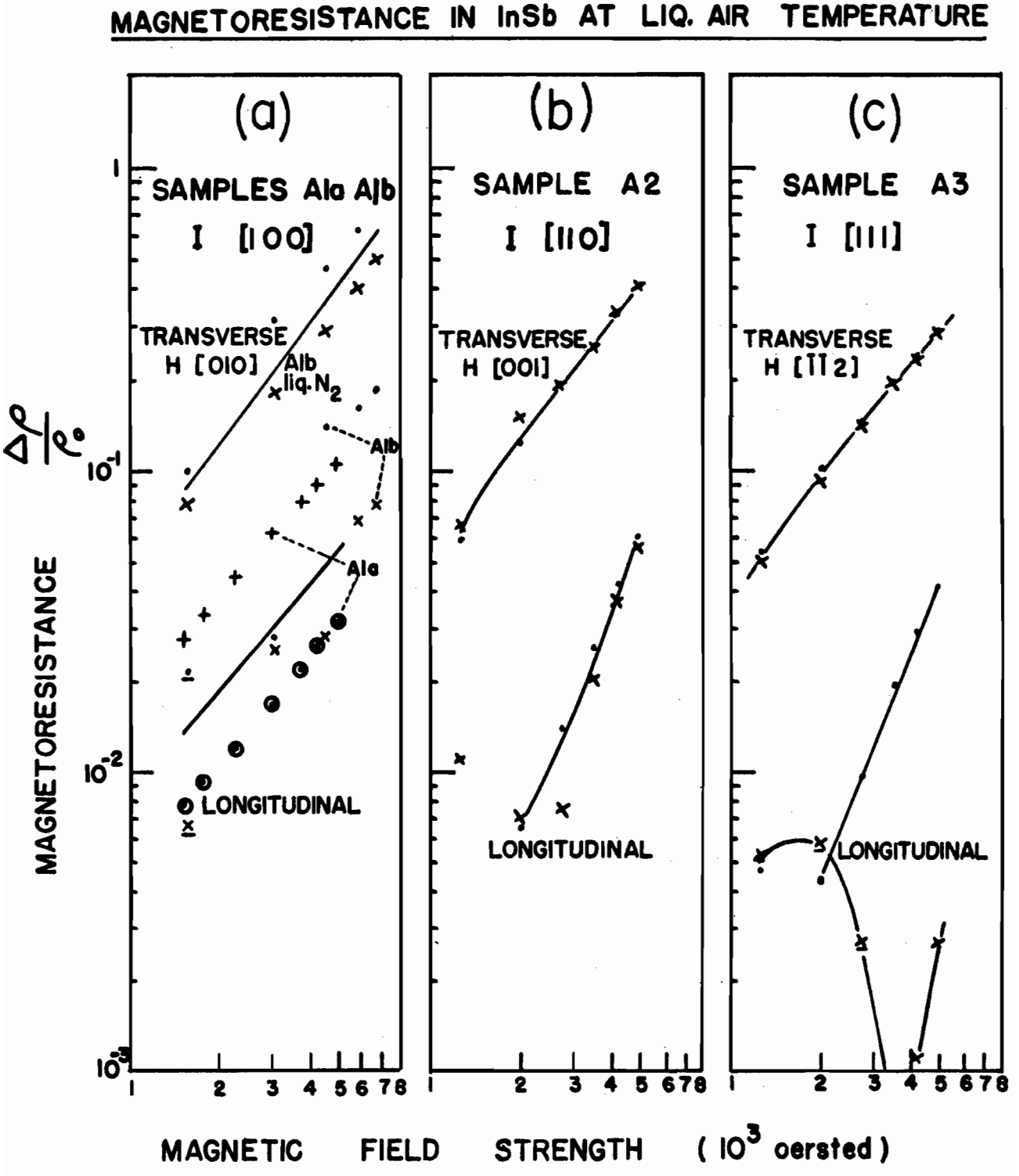

Fig. 30 Magnetic field dependence of the transverse and longitudinal magnetoresistance in the indium antimonide samples Ala, Alb, A2 and A3 at liquid air temperature where the points • and ⊙ refer to the upper probe pairs and × and + to the lower probe pairs. Underlined points represent negative values.

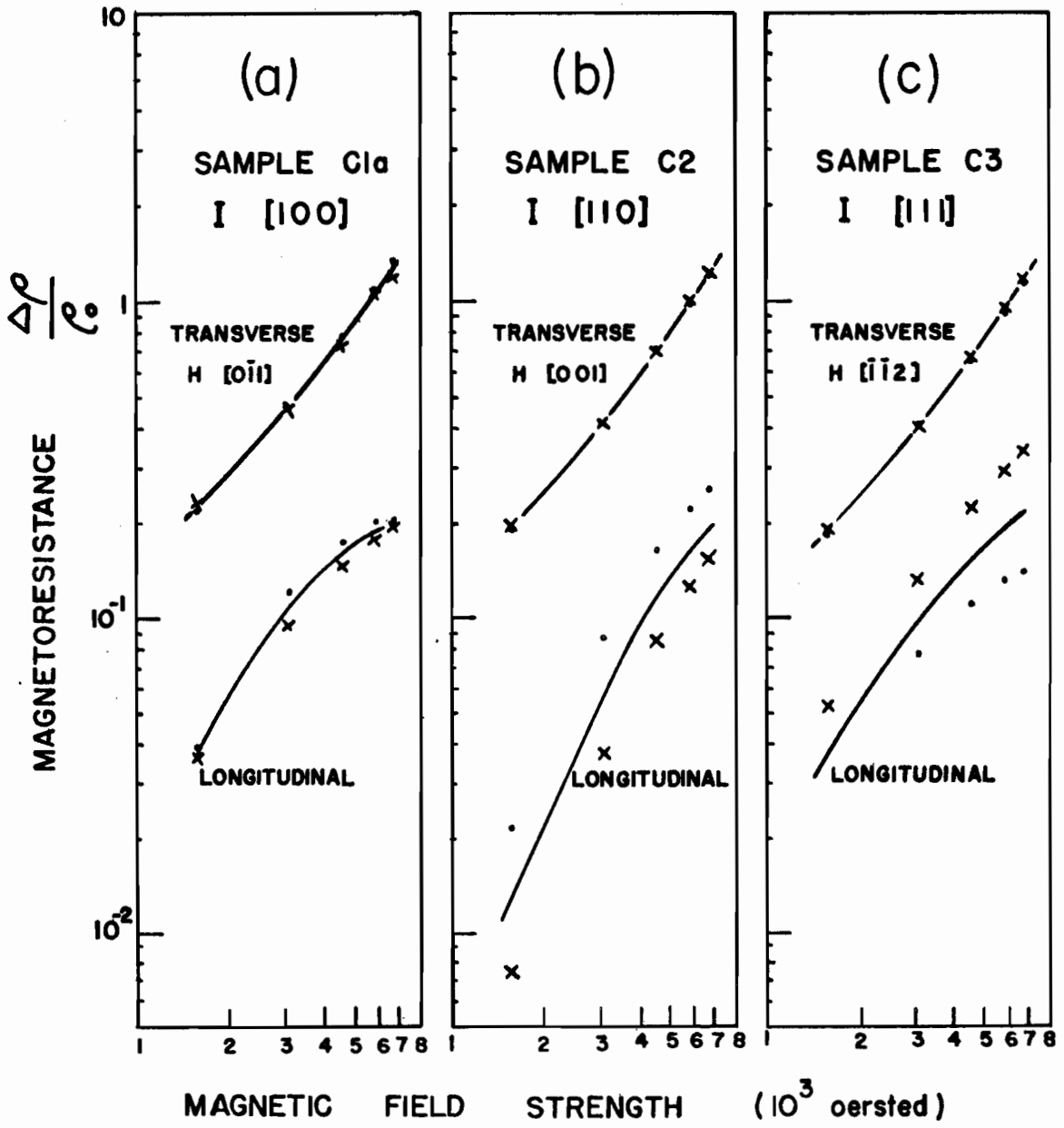

Fig. 31 Magnetic field dependence of the transverse and longitudinal magnetoresistance in the indium antimonide samples C1a, C2 and C3 at liquid nitrogen temperature where the points • refer to the upper probe pairs and × to the lower probe pairs.

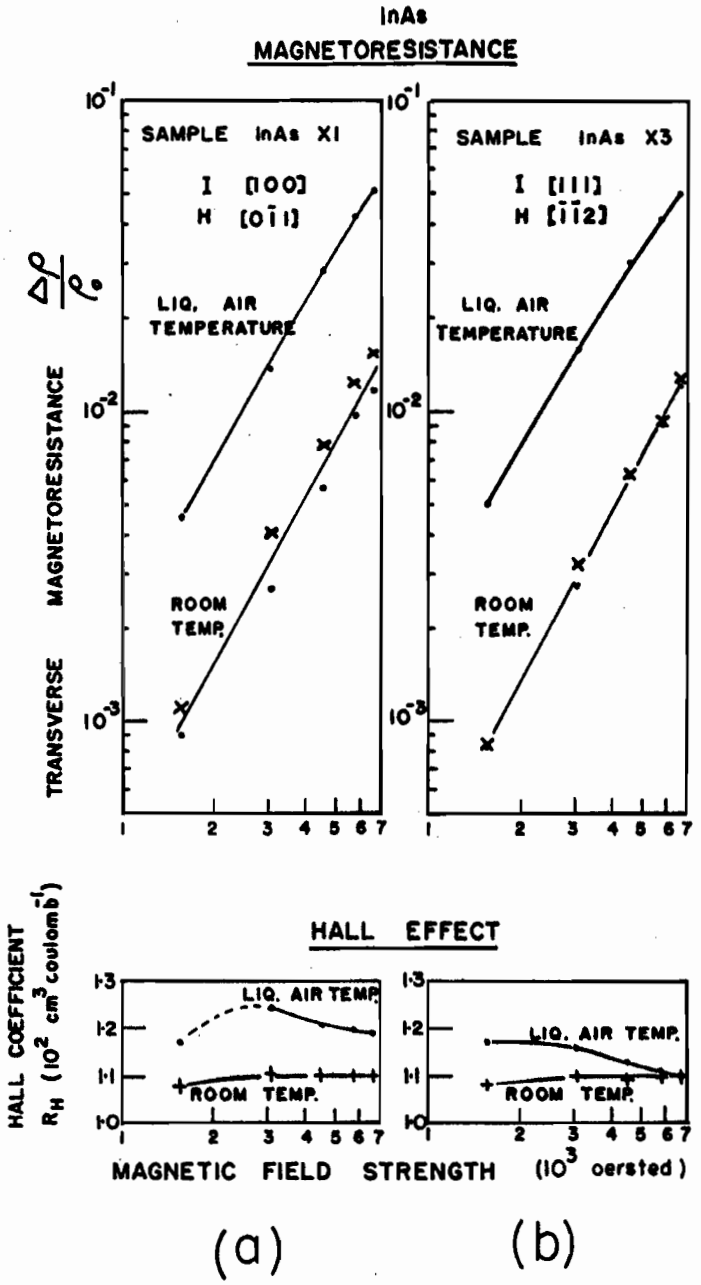

Fig. 32 Magnetic field dependence of the transverse magnetoresistance ($\Delta\rho/\rho_0$) and Hall coefficient (R_H) at room and liquid air temperatures. For $\Delta\rho/\rho_0$ the points • refer to the upper probe pairs and × to the lower probe pairs; for R_H, the points • refer to probe pair 2 and + refer to average values measured on the two probe pairs 1 and 2.

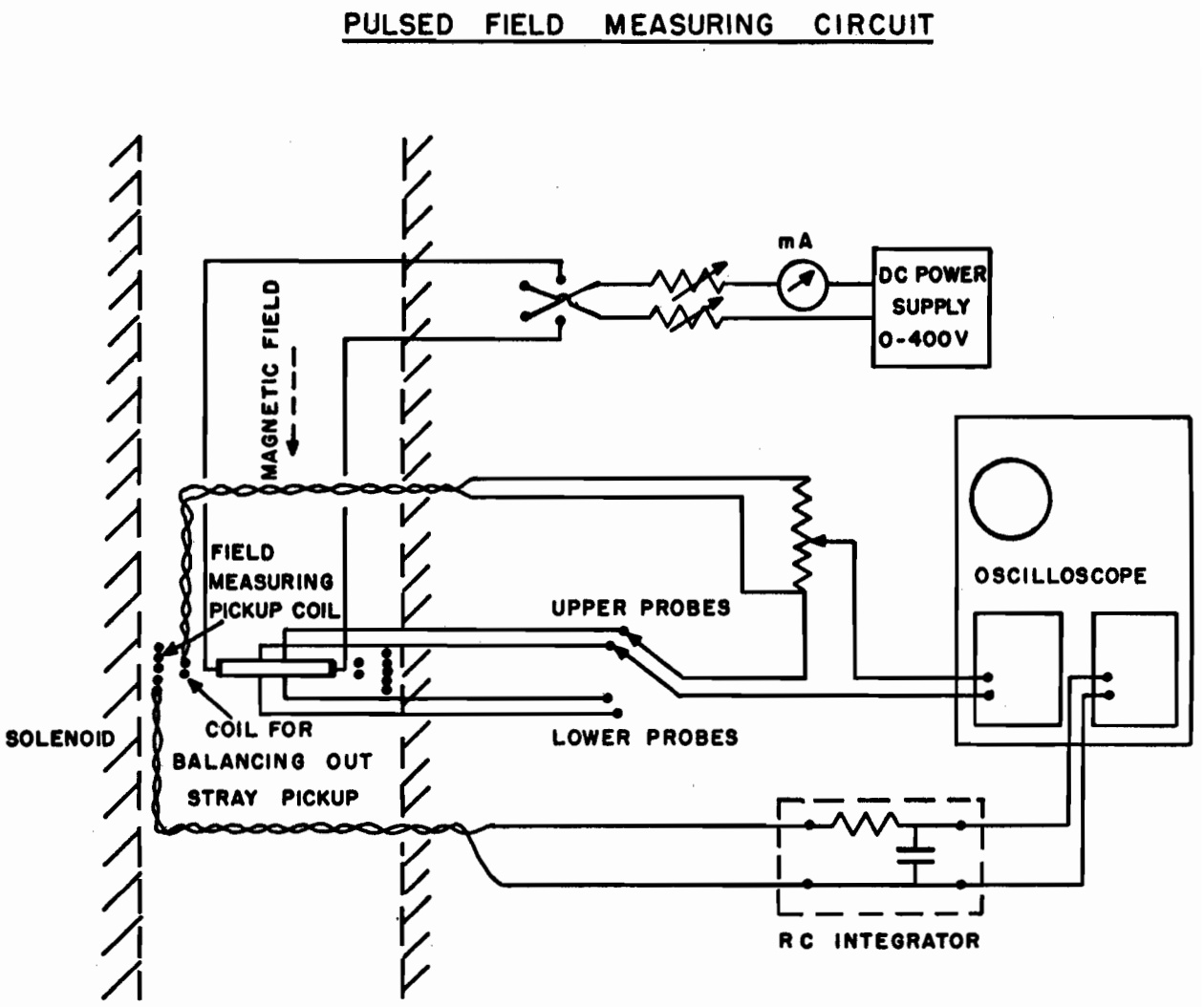

Fig. 33 Schematic experimental arrangement for the high pulsed field measurements.

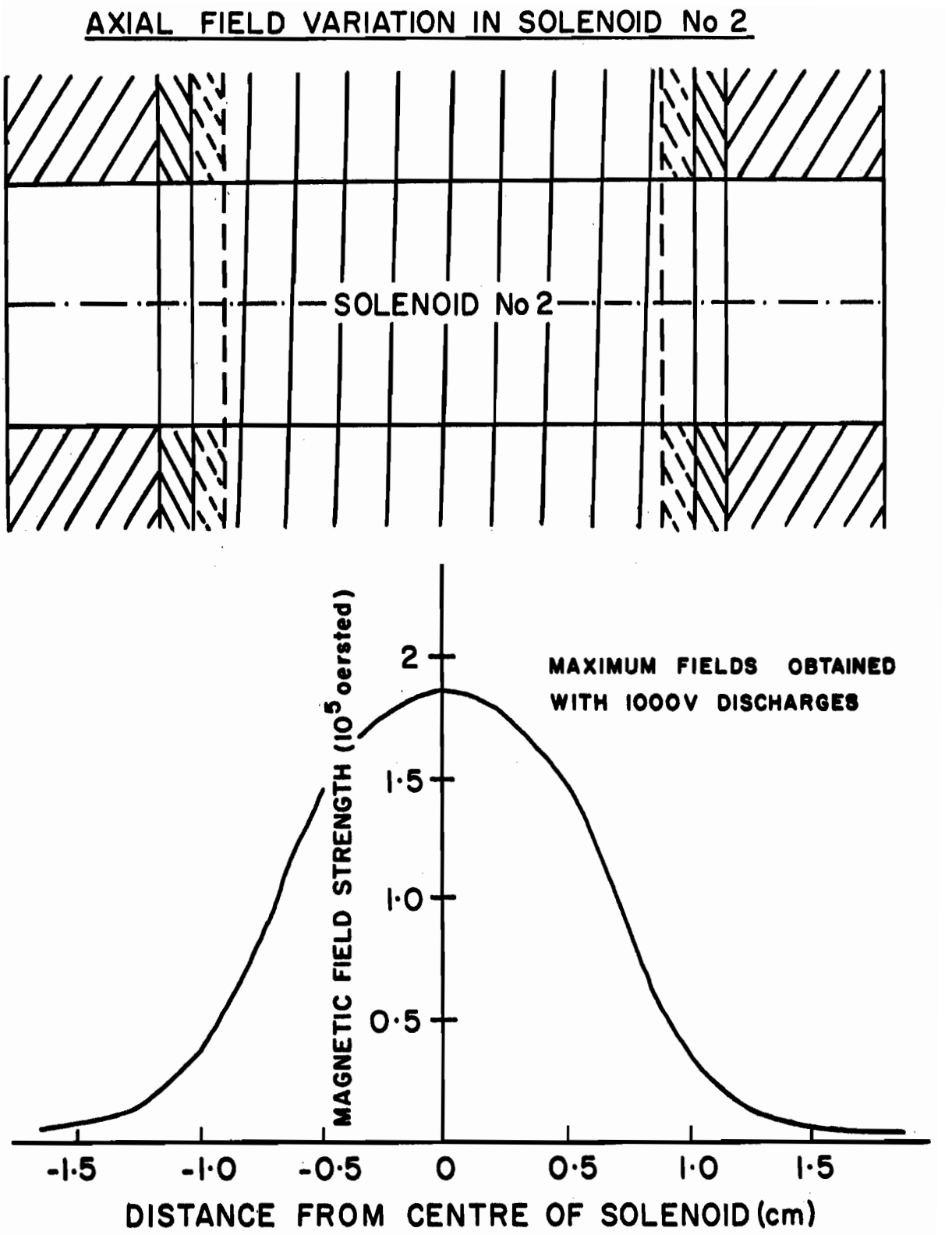

Fig. 34 Variation of the peak value of magnetic field along the axis of solenoid No. 2 measured with a pickup coil during 1000 volt discharges.

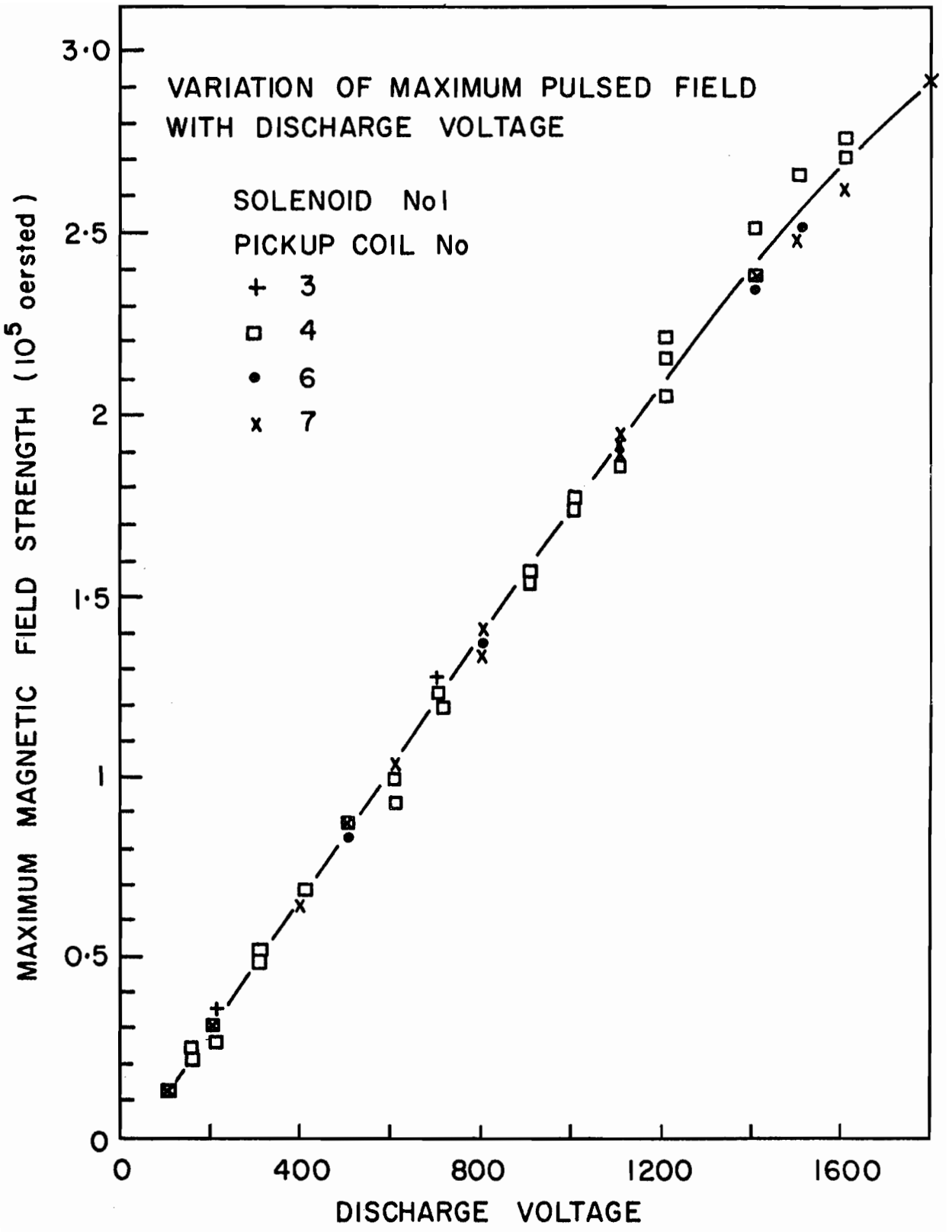

Fig. 35 Plot of peak magnetic field in solenoid No. 1 against discharge voltage using various pickup coils.

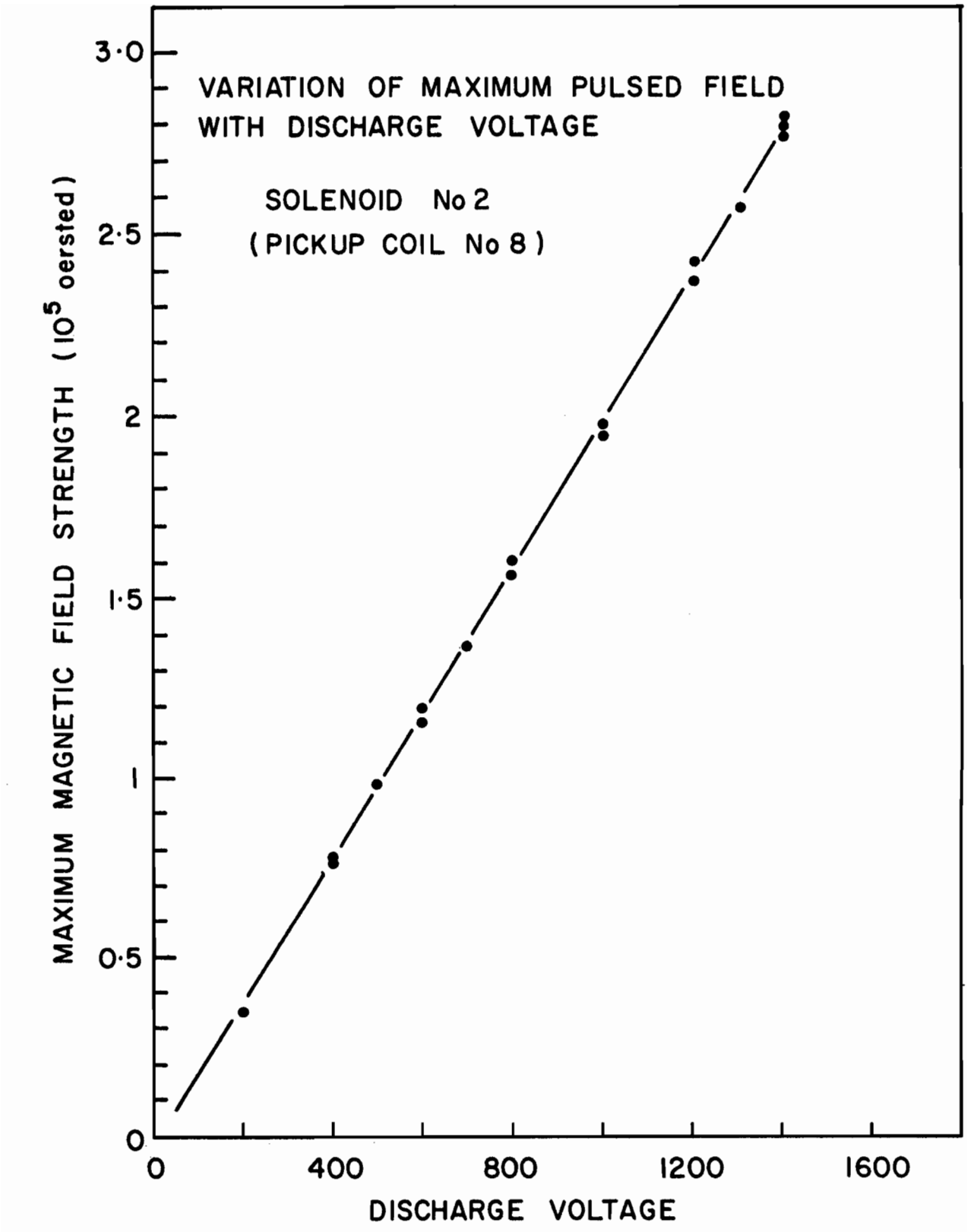

Fig. 36 Plot of peak magnetic field in solenoid No. 2 against discharge voltage.

OSCILLOSCOPE PHOTOGRAPHS TAKEN DURING 500V DISCHARGES

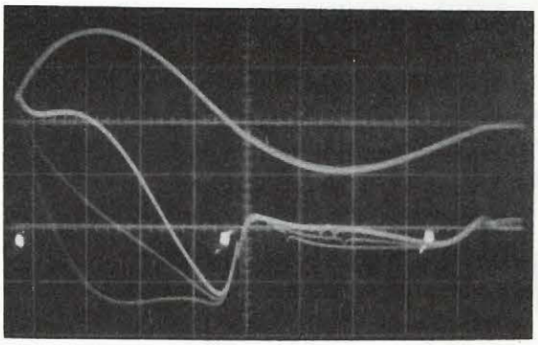

500V DISCHARGE

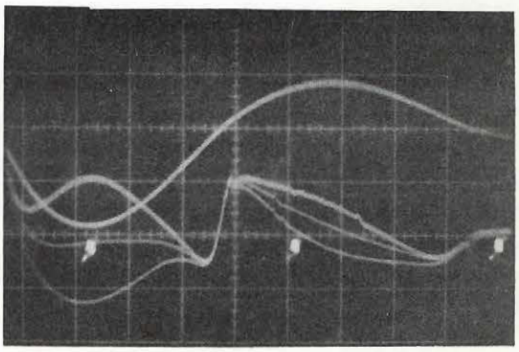

-500V DISCHARGE

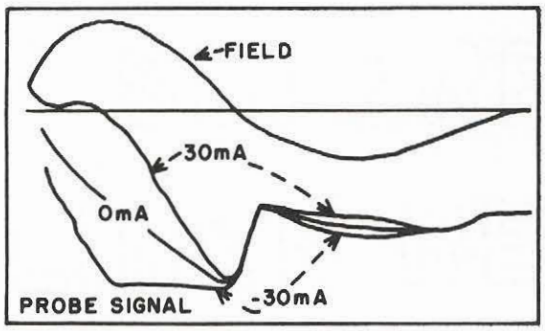

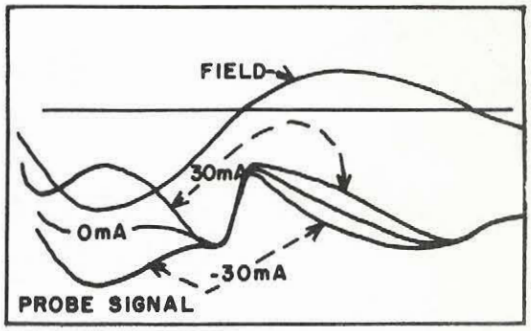

DETAILS

DATE:	4th JANUARY 1961	SAMPLE CURRENTS:	30mA (thicker trace), 0 and -30mA
SAMPLE:	In Sb C1b	OSCILLOSCOPE:	551 SER. No 1030
PROBES:	LOWER PAIR	MAG. FIELD SCALE:	1V/cm
SOLENOID:	No 1	PROBE SIGNAL SCALE:	50mV/cm
PICKUP COIL:	No 6	TIME SCALE:	20μsec/cm

Fig. 37 Oscilloscope photographs showing the magnetoresistance effect (plus a stray component of Hall effect) in an indium antimonide sample taken during six 500V discharges through the high field solenoid.

OSCILLOSCOPE PHOTOGRAPHS TAKEN DURING 800V DISCHARGES

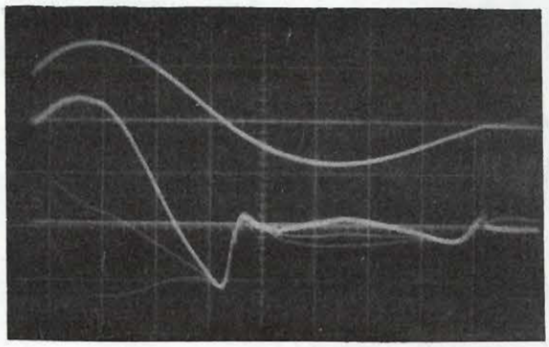

800V DISCHARGE

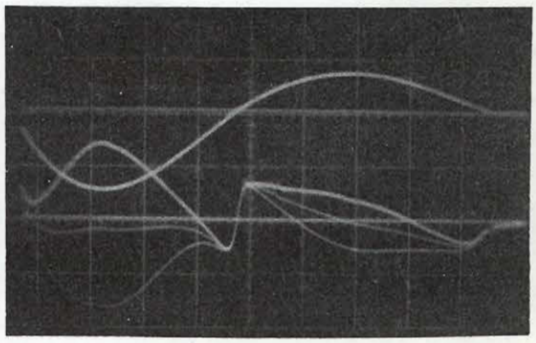

-800V DISCHARGE

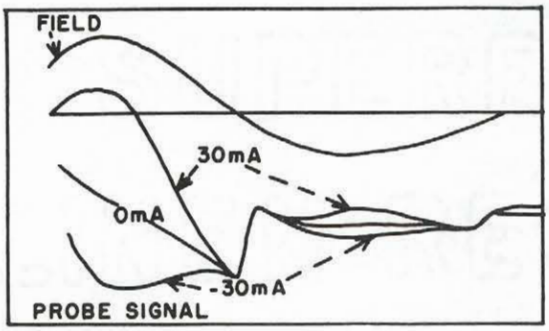

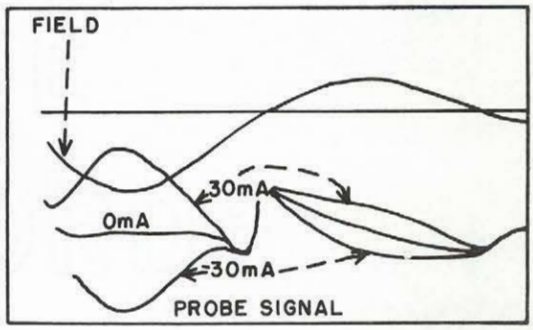

DETAILS

DATE :	4th JANUARY 1961	SAMPLE CURRENTS :	30mA (thicker trace), 0 and -30mA
SAMPLE :	In Sb C1b	OSCILLOSCOPE :	551 SER. No 1030
PROBES :	LOWER PAIR	MAG. FIELD SCALE :	2V/cm
SOLENOID :	No1	PROBE SIGNAL SCALE :	100mV/cm
PICKUP COIL :	No6	TIME SCALE :	20μsec/cm

Fig. 38 Oscilloscope photographs showing the magnetoresistance effect (plus a stray component of Hall effect) in an indium antimonide sample taken during six 800V discharges through the high field solenoid.

OSCILLOSCOPE PHOTOGRAPHS TAKEN DURING 600V DISCHARGES WITH DIFFERENT SAMPLE CURRENTS

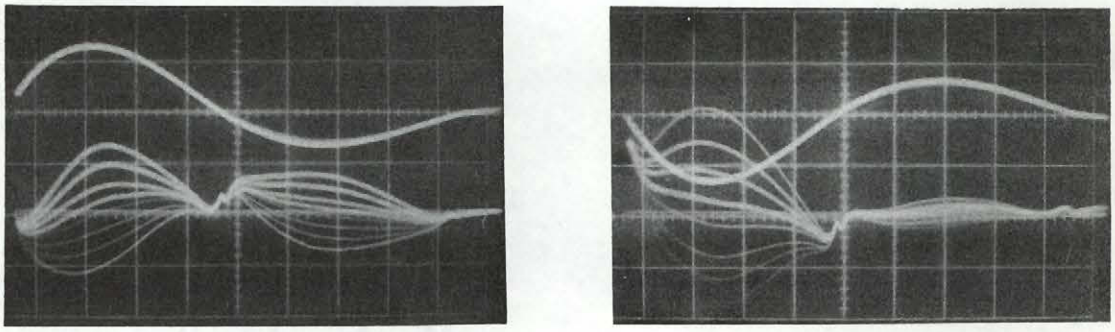

600V DISCHARGE

-600V DISCHARGE

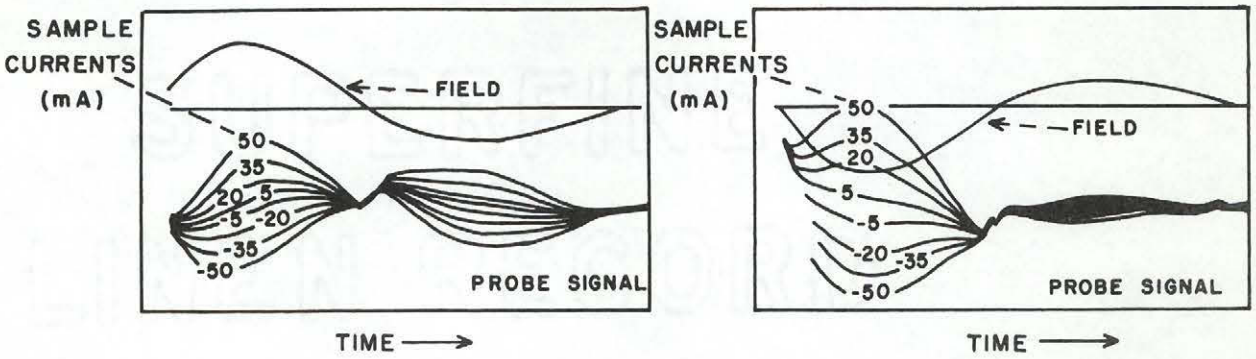

DETAILS

DATE:	6th JANUARY 1961	OSCILLOSCOPE:	551 SER. No 1030
SAMPLE:	In Sb Clb	MAG. FIELD SCALE:	2V/cm
PROBES:	UPPER PAIR	PROBE SIGNAL SCALE:	200mV/cm
SOLENOID:	No 1	TIME SCALE:	20 μ sec/cm
PICKUP COIL:	No 7		

Fig. 39 Oscilloscope photographs showing the magnetoresistance effect (plus a stray component of Hall effect) at various currents in an indium antimonide sample taken during 600V discharges through the high field solenoid.

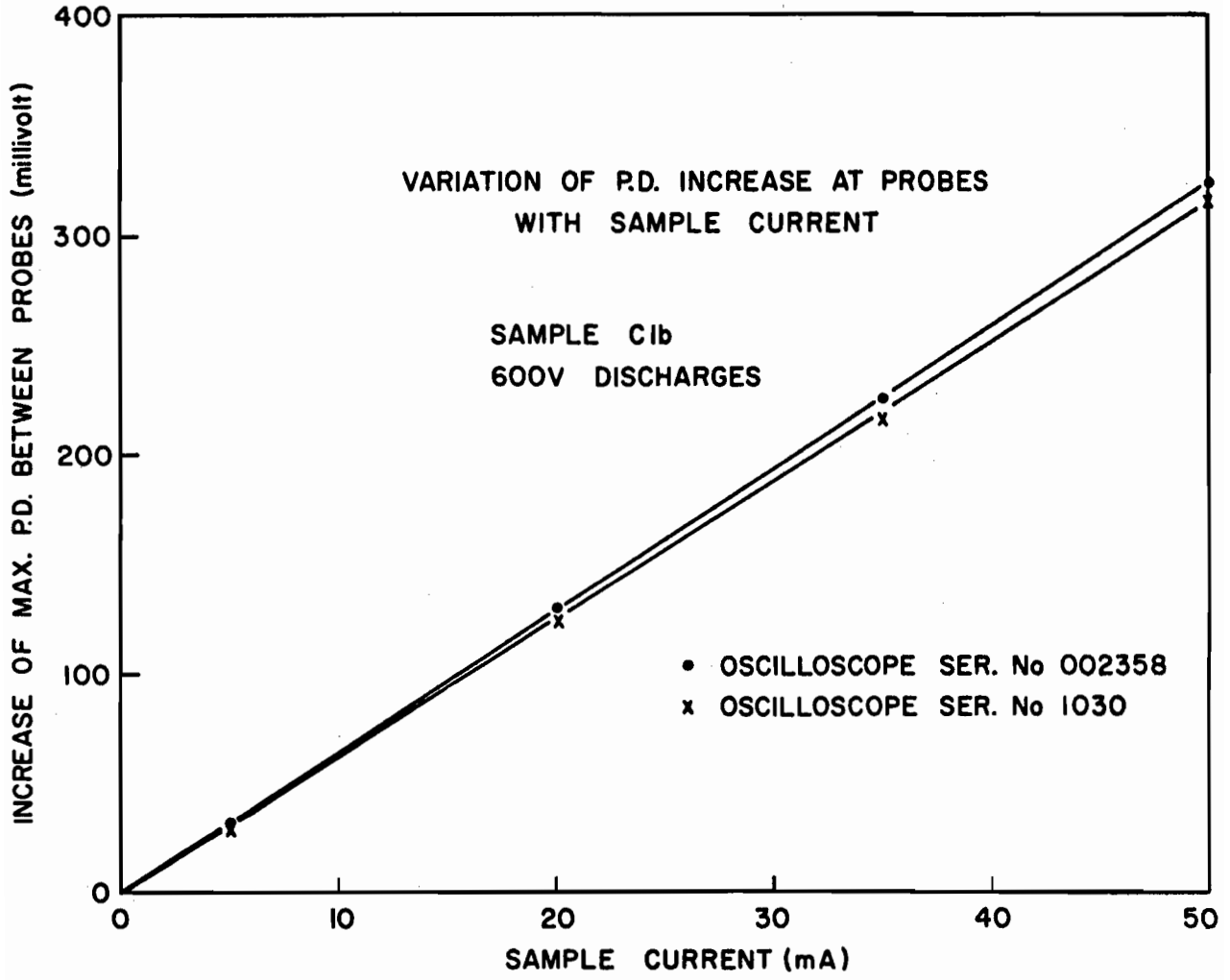

Fig. 40 Variation with sample current of the peak signal at the conductivity probes, on an indium antimonide sample during 600V discharges (one set of points was obtained from the photographs in fig. 39).

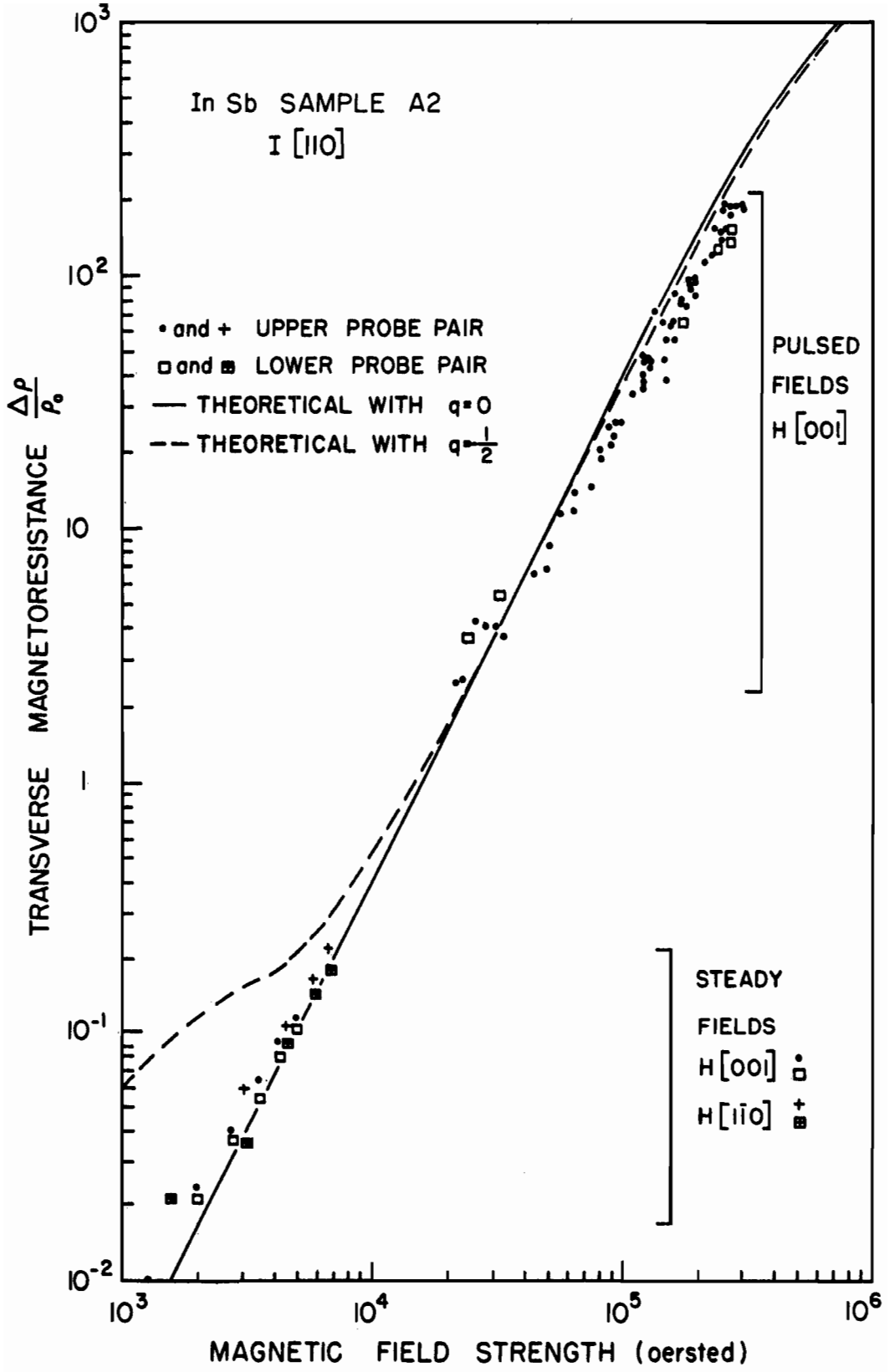

Fig. 41 Variation of transverse magnetoresistance with magnetic field strength in indium antimonide sample A2. The theoretical lines shown were calculated from the carrier concentrations and mobilities in the sample assuming relaxation times for the electrons and holes to be independent of energy ($\mathcal{E}$) or to have an $\mathcal{E}^{-1/2}$ dependence.

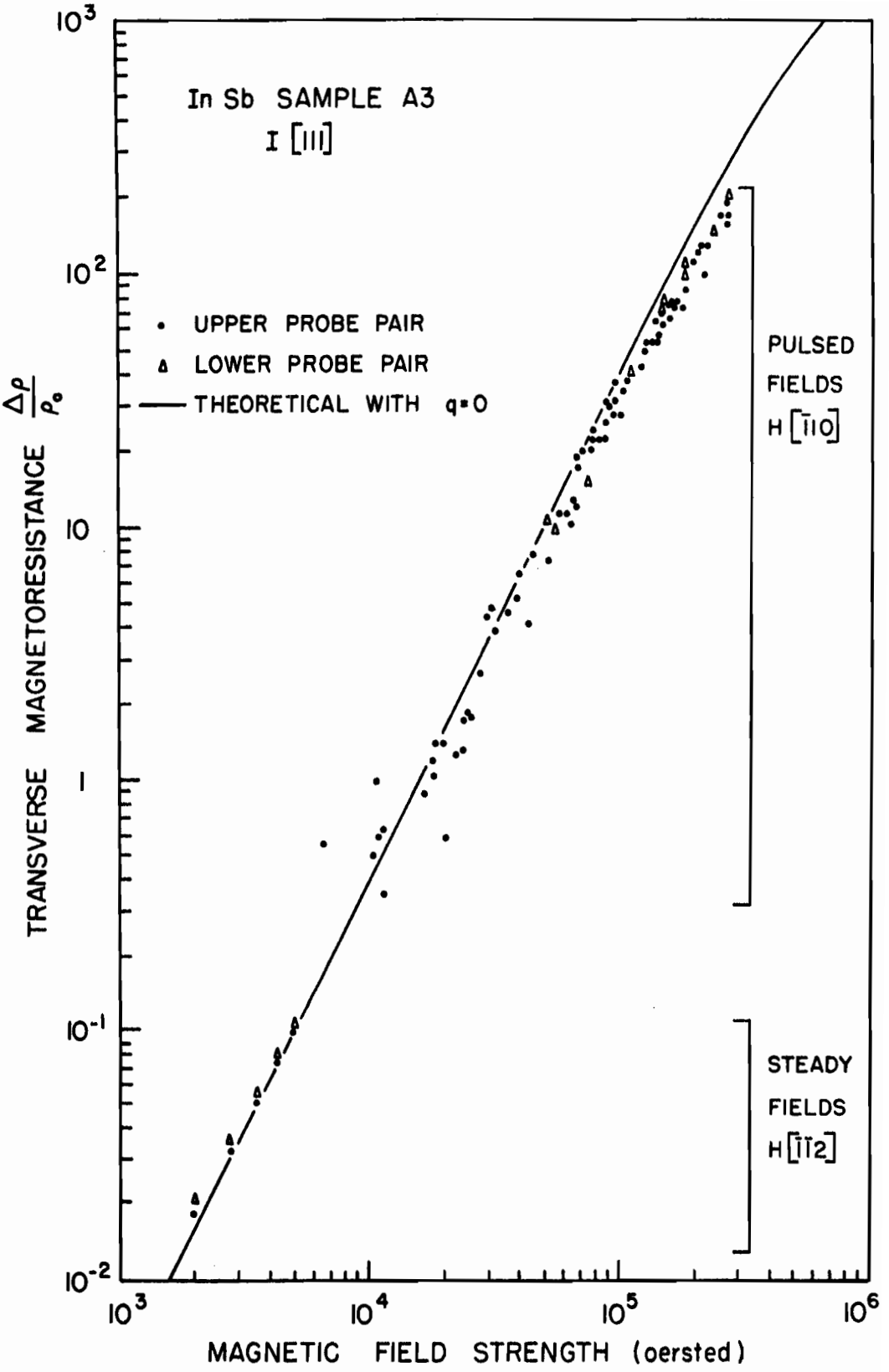

Fig. 42 Variation of the transverse magnetoresistance with magnetic field strength in indium antimonide sample A3. The theoretical line shown was calculated for the sample assuming the electron and hole relaxation times to be independent of energy.

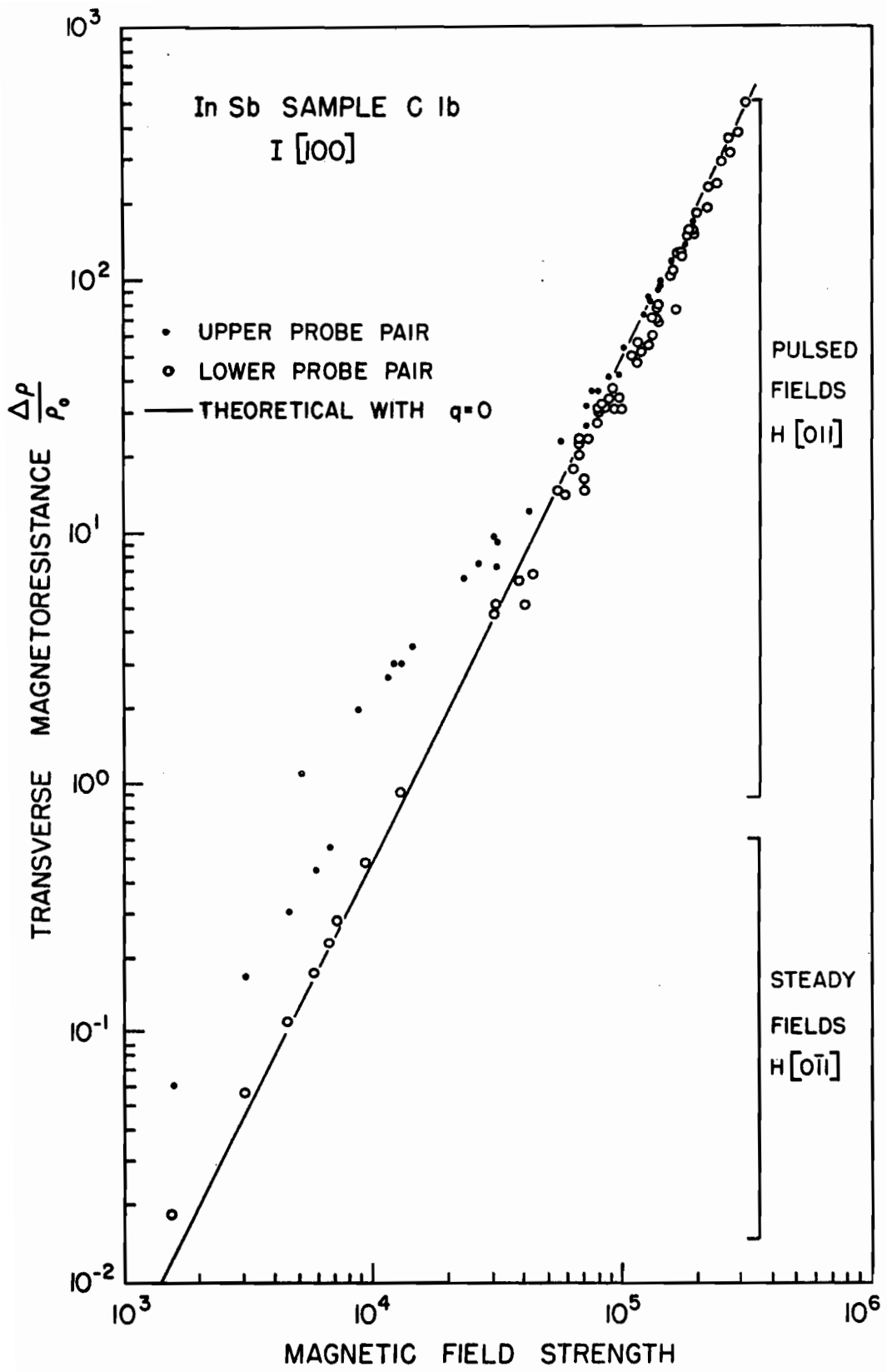

Fig. 43 Variation of the transverse magnetoresistance with magnetic field strength in indium antimonide sample C1b. The theoretical line shown was calculated for the sample assuming the electron and hole relaxation times to be independent of energy.

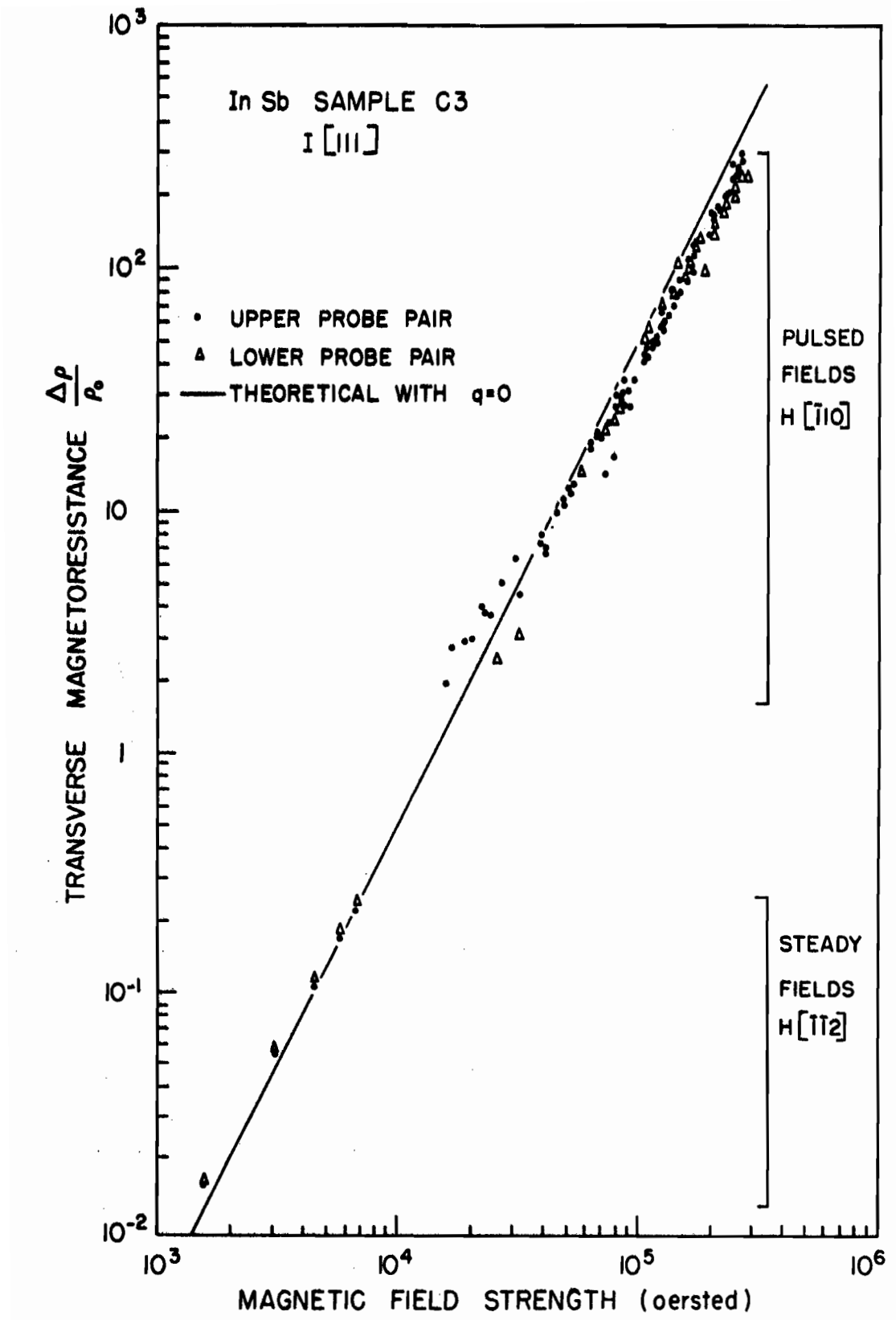

Fig. 44 Variation of the transverse magnetoresistance with magnetic field strength in indium antimonide sample C3. The theoretical line shown was calculated for the sample assuming the electron and hole relaxation times to be independent of energy.

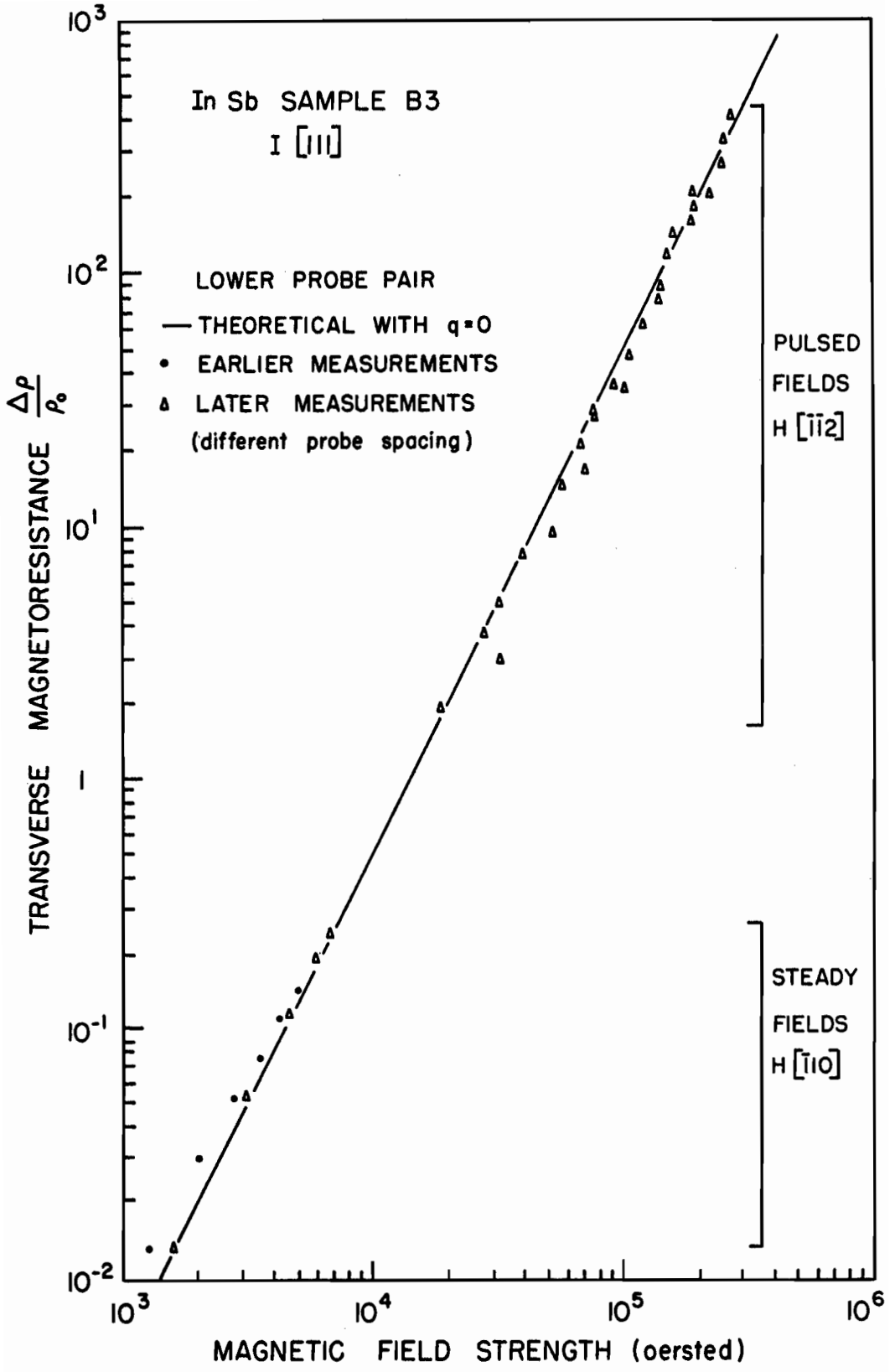

Fig. 45 Variation of the transverse magnetoresistance with magnetic field strength in indium antimonide sample B3. The theoretical line shown was calculated for the sample assuming the electron and hole relaxation times to be independent of energy.

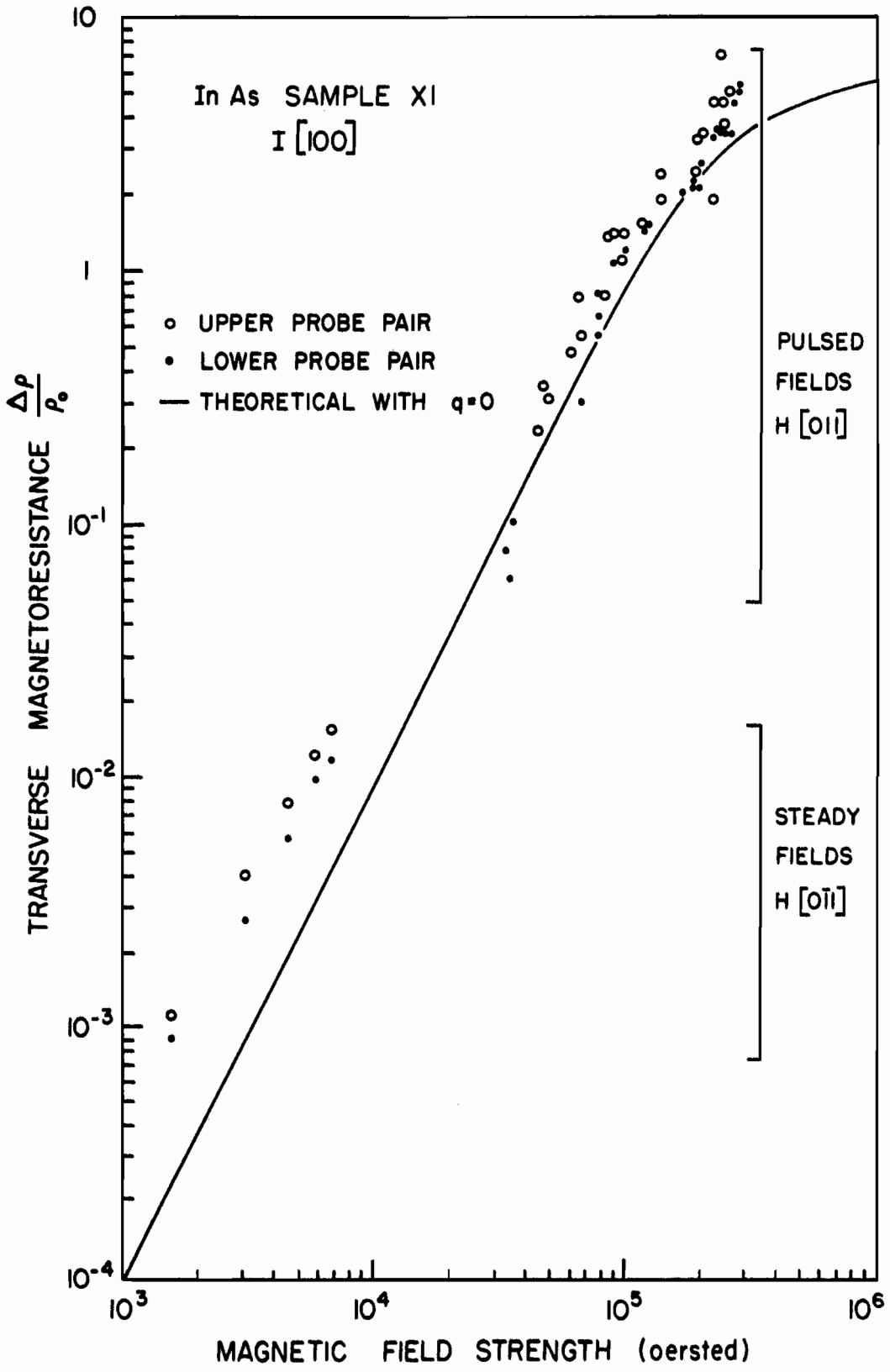

Fig. 46 Variation of the transverse magnetoresistance with magnetic field strength in indium arsenide sample X1. The theoretical line shown was calculated for the sample assuming the electron and hole relaxation times to be independent of energy.

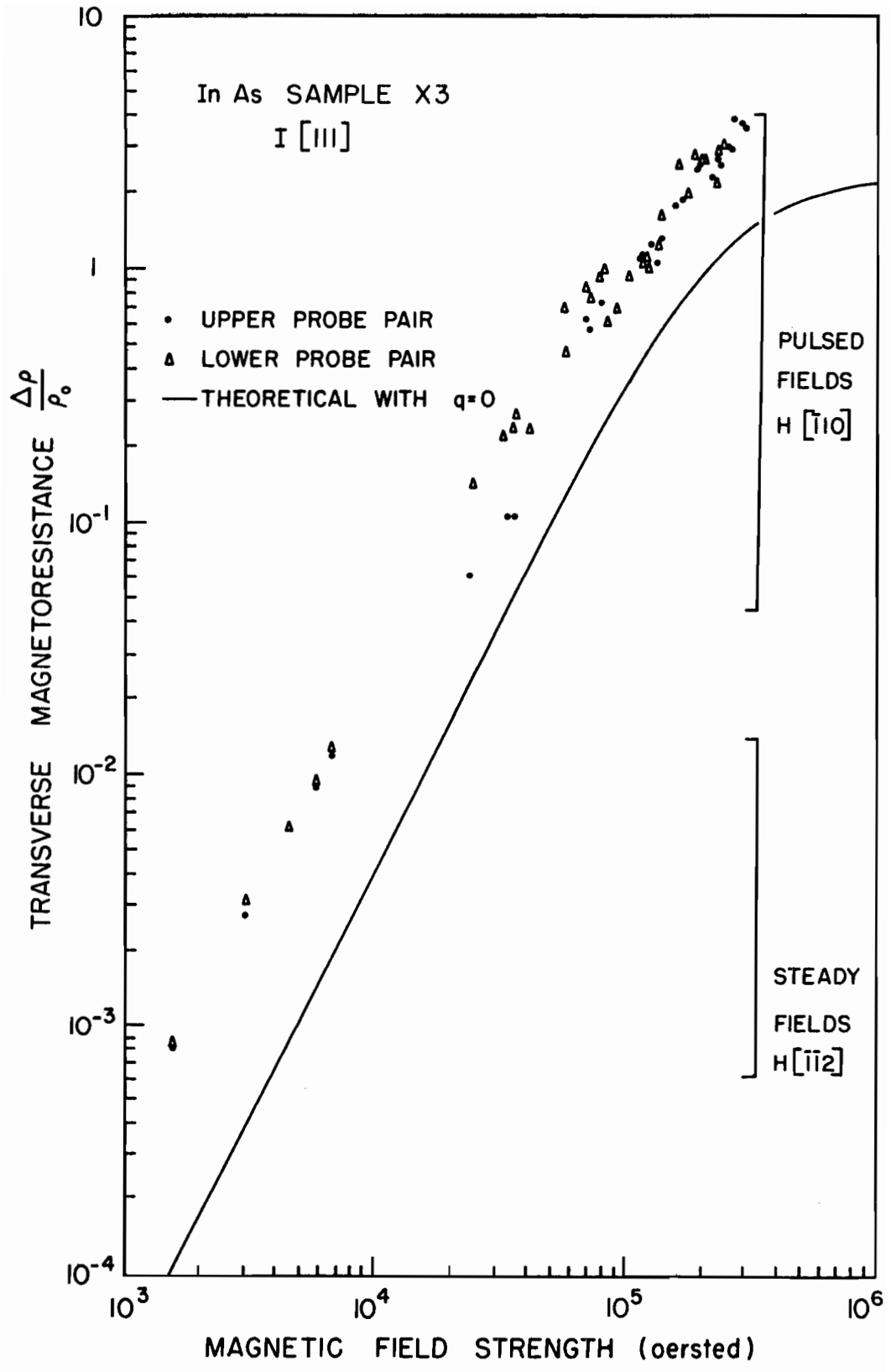

Fig. 47 Variation of the transverse magnetoresistance with magnetic field strength in indium arsenide sample X3. The theoretical line shown was calculated for the sample assuming the electron and hole relaxation times to be independent of energy.

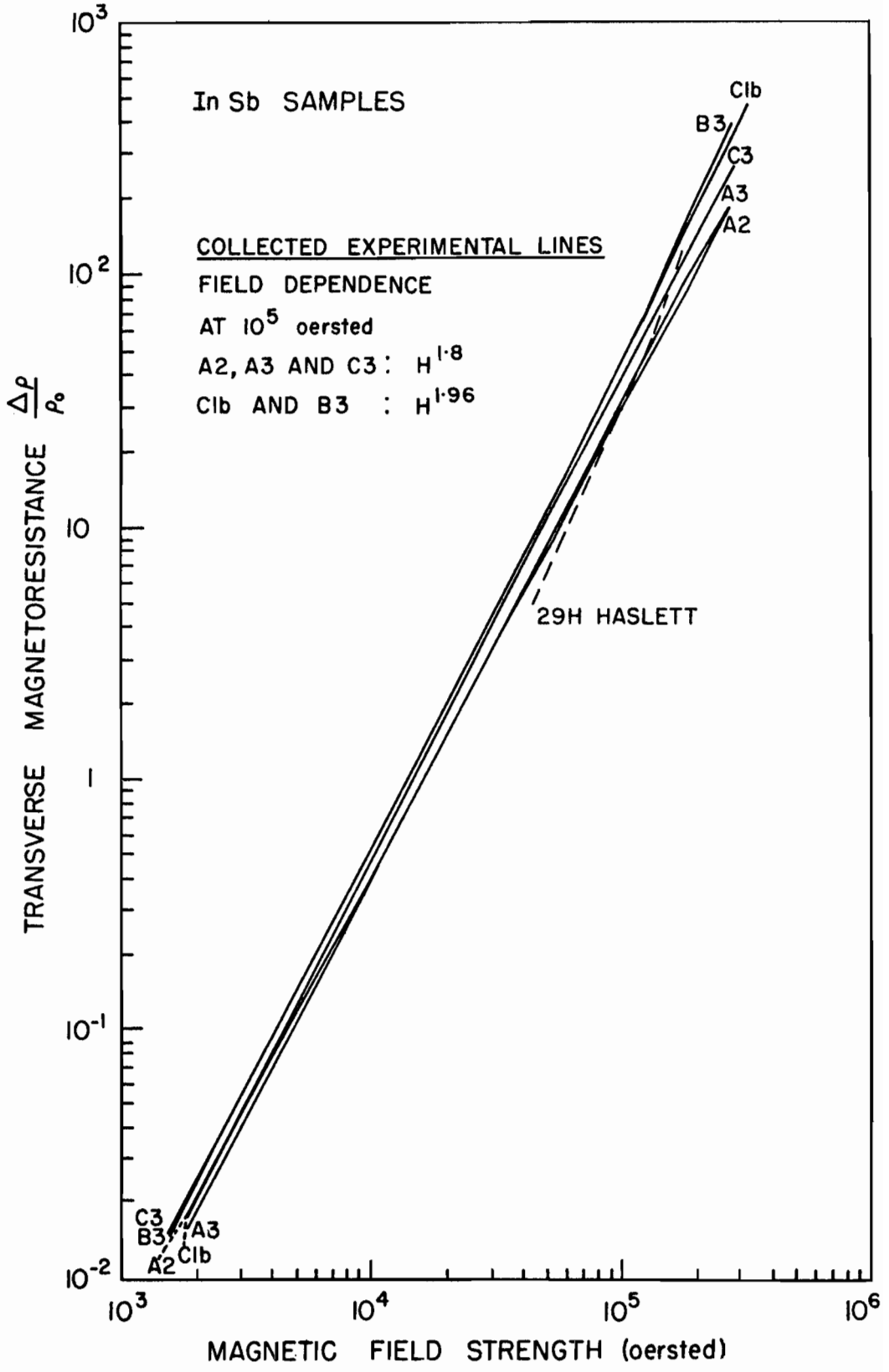

Fig. 48 Variation of transverse magnetoresistance with magnetic field strength in the indium antimonide samples obtained from average lines drawn through the experimental points in figs. 42 to 45.

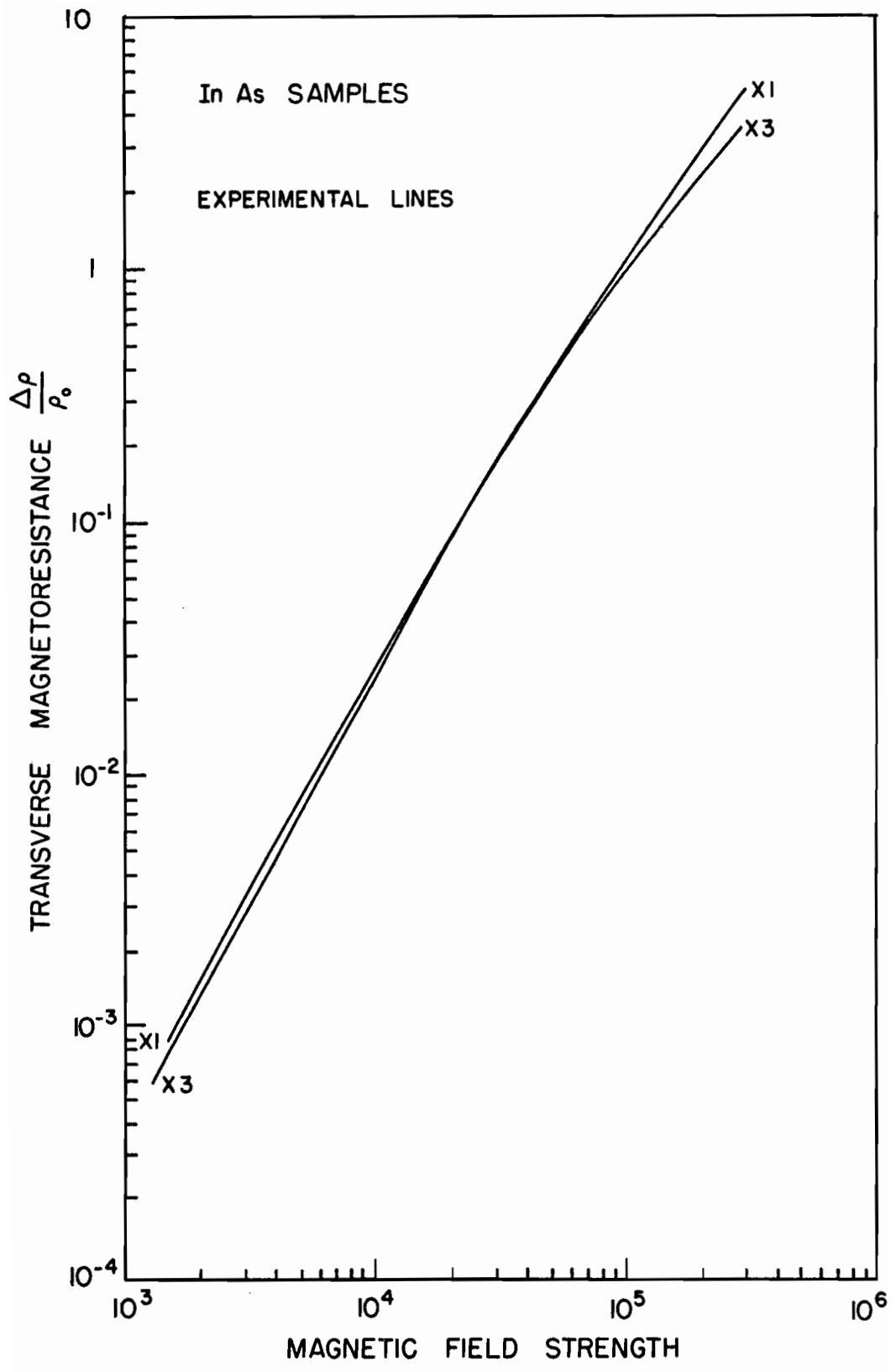

Fig. 49 Variation of transverse magnetoresistance with magnetic field strength in the two indium arsenide samples obtained from average lines drawn through the experimental points in figs. 46 and 47.

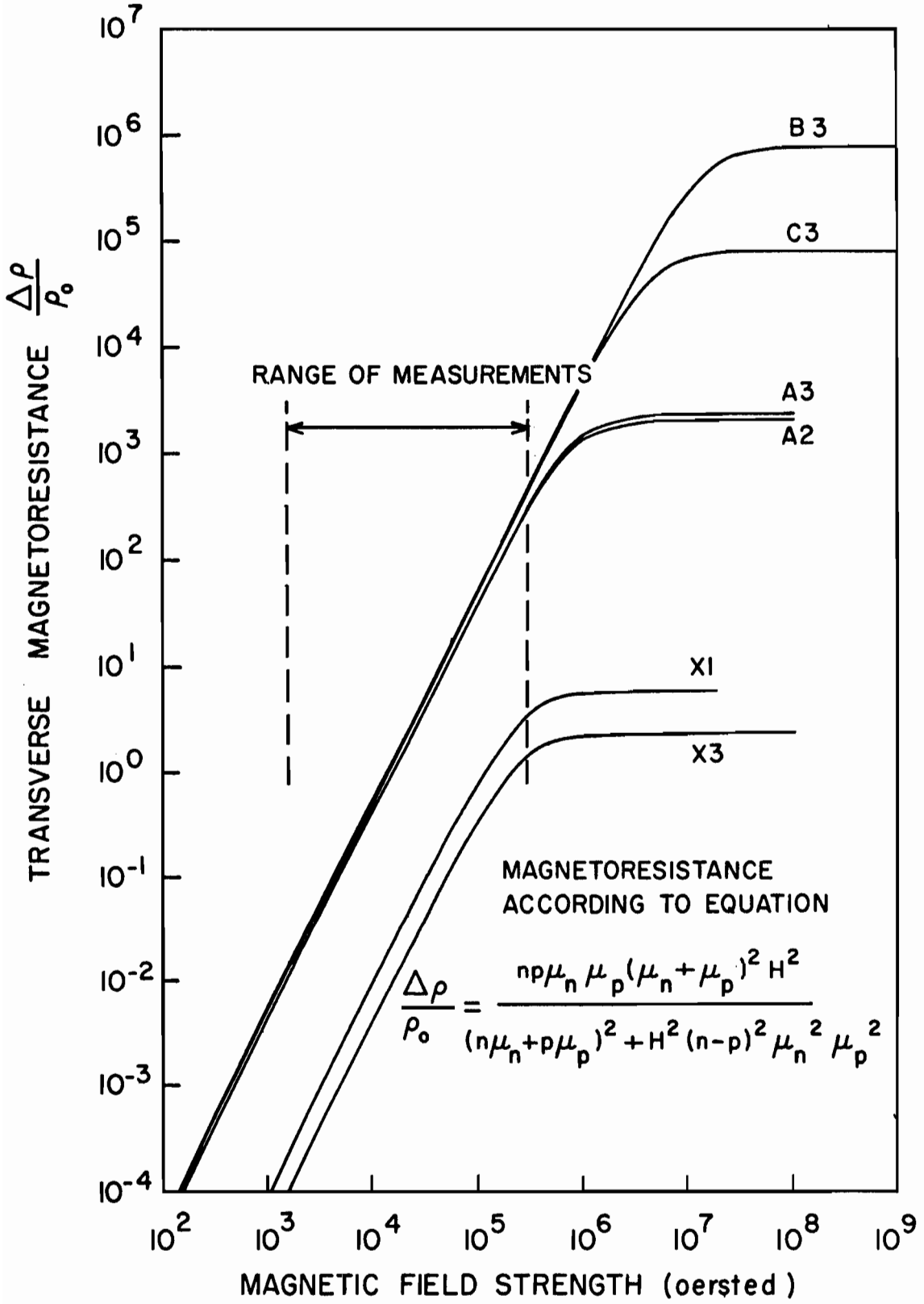

Fig. 50 Calculated variation of transverse magnetoresistance with magnetic field strength for the various samples using the equation shown which assumes relaxation times to be independent of energy.

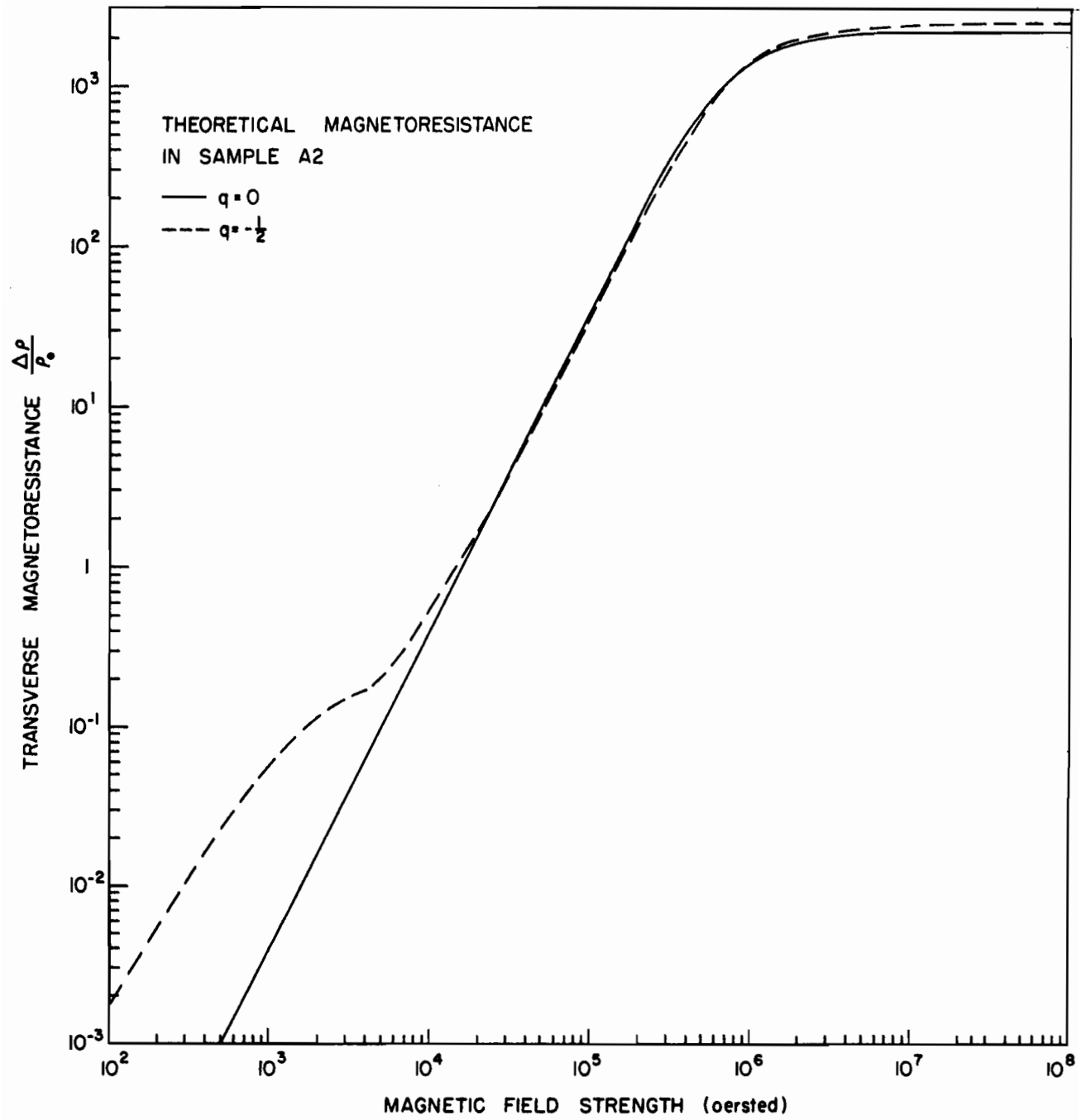

Fig. 51 Comparison of the variation of transverse magnetoresistance with magnetic field strength calculated for sample A2 assuming relaxation times to be independent of energy (solid line) and proportional to $\mathcal{E}^{-1/2}$ (broken line).

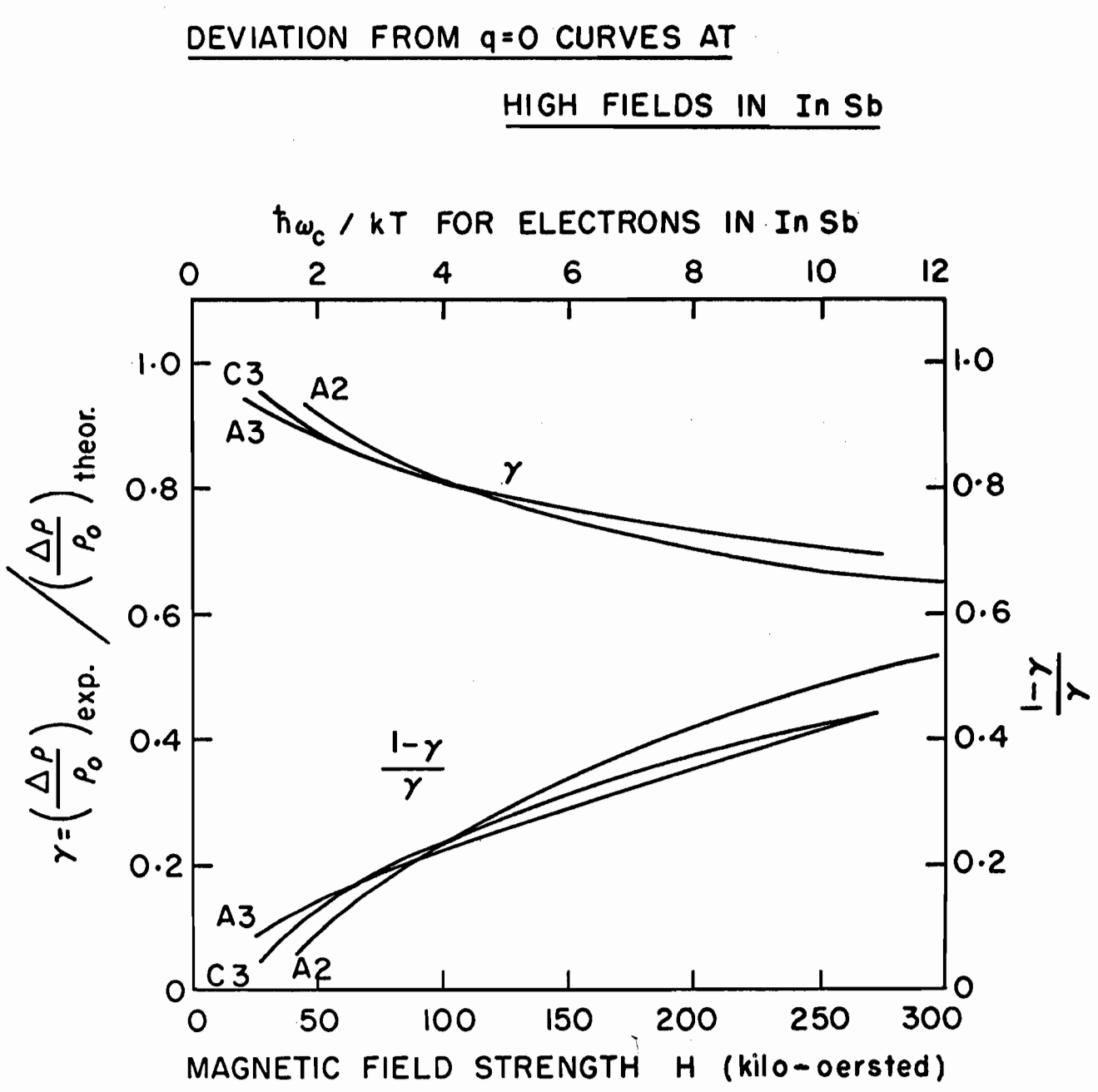

Fig. 52 Variation at the higher fields of the ratio of the average measured magnetoresistance to theoretical values (assuming $q = 0$) for the samples A2, A3 and C3.

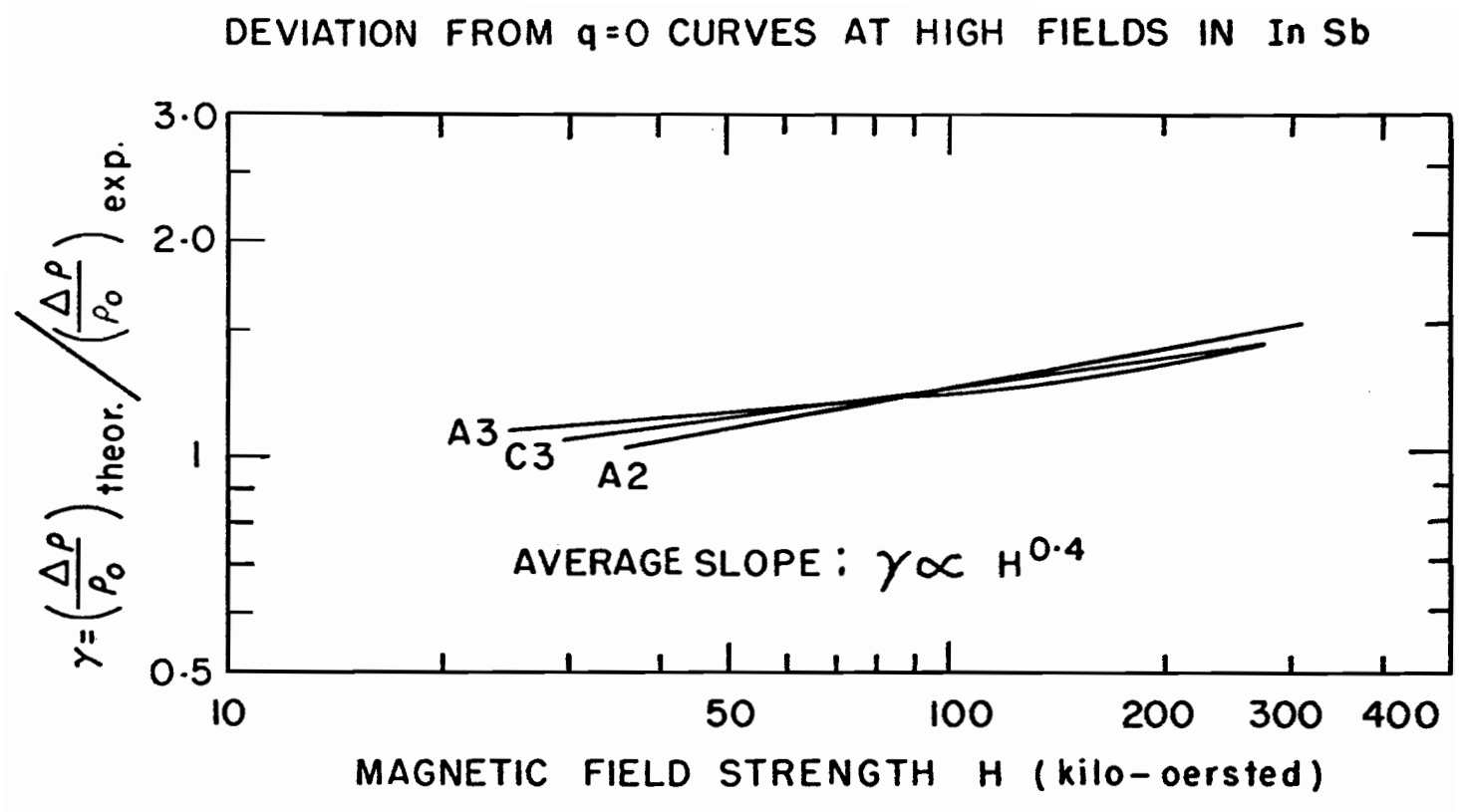

Fig. 53 Log-log plot of the ratio of the theoretical magnetoresistance (assuming $\zeta = 0$) to the average measured values for samples A2, A3 and C3.